UNIVERSITY OF CALIFORNIA SAN DIEGO

PSME3 Regulates Migration and Differentiation of Myoblasts

A Dissertation submitted in partial satisfaction of the requirements
for the degree Doctor of Philosophy

in

Neurosciences

by

Kenneth David Kuhn

Committee in charge:

Professor Brenda Bloodgood, Chair
Professor Martin Hetzer, Co-Chair
Professor Nicola Allen
Professor Sreekanth Chalasani
Professor Maria Marchetto

2025

The Dissertation of Kenneth David Kuhn is approved, and it is acceptable in quality and form for publication on microfilm and electronically.

University of California San Diego

2025

EPIGRAPH

We carve out groups of stars in the heavens, and call them constellations, and the stars patiently suffer us to do so—tho if they knew what we were doing, some of them might feel much surprised at the partners we had given them…

we humanly make an addition to some sensible reality, and that reality tolerates the addition.

William James

TABLE OF CONTENTS

LIST OF FIGURES

LIST OF TABLES

LIST OF ABBREVIATIONS

PSME3	Proteasome Activator Subunit 3 (PA28γ, 11s REGγ, or Ki nuclear autoantigen)
MHC	Major histocompatibility complex
NLS	Nuclear localization signal
BAG	Bcl2-associated athanogene
ARF	$p14^{ARF}$
MEF	Mouse embryonic fibroblast
PTM	Post-translational modification
MAPK	Mitogen activated protein kinase
ERK	Extracellular-signal-regulated kinase
O-GlcNAc	O-linked β-N-acetylglucosamine
Ddx6	DEAD box polypeptide 6
P-bodies	Processing bodies
SRC-3AIB1	Steroid receptor coactivator-3
RBM3	RNA Binding Motif Protein 3
PKAcα	Protein kinase A catalytic subunit-α
TAA	Tumor-associated antigen
PTP	Pioneer translation products
PML	Promyelocytic leukemia protein
RNAPII	RNA pol II
LIM-HD	LIM homeodomain
CLIM	Cofactor of LIM-HD proteins
5-FU	5-fluorouracil

EAE	Experimental autoimmune encephalomyelitis
BSMCs	Bone marrow stromal cells
MyoD	Myogenic Differentiation (protein)
RPRD1A	Regulation of Nuclear Pre-MRNA Domain Containing 1A
NUDC	Nuclear distribution C
CCT	Coiled-coil terminus
CID	C-terminal domain (CTD)-interacting domain
TSS	Transcriptional start site
TCF	T cell-specific factor
LIS1	Lissencephaly protein 1
HOP	Hsp70-Hsp90 organizing protein
MTOC	Microtubule organizing center
CHIP	Carboxyl terminus of HSC70-interacting protein
CUT&RUN	Cleavage Under Targets & Release Using Nuclease
PLA	Proximity Ligation Assay
DSB	Double strand DNA break
APC	Adenomatous Polyposis Coli
ITGB3	Integrin Beta-3
MHC	Myosin heavy chain
siScr	Scrambled siRNA
Cdel	C-terminal deletion mutant

ACKNOWLEDGEMENTS

I would first like to thank the members of the Hetzer lab, in all of its iterations, for the abundant patience and kindness they showed to an often hapless graduate student. Without their guidance I may still yet be struggling to get a clean Western blot result, and without whose friendship and support I would have given up on this whole endeavor several times over. I am particularly grateful to my fellow Salk lab members Rafael Arrojo e Drigo, Juliana Capitanio, and Jeanae Kaneshiro for helping me gain my footing in the lab after I first arrived, and for guiding me through my riskiest projects. I further owe a great debt to all the Hetzer lab members who were part of the lab after our relocation to Austria: to Sabine for her herculean organization efforts and boundless hospitality, to Manuel for commiseration in the face of struggles common to every scientist, and to Anjali and JQ for their earnest friendship.

I would especially like to thank, in connection with this work, Rae, who not only showed unreasonable levels of forbearance even amidst the countless disturbances to which I surely subjected his peace of mind while we were benchmates, but also long after my relocation to Austria, when he continued to express genuine interest in my project and helped me achieve the best result at every step of my scientific journey. Where it might have engendered ire in any other, Rae only radiated kindness, and for that I owe him a great deal. Without Rae's insight, wisdom, and expertise, this project simply would not exist.

That I should ever have become a natural scientist at all, I owe to my mother and father, who, at every critical juncture of my life, provided me with the freedom of choice, the means to exercise it, and unconditional support no matter which path I settled on. I thank my siblings Gret and Max not only for being family, but also dear friends throughout this work. I thank David Brusick for guiding me along the path of a professional biologist, and for reminding me that,

compared to graduate students sixty years ago, I really am living the good life. It made those long nights in the lab with only negative results for company a bit more bearable. I'm indebted to all my friends, both in San Diego and Vienna, for their steadfast support through my time in graduate school. I would also like to thank Saki, who was available to listen to me explain (incorrectly) why the next RNA sequencing experiment was certain to show positive results, and for making the most grueling data analysis work into an enjoyable experience. In retrospect, Saki always seemed to be one step ahead of me, and I owe her a great debt for not only her clarity of thought, but her insistence on its prescience.

I am forever grateful to my committee members, without some of whom, I might never have arrived in San Diego at all. Thank you, Nicola, for being so welcoming when I first arrived at the Salk to interview for the neuroscience program, and for hosting me for a very educational rotation. Thank you, Shrek, for providing frank and actionable advice when I needed it most. Thank you, Brenda, for your support and providing the seed for this project, which would never have happened without your suggestion. And thank you, Carol, for your insightful feedback on my project, and for helping me be confident in accuracy and rigor.

Finally, I would like to thank my advisor, Martin Hetzer. Martin has put my development at the forefront, even when faced with the superhuman tasks of leading a lab of roughly twenty members, organizing an entire institute's response to the COVID pandemic, relocating the lab across a continent and an ocean, and running a world-class research institution. I fear I may still fail to appreciate how many pressing tasks he had to set out of his mind each time we met, and yet that may only be further testament to his remarkable fortitude. Thank you, Martin, for giving me the freedom to take big risks, ask big questions, and make big mistakes, and for always

guiding me back to the right path before I strayed too far. Without it, I wouldn't be half the scientist I am today.

Chapters 2 and 3, in part, have been submitted to and are under review for publication at Life Science Alliance. The dissertation author was the primary researcher and author of this paper and is accompanied by Ukrae H. Cho and Martin W. Hetzer.

VITA

2014-2018 Bachelor of Science in Biology, University of Virginia

2018-2025 Doctor of Philosophy in Neurosciences, University of California San Diego
Salk Institute
Institute of Science and Technology Austria

PUBLICATIONS

Kuhn, K. D.; Cho, U. H.; Hetzer M. W. PSME3 Regulates Migration and Differentiation of Myoblasts. In review, Life Science Alliance.

Kuhn, K. D.; Edamura, K.; Bhatia, N.; Cheng, I.; Clark, S. A.; Haynes, C. V.; Heffner, D. L.; Kabir, F.; Velasquez, J.; Spano, A. J.; Deppmann, C. D.; Keeler, A. B. Molecular Dissection of TNFR-TNFα Bidirectional Signaling Reveals Both Cooperative and Antagonistic Interactions with P75 Neurotrophic Factor Receptor in Axon Patterning. Molecular and Cellular Neuroscience, 2020, 103, 103467. https://doi.org/10.1016/j.mcn.2020.103467.

Beer, K. B.; Rivas-Castillo, J.; **Kuhn, K.**; Fazeli, G.; Karmann, B.; Nance, J. F.; Stigloher, C.; Wehman, A. M. Extracellular Vesicle Budding Is Inhibited by Redundant Regulators of TAT-5 Flippase Localization and Phospholipid Asymmetry. Proceedings of the National Academy of Sciences, 2018, 115. https://doi.org/10.1073/pnas.1714085115.

ABSTRACT OF THE DISSERTATION

PSME3 Regulates Migration and Differentiation of Myoblasts

by

Kenneth David Kuhn

Doctor of Philosophy in Neurosciences

University of California San Diego, 2025

Professor Brenda Bloodgood, Chair
Professor Martin Hetzer, Co-Chair

The acquisition of cellular identity requires large-scale alterations in cellular state. A cell must not only reorganize its nuclear contents to facilitate the expression of necessary genes while silencing those required for stem-like character, but differentiation also often entails dramatic reorganization of the cytoplasmic contents. The number of proteins required for this process is prodigious and may well count among its number the non-canonical proteasome activator

PSME3. PSME3 is known to regulate diverse cellular processes in both the nucleus and cytoplasm, but its importance for differentiation remains unclear. To this end, we have undertaken a series of studies using the C2C12 mouse myoblast cell line.

In Chapter 1, I provide a detailed introduction of proteasome biology with a particular focus on PSME3. I discuss major findings pertaining to PSME3's function, enumerate its many degradation targets, discuss its known biochemical properties, and note the existing evidence for its role in differentiation.

In Chapter 2, I investigate the association of PSME3 with the chromatin and find its widespread association with highly active promoter regions. I further identify the transcriptional protein RPRD1A as an interaction partner that may facilitate this association. Finally, I demonstrate that, though it associates with highly active genes, loss of PSME3 has no effect on gene expression across differentiation.

In Chapter 3, I show that PSME3 is important in differentiating myoblasts for its ability to regulate cell migration and the formation of myotubes. I demonstrate that loss of PSME3 is accompanied by an altered abundance of cell-adhesion-related proteins, which may be affected by an interaction of PSME3 with the chaperone NUDC. I attempt to elucidate a potential mechanism for these functions and show PSME3 mediates differentiation in a cell-intrinsic, proteasome-independent mechanism.

In Chapter 4, I analyze the sum of my work, place it into the broader context of PSME3 function, and speculate on what future efforts would prove fruitful to better understand this elusive protein.

Chapter 1 Introduction

1.1 Proteasome Biology

The proteasome is the principal protease in both the nucleus and cytoplasm of eukaryotic cells. It is responsible for both the timely degradation of proteins involved in several central cellular processes, including transcription, signal transduction, and cell division, as well as the disposal of old or damaged protein molecules (Bard et al., 2018). As such, the proteasome serves a critical role in cellular physiology.

The proteasome is composed of two major functional units. The first is its barrel-like core, termed the 20s proteasome, while the second is a regulatory cap which can bind to either end, of which there are many types. The 20s component is composed of four stacked rings each of seven components. The two inner rings are composed of beta subunits form a cavity containing catalytic threonine proteases, and the outer rings of alpha subunits form a 13 Å pore through which proteasomal substrates must pass before being degraded (Stadtmueller and Hill, 2011). Three distinct types of proteolytic activities are performed within the proteasome: chymotryptic, tryptic, and caspase-like (Geng et al., 2012). Though in certain cases the 20s proteasome is capable of unassisted degrading proteins, most proteasomal activity has been described in the context of its association with regulatory caps, which alter the set of recognized substrates, open the pore of the 20s core, and, in some cases, alter its catalytic activity (Deshmukh et al., 2023). It should be noted that, as the 20s subunit is symmetrical, two distinct caps may associate with a single proteasome at either end. The function of these “hybrid” proteasomes remains elusive and is an active area of study (Thomas et al., 2023).

The most well-studied of these regulatory caps is the 19s subunit, which, together with the 20s core, forms what is known as the 26s proteasome. The 19s subunit is a large heteromeric structure which recognizes its cargo through the presence of ubiquitin, which canonically is conjugated in a chain by lysine residue 48 of the ubiquitin molecule (though monoubiquitination,

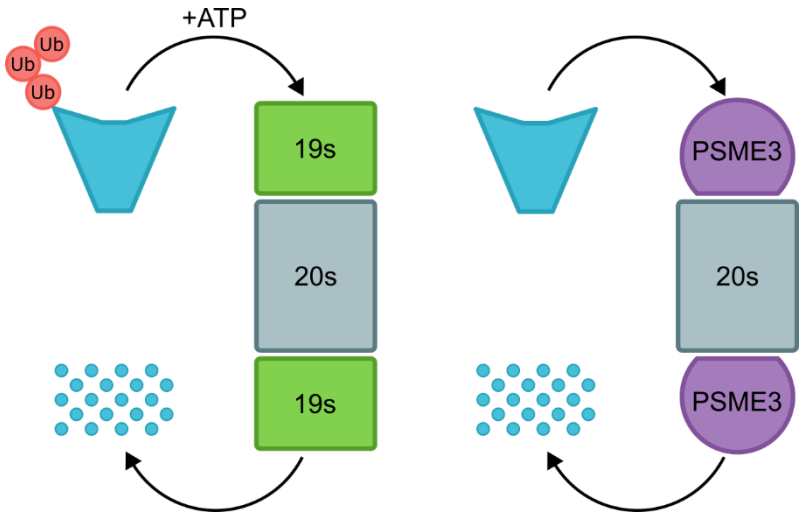

Figure 1.1: The Structure of the Proteasome. The proteasome is composed of both the catalytic 20s core responsible for protein degradation, as well as an adaptor subunit. The canonical cap, termed the 19s, is a large protein complex that recognizes cargo through the presence of a polyubiquitin chain and unfolds these target proteins using ATP prior to insertion into the 20s core. PSME3 is an alternative regulatory subunit and is distinct from the 19s cap in that it neither recognizes ubiquitin nor requires ATP to translocate its substrates into the 20s core.

SUMOylation, or the presence of intrinsically disordered domains may also serve as degradation cues) (Ben-Nissan and Sharon, 2014; Manohar et al., 2019; Son et al., 2023). This signal is recognized by one of several ubiquitin-binding protein components contained within the ring of the 19s subunit (Rousseau and Bertolotti, 2018). Through ATP hydrolysis, the target protein is unfolded and translocated into the 20s core, while several deubiquitinating components of the 19s simultaneously remove the conjugated ubiquitin chains (Majumder and Baumeister, 2019). This process is further aided by the capacity of the 19s subunit to allosterically stimulate the opening of the entry pore into the 20s core through a "key in a lock" mechanism through association of the C-termini of several 19s subunits with the alpha ring of the 20s core (Smith et al., 2007). The 19s-capped form of the proteasome represents, in most cell types studied, 30% of all cellular proteasome complexes by number, second only to the uncapped 20s, which represents 50% (Ben-Nissan and Sharon, 2014; Brooks et al., 2000; Fabre et al., 2013; Savulescu and Glickman, 2011; Tanahashi et al., 2000).

However, alternative regulatory caps of the proteasome have been found that do not rely on ATP for the unfolding and translocation of the target protein, or on ubiquitin for substrate recognition. The two major groups represented in this family are the PA28 proteins and PA200. PA200 is a large, monomeric protein found exclusively in the nucleus and has been found to be important for degradation of histones to facilitate repair after DNA damage, enable spermatogenesis, and maintain the stability of histone marks (Jiang et al., 2021; Qian et al., 2013; Z.-H. Zhang et al., 2020). Though the 19s subunit is the most observed cap in most cell types, PA200 has been shown to associate with 90% of proteasome complexes in testicular tissues, indicating a particularly specialized role (Qian et al., 2013; Ustrell et al., 2002). While the general mechanism for substrate recognition by PA200 is unclear, it is known to recognize

acetylated histones through its bromodomain (BRD)-like domain (Mandemaker et al., 2018; Qian et al., 2013). Further, PA200 possesses the ability to open the pore of the 20s core, as well as allosterically influence the character of its proteolytic activity from chymotrypsin-like to trypsin-like (Thomas et al., 2023).

Like the 20s, 19s, and PA200 subunits, the PA28 family of regulatory subunits was present in the ancestor common to all eukaryotes (Fort et al., 2015). However, this early organism possessed only a single ancient PA28 protein which was to undergo several duplications in jawed vertebrates. As such, mammals express three members of the PA28 family: PA28α (PSME1), PA28β (PSME2), and PA28γ (PSME3, though also known as 11s REGγ or Ki nuclear autoantigen). One likely hypothesis is that PA28γ (hereafter referred to as PSME3) represents the slow-evolving ancestral variant, and so retains the functions that that protein possessed, while PA28α and PA28β were freed to develop new roles (Fort et al., 2015).

PA28α and PA28β form a heteroheptamer commonly known as PA28αβ, which generally possesses a cytoplasmic localization (Thomas et al., 2023). Like the 19s subunit, PA28αβ can effect structural changes in the 20s core to elicit pore opening and substrate entry (Knowlton et al., 1997; Stadtmueller and Hill, 2011; Sugiyama et al., 2013; Whitby et al., 2000). While PA28αβ appears to have no intrinsic capacity to regulate the proteolytic properties of the 20s subunit (Sijts and Kloetzel, 2011), it possesses the ability to act as a "smart sieve" which only allows exit from the 20s core by peptides that are of the proper length for antigen presentation (Cascio, 2021; Raule et al., 2014). Further, its ability to stimulate the opening of the 20s pore can result in a 200-fold increase in peptide degradation rates (Realini et al., 1997; Thomas and Smith, 2022) and may be related to its ability to form a partially closed pore, bound by a highly flexible cap (Chen et al., 2021; S. C. Xie et al., 2019). Expression of PA28αβ is induced by exposure to

interferon-γ, which simultaneously elicits the expression of alternative catalytic beta subunits of the core 20s particle that display altered cleavage preferences and catalytic rates (Sijts and Kloetzel, 2011). As a result, the altered 20s/PA28αβ complex is also referred to as the immunoproteasome, as it appears especially well suited to the production of small antigenic peptides for presentation on major histocompatibility complex (MHC) Class-I molecules (Cascio, 2014; Li and Rechsteiner, 2001). Indeed, mice lacking PA28αβ show a 50% divergence from the repertoire of peptides presented by wild-type animals by MHC Class-I (Kincaid et al., 2011).

Compared to PA28αβ, the structure and function of PSME3 remains less well understood. PSME3 forms a homoheptamer that is found predominantly in the nucleus, but how it interacts with the proteasome and the effects thereof are unclear, and the plausible hypotheses are limited only by what has been discovered to be true for the other proteasome activators. Some studies suggest that PSME3 can alter the relative activities of the various proteolytic functions of the core proteasome similar to PA200, while other studies suggest that no such role exists, and that PSME3 instead stimulates the 20s core only by opening its pore to allow substrate entry (Thomas and Smith, 2022; Thomas et al., 2023). Others propose that, like PA28αβ, PSME3 may form a "smart sieve" to regulate the types of products that are able to leave the 20s core (Toste Rêgo and da Fonseca, 2019). The most recent results indicate that PSME3 stimulates the trypsin-like activity of the proteasome and, while it may open the pore, it likely does not act as a selective sieve. The lack of clear structural information on PSME3 association with the 20s subunit makes such research difficult, and only recent work has indicated that PSME3 may dock into the 20s subunit through association with its C-terminal domain in a manner similar to the PA28αβ complex (Chen et al., 2022; Jonik-Nowak et al., 2018). The means by which PSME3 recognizes

its substrates are similarly mysterious, as PSME3 has been documented to degrade such diverse proteins as p53, p21, SRC-3/AIB1, Smurf1, Oct-1, Hepatitis C virus core protein, and SARS-CoV-2 nucleocapsid protein (Thomas et al., 2023). Several of these known targets possess extensive intrinsically disordered domains, which may, however, suggest a potential mechanism for substrate recognition. Indeed, PSME3 was found to be capable of enhancing the degradation rates of unfolded proteins *in vitro*, and not their native counterparts (Frayssinhes et al., 2021).

1.2 PSME3 Biology

PSME3 Expression, Modification, and Localization

PSME3 is expressed ubiquitously throughout the body, though it is found in especially high levels in the brain, testes, and spleen (Noda et al., 2000; Yu et al., 2010). Curiously, only a small fraction of total cellular PSME3 was found to associate with the 20s proteasome in a survey of nine human cell lines (though has been documented to increase under conditions such as DNA damage and cancer progression), which is consistent with several potential proteasome-independent functions, as discussed below (Cascio, 2021; Fabre et al., 2014; Welk et al., 2016).

PSME3 is largely observed to possess a nuclear localization, which is due to its two nuclear localization signals (NLSs) (Cascio, 2021). The first, composed of amino acids KKRR at positions 85-88, likely represents a classical monopartite NLS recognized by the importin α/β pathway (Kosugi et al., 2009). The second NLS, found near the C-terminal at amino acids 243-246 and reading KRPR, is likely recognized by the same machinery, but appears to be dispensable for nuclear localization when the 85-88 NLS is present (Zannini et al., 2008).

Under certain circumstances, PSME3 may relocalize from the nucleus into various parts of the cytoplasm. In SH-SY5Y cells, hypertonic stress results in the formation of cytoplasmic PSME3-containing punctae, which also are associated with Bcl2-associated athanogene 2 (BAG2), Hsp70, and the 20s proteasome (Carrettiero et al., 2022). Whether this represents a

dynamic relocalization of PSME3 from the physiological state is unclear, as the localization of PSME3 under normal conditions was not shown in these cells.

A mechanism for the regulation of PSME3 localization has been discovered, though how generalizable it is and whether other mechanisms exist remain unknown. PSME3 can be SUMOylated by SUMO-1, -2, -3, or $p14^{ARF}$ (ARF) at residues including K6, K14, and K12, which results in its export from the nucleus into the perinuclear cytoplasm (Kobayashi et al., 2013; Wu et al., 2011). This alters its access to client proteins and allows it to degrade cytoplasmic cell cycle regulator p16 in mouse embryonic fibroblasts (MEFs). This relocalization also appears to regulate the stability of PSME3, as SUMOylated PSME3 was found to be rapidly degraded once in the cytoplasm.

Other post-translational modifications (PTMs) of PSME3 have been documented. Phosphorylation of PSME3 by mitogen activated protein kinase (MAPK)/extracellular-signal-regulated kinase (ERK) kinase kinase 3 (MEKK3) results in stabilization of PSME3 levels in Cos-7 cells through an unknown mechanism (Hagemann et al., 2003). Further, O-linked β-N-acetylglucosamine (O-GlcNAc) at serine 111 of PSME3 was found to promote its degradation of DEAD box polypeptide 6 (Ddx6), an RNA helicase required for the development of cytoplasmic processing bodies (P-bodies), which contain mRNA prior to their decay or release for translation (Pecori et al., 2021). Loss of this glycosylation mark was sufficient to stabilize Ddx6 and result in the exit of embryonic stem cells from their pluripotent state. Finally, acetylation of lysine 195 on PSME3 promotes its heptamerization, and mutation of this site impairs complex formation (Liu et al., 2013). The structural consequences for PSME3 of such modifications have not been uncovered, and how exactly they affect its function largely remains a mystery.

Five splicing variants have been discovered for PSME3 (Bethesda (MD): National Library of Medicine (US), National Center for Biotechnology Information, 1988). The best-studied isoform contains eleven exons and produces a protein of 254 amino acids long. It is the only variant to possess the long C-terminal domain known to be required for 20s proteasome interactions (Thomas et al., 2023). All other documented transcripts contain only a subset of these exons, with allowance for some truncations, except for exon 2, which is only present in three of the less-studied variants and notably absent in the main splicing isoform. The function of this additional exon is unclear, as are the functions of these lesser-known splicing variants.

PSME3 Functions

The first definitive demonstration that PSME3 is capable of mediating protein degradation in combination with the 20s subunit was performed with the steroid receptor coactivator-3 (SRC-3AIB1) in 2006 (Li et al., 2006). In the years since, several other degradation targets have been proposed. Several of these targets and their associated functions may be found in Table 1.1 (note that the criterion for inclusion in this table is a demonstrated stabilization of the substrate upon PSME3 loss rather than *in vitro* evidence of degradation).

Table 1.1: A non-exhaustive list of PSME3 degradation targets and their functions.
PSME3 Functions

Substrate Name	Substrate Function
p53 (Zhang and Zhang, 2008)	Induction of apoptosis, cell cycle arrest, or senescence
Smurf1 (Nie et al., 2010)	Degradation of BMP-Smad, Wnt and RhoA
Oct-1 (Fan et al., 2019)	Induction of transcription of scavenger receptor LOX-1 in macrophages
CK1ε (Chen et al., 2018)	Regulation of cell division, differentiation, and apoptosis
p16, p19, p21 (Chen et al., 2007)	Cell cycle regulation
MAFA (Kanai et al., 2011)	Regulation of lens development
SRC-3/AIB1 (Li et al., 2006)	Tumorigenesis-related gene transcription
GSK3β (L. Li et al., 2015)	Regulation of Wnt/β-catenin signaling
PTTG1 (Ying et al., 2006)	Coupling of sister chromatids before anaphase
HCV core protein (Moriishi et al., 2007)	Encapsulation of HCV genomic RNA
SARS-CoV2 nucleocapsid protein (H. Zhang et al., 2020)	Encapsulation of SARS-CoV2 genomic RNA
Klf2 (Sun et al., 2016)	Negative regulation of NF-κB
RBM3 (Xie et al., 2023)	RNA homeostasis
LHX2 (Gao et al., 2021)	Potentiation of Wnt signaling in stem cells
IκBε (Xu et al., 2016)	Sequestration of NF-κB away from chromatin
SirT1 (Dong et al., 2013)	Cellular deacetylation
PKAca (Liu et al., 2014)	Cell signaling
IFR8 (Zhou et al., 2020)	Myeloid cell maturation transcription
SMAD7 (Jiao et al., 2020)	TGF-β signaling antagonism
c-Myc (Chen et al., 2018)	Transcriptional activation
LATS1 (Wang et al., 2018)	Regulation of mitosis

The functions of PSME3 are just as diverse as its many degradation targets. Though, perhaps somewhat surprisingly, PSME3 is not an essential protein, and mice that lack PSME3 survive through development (Murata et al., 1999). However, several phenotypes become apparent. In line with PSME3's role in the degradation of several cell cycle regulators, mice lacking PSME3 have a stunted growth rate and reduced adult body mass compared to wildtype counterparts. A study of fibroblasts isolated from these animals revealed a reduced fraction of cells in S or G2/M phase of mitosis (Barton et al., 2004). This may be the result of a reduction in the length of S phase duration (Fesquet et al., 2021), though other studies in both human cancer cells and in Drosophila demonstrate an arrest at the G1/S transition upon PSME3 loss (Lei et al., 2020; Masson et al., 2001), which is plausibly the result of the stabilization of p21 (Chen et al., 2007; Li et al., 2007).

In addition to reduced growth rates, mice lacking PSME3 also experience a more rapid age-related decline in health. These mice show an earlier, more rapid loss of body mass, and increased mortality starting at 60 weeks of age, which is accompanied by an increase in signs of DNA damage (Li et al., 2013). These effects are generally understudied, but the authors of this work suggest that a global increase in p53 levels across bodily tissues may be responsible for the accelerated aging observed in these animals.

Despite early characterization of PSME3 KO mice as fully fertile (Barton et al., 2004; Murata et al., 1999), subsequent studies discovered that loss of PSME3 results in reduced sperm number and motility, potentially through and elevation of p53-mediated repression of Plzf expression, a protein necessary for the early stages of spermatogenesis (Gao et al., 2019). This finding recalls the observation that loss of another proteasomal cap PA200 results in similar failures in spermatogenesis. Indeed, concurrent loss of both PA200 and PSME3 result in

complete male infertility, a stronger phenotype than loss of either alone (Huang et al., 2016). While sperm are still produced in these double knock-out animals and retain the formal capacity to fertilize an egg, they exhibit remarkable motility defects. This is accompanied by high levels of oxidative damage markers and an increase in ubiquitin staining in sperm cells, indicating deficit in proteasomal function.

In line with its role as a negative regulator of both p53 and p21, PSME3 is upregulated in several forms of cancer. Indeed, upregulation of PSME3 has been associated with an increase in cell proliferation rates, migration rates, and invasive capacity in endometrial, thyroid, breast, and lung cancers, as well as renal carcinomas and multiple myelomas (Bhatti et al., 2019; Chen et al., 2018; Liu et al., 2018; Tong et al., 2020; Wang et al., 2015; Yi et al., 2017). In addition, PSME3 is a known negative regulator of the oncogenic proteins SRC-3/AIB1, a transcriptional coactivator capable of regulating cell proliferation and migration in myriad cancers (Li et al., 2006; Mao et al., 2008), and PTTG1, a mitotic checkpoint protein often overexpressed in thyroid cancer (Ying et al., 2006).

PSME3 levels have also been negatively correlated with rates of apoptosis. Fibroblasts derived from mice lacking PSME3 show an increase in rates of apoptosis (Murata et al., 1999), and a correlation has been established between PSME3 levels and susceptibility to apoptosis in several cancer lines (Cascio, 2021). This is potentially the result of an increase in caspase activity through increased levels of p53 in the absence of PSME3 (Moncsek et al., 2015).

Additionally, PSME3 appears to have a role in regulating immune function. Mice lacking PSME3 display a slightly reduced number of CD8+ T cells and a reduced ability to clear a pulmonary fungal infection but were found to have no alterations in antigen presentation by the MHC Class-I complex in a physiologically normal state (Barton et al., 2004; Murata et al.,

1999). Indeed, PSME3, unlike PA28αβ, reduces rather than increases the variability of peptides that are suitable for MHC Class-I presentation (Frayssinhes et al., 2021). Overexpression of PSME3 was found to reduce the presentation of tumor-associated antigens (TAAs) through destruction of pioneer translation products (PTPs) generated in the nucleus from nascent mRNAs (Boulpicante et al., 2020). Additionally, a positive feedback loop has been discovered between PSME3 and NF-κB in mouse macrophages in response to bacterial infection, such that PSME3 degrades KLF2, an inhibitor of NF-κB activity, which then in turn increases PSME3 expression. When PSME3 is lost, so is the positive interaction between PSME3 and NF-κB activity, thus weakening the host's immune response (Sun et al., 2016). Curiously, a separate study demonstrates a negative regulation of NF-κB by PSME3 in mouse macrophages of similar preparation; the cause for this discrepancy remains unclear (Yan et al., 2014). Nevertheless, the bulk of evidence appears to indicate a positive regulation of NF-κB by PSME3 (Liu et al., 2018; Yan et al., 2014).

However, degradation of KLF2 is not the only means PME3 possesses to regulate NF-κB signaling. PSME3 may also degrade NF-κB regulator IκBε, which sequesters NF-κB from the chromatin so it may not regulate transcription (Xu et al., 2016). This study was also performed in mice, but in intestinal crypt cells in mice treated with dextran sodium sulfate in an experimental model of colitis. This mechanism of regulation was later found to also occur in Leydig cells (T. Xie et al., 2019). Whether this additional regulatory mechanism occurs in mouse macrophages (where degradation rates of the closely related protein IκBα were unchanged by PSME3 loss) remains unclear (Sun et al., 2016).

Further functions continue to be attributed to protein degradation by PSME3, and enumeration of each of these functions will likely not shed light on any additional principles of

its function. Suffice it to say, PSME3 has been implicated in protecting against a high fat diet by elevating levels of SirT1 (Dong et al., 2013), regulate vascularization through degradation of PKAca and subsequent alteration of FoxO1 activity (Liu et al., 2014), promote aortic dissection by inhibiting RBM3 (Xie et al., 2023), and regulate the hair cycle by stabilizing Lgr5 in hair follicle stem cells (Gao et al., 2021). It is clear that PSME3 performs wide-ranging functions within the cell, many of which likely remain to be uncovered.

That said, the various functions ascribed to PSME3 seem to outnumber the sum of its degradation targets, and some functions have been attributed to PSME3 without the identification of a corresponding proteolytic event. For example, PSME3 localizes to sites of DNA damage and recruits both 20s and 19s proteasome components to facilitate DNA repair. As a result, loss of PSME3 sensitizes several cell types to radiation treatment (Levy-Barda et al., 2011; Zhu et al., 2024). Further, though no functional consequences for gene transcription or mRNA splicing were observed, loss of PSME3 has also been found to regulate promyelocytic leukemia protein (PML) body number (Zannini et al., 2009), alter nuclear speckle structure, and impair recruitment of splicing factors to sites of active transcription (Baldin et al., 2008), while an overexpression of PSME3 was shown to disrupt Cajal body structure (Cioce et al., 2006).

Indeed, some functions of PSME3 have been explicitly demonstrated to occur entirely independently of the 20s proteasome. For example, PSME3 has been shown to localize to the chromosomes in telophase and to be necessary for mitotic arrest following spindle damage (Zannini et al., 2008). As such, loss of PSME3 function was associated with aneuploidy, supernumerary centrosomes, and multipolar spindles in U2OS cells as well as primary fibroblasts from transgenic mice. Strikingly, the mitotic arrest phenotype can be rescued by expression of a PSME3 variant that can no longer associate with the 20s proteasome, thus

rendering it incapable of effecting protein degradation. A similar mutation was found to have no effect on PSME3's ability to regulate global heterochromatin compaction in conjunction with HP1β (Fesquet et al., 2021). We discuss the possibility of these proteasome-independent functions in the following section.

Mechanisms of PSME3 Action

As discussed earlier, information about the interactions between PSME3 and the 20s proteasome are sparse, and only in the last two years have high resolution protein structures been produced (Chen et al., 2021; Thomas et al., 2023). However, these studies have revealed a remarkable structural similarity between PSME3 and PA28αβ when bound to the core proteasome. Most functional knowledge about PSME3 interactions come indirectly from studies of these closely related proteins, and so a brief discussion of the structural similarities between the PA28 members becomes necessary (Zhang et al., 1998).

The structure of the PA28 monomers (including PSME3) consists of four alpha-helices of 33-45 residues in length (Knowlton et al., 1997). The C-terminal tails (considered to be somewhere between 10 and 14 residues in length) of each monomer tucks into the outer surface of the 20s proteasome to mediate binding (Cascio, 2021; Fesquet et al., 2021; Ma et al., 1993; Smith et al., 2007; Stadtmueller and Hill, 2011). The linker region between helices one and two contains a highly disordered linker region not resolved by crystallography (Rechsteiner et al., 2000), while the highly conserved region between helices two and three, termed the "activation loop," is necessary for proteasome activation (namely, gate opening) (Cascio, 2021; Zhang et al., 1998).

The discovery of this activation loop was the result of a mutagenesis study performed on PA28α (Zhang et al., 1998). While many point substitutions are sufficient to abrogate 20s-binding capacity of PA28α, a specific mutation in the activation loop, N146Y, had no effect on

20s-binding but destroyed all proteasome-activation properties of PA28α in a dominant-negative fashion. A similar mutation in PSME3, N151Y, was found to produce a similar disruption of proteasome activation without impairing PSME3's physical association with the 20s core. Also of note was the observation that mutations in the homolog-specific insert region were found to be dispensable both for oligomerization of PA28α and its activation of the proteasome. A further mutation near the end of helix three, K188E/D, was found to generate a hyperactive PSME3 variant which could stimulate not only the trypsin- but also the chymotrypsin-like activity of the 20s core (Li et al., 2001). Whether this helix is the region that mediates the long-range allosteric interactions necessary for the physiological stimulation of the core particle's trypsin-like activity is unclear, and requires additional biophysical evidence (Thomas and Smith, 2022).

These mutations have been used as a toolkit to investigate the various functions of PSME3. For example, in the investigation of degradation of SRC-3/AIB1, it was found that overexpression of the N151Y mutant was unable to induce degradation of this target protein (Li et al., 2006). While it is firmly established that asparagine 151 is critical for activation of the proteasome, and therefore necessary for PSME3-mediated protein degradation, it has recently been discovered that PSME3 may perform several proteasome-independent functions. For example, it was found that PSME3 mutations in the activation loop G150S and N151Y (both of which render the protein unable to activate, but still able to bind the proteasome) or mutation at the C-terminal residue P245Y (which abrogates proteasome binding entirely) had no effect on PSME3's ability to degrade p53 (Zhang and Zhang, 2008). Instead, PSME3 was found to facilitate the interaction of MDM2 and p53 through its homolog specific insert region. MDM2 is thereby able to ubiquitinate p53 and induce its degradation by the canonical 26s proteasome. In a similar, though less thoroughly investigated example, mutations either at N151Y or K188D (the

hyperactive mutant) were sufficient to alter the degradation rates of known PSME3 target p21 but have no effect on degradation of MAFA (Kanai et al., 2011). In a separate study, it was found that deletion of the final fourteen amino acids at the C-terminal, a manipulation akin to mutation at P245, has no effect on PSME3's ability to regulate the compaction of H2B histones in heterochromatic regions (Fesquet et al., 2021). It is therefore likely that PSME3 may serve many additional functions independent of its ability to directly activate the proteasome.

A function for proteasomal activators independent of protein degradation is not without precedent. The 19s cap has been shown to remodel the multifunctional co-activator complex SAGA through a 20s-independent mechanism, and instead likely employs only its chaperone-like activity to achieve this goal (Lim et al., 2013). Further, mutations of the 19s are sufficient to induce transcriptional defects in basic *in vitro* systems derived from yeast cell extracts (Ferdous et al., 2001). Other examples of proteolysis-independent functions of the 19s cap have been described, including processing of the Gal4 transcription factor in yeast, though the absence of the 20s complex has not been definitively established (McCann and Tansey, 2014).

Altogether, while these results firmly indicate that PSME3 may associate with the 20s proteasome to mediate protein degradation, this is not its sole mechanism of action. What the mechanism of these functions may be is uninvestigated, though may conceivably be through chaperone or scaffold-like activities.

1.3 The Proteasome and Transcription

The 26s Proteasome in Transcription

Despite being possessed of several nuclear-specific regulatory subunits, the canonical 26s proteasome, often restricted to the cytoplasm in conception, may be found in the nucleus as well, and the varied challenges that face the transcriptional system provide ample opportunity for contribution by this versatile complex (Geng et al., 2012).

Indeed, discovery of proteasomal subunits at active transcriptional complexes predated the characterization of the subunits themselves (McCann and Tansey, 2014). A mutation in a component of the 19s cap, termed Sug1 (also known as PSMC5), was found to act as a suppressor for a C-terminal deletion of the Gal4 gene in yeast (Swaffield et al., 1992). Sug1 was soon found in a preparation of RNA pol II (RNAPII) holoenzyme and was therefore considered to be a component thereof (Kim et al., 1994). It was only after this fraction was further found to copurify with a protein fraction containing proteolytic activity that it was identified as a component of the 26s proteasome (Rubin et al., 1996). Despite not serving as a core component of the RNAPII holoenzyme, following studies showed a clear relationship between levels of transcription and presence of the proteasome. Induction of the Gal1-10 promoter in yeast rapidly recruits PSMC5 not only to the promoter where Gal4 binds, but also the entire length of the gene body (Geng and Tansey, 2012). Furthermore, cessation of transcription results in rapid dissociation of the proteasome from the gene. This phenomenon appears to be generalizable, as transcriptional activity in yeast appears to be positively correlated with proteasome binding at a genomic level (Auld et al., 2006).

Proximity alone does not imply function, though important roles for the 26s proteasome in the regulation of transcription have since been uncovered, and certainly protein degradation by the proteasomal is a central component. Proteasomal inhibition results in global increases in ubiquitination of chromatin-bound proteins by 80% (Catic et al., 2013). These changes are especially enriched near transcriptional start sites and appear to be critical for proper regulation of transcription. Inhibition of the proteasome for six hours results in an 8.1-fold increase in log 2 gene expression variance, revealing the importance of protein turnover at the chromatin.

Several degradation targets of the 26s proteasome at the chromatin have been identified and studied in detail. In line with its association with active promoters, the 26s proteasome is involved in regulation of transcriptional activation. Glucocorticoid receptors are rapidly cycled at the chromatin through the combined action of chaperones and the proteasome, which serve to finely tune their transcriptional activity (Stavreva et al., 2004). Further, the valence of transcription factor activity, determined by their association with different co-activators, is subject to proteasomal regulation. Association of the LIM homeodomain (LIM-HD) transcription factors with cofactor of LIM-HD proteins (CLIM) cofactors repress their transcriptional activation function. CLIM factors may be degraded by the 26s proteasome, altering LIM-HD-activated gene expression (Ostendorff et al., 2002). Finally, transcriptional activators, such as Gal4, may require proteolytic processing by the 26s proteasome before they are capable of activating transcription (Lipford et al., 2005; McCann and Tansey, 2014).

While proteasomal inhibition does not universally impede transcription, there may still exist a role for it in the regulation of transcriptional initiation, elongation, and termination. The 26 proteasome may be recruited to the transcriptional elongation complex, and mutations in the 19s subunit result in impaired displacement of histones ahead of the advancing RNA polymerase complex (Chaves et al., 2010; Pan et al., 2013). Further, inhibition of the proteasome may cause the polymerase complex to ignore transcriptional termination sites (Gillette et al., 2004). Finally, though evidence for a common mechanism is lacking, inhibition of the proteasome or mutation of the 19s subunit may result in changes in deposition of repressive histone marks, having an additional effect on transcription patterns (Ezhkova and Tansey, 2004).

PSME3 and Transcription

Just as the importance of the 26s proteasome in the regulation of transcription is well-established, examples of PSME3 performing similar function are abundant. PSME3 is

documented to degrade many transcription factors and their regulators (see table 1.1). Particularly well-studied are the gene expression changes that occur downstream of PSME3's regulation of NF-κB, which regulates expression of CRAMP and iNOS in macrophages in response to an immune challenge, and cytokines in colon epithelial cells in response to dextran sulfate treatment (Sun et al., 2016; Wang et al., 2018; Xu et al., 2016). Other changes in gene expression resulted from the study of PSME3's regulation of SMAD signaling molecules, LGR5, FOXO1, RBM3, NF-κB, LHX2, IRF8, c-Myc, PKA, SRC-3/AIB1, and p53 (Gao et al., 2021; Jiao et al., 2020; Liu et al., 2014; S. Li et al., 2015; Li et al., 2006; T. Xie et al., 2019; Xie et al., 2023; Yan et al., 2014; Zhang and Zhang, 2008; Zhou et al., 2020). Additionally, loss of PSME3 in several cancer types resulted in the altered expression of several markers of aggressiveness, including E-cadherin, N-cadherin, vimentin, and other EMT transcription factors, wherein a degradation target was not specifically identified (Bhatti et al., 2019; Tong et al., 2020; Yi et al., 2017).

However, beyond the regulation of the levels of specific transcription factors, evidence for a more generalized regulation of gene expression by PSME3 is lacking. Indeed, PSME3 was shown to be critical for global compaction of heterochromatin and the nuclear speckle (Baldin et al., 2008; Fesquet et al., 2021), but depletion of PSME3 in stable cell lines had no effect on the splicing of several endogenous or exogenously expressed genes (Baldin et al., 2008). Further, global levels of 5-fluorouracil (5-FU) incorporation, a measure of bulk transcription, were unaffected by either an increase or decrease in PSME3 abundance (Baldin et al., 2008; Cioce et al., 2006), suggesting that a loss of PSME3-mediated chromatin compaction does not translate to changes in gene expression. Of course, several published examples of instances where PSME3 does not influence the mRNA level of several select genes exist, though this evidence is naturally

quite fragmentary (Dong et al., 2013; Liu et al., 2018). As no global study of the expression of individual genes had been performed, generalized conclusions could not yet be made.

1.4 The Proteasome and Differentiation

The specification of cell identity, by which a stem cell acquires the characteristics to carry out the specialized functions of any tissue in the body, requires a major restructuring of many cellular systems, including gene expression patterns (Strober et al., 2019). Unsurprisingly, the proteasome, with its generalized function in proteostasis and specialized role in regulating gene expression, is widely implicated as an important factor for cellular differentiation (Ashok et al., 2024; Bax et al., 2019; Dasuri et al., 2011; Konstantinova et al., 2008; Leng et al., 2019; Pinto et al., 2016; Podenkova et al., 2023; Schröter and Adjaye, 2014; Uyama et al., 2012).

The study of PSME3, specifically, in differentiation remains in its incipient stages. In one study, PSME3 was found to degrade transcription factor IRF8 in dendritic cells, such that loss of PSME3 resulted in an increase in surface expression integrin αvβ8, a consequent increase in active TGF-β1, and a polarization of Th17 cells towards a non-inflammatory identity in an experimental autoimmune encephalomyelitis (EAE) model (Zhou et al., 2020). In another study, PSME3 promoted osteogenic differentiation and inhibited adipogenic differentiation of bone marrow stromal cells (BMSCs) through interaction with Wnt5α and activation of the Wnt/β-catenin signaling pathway (Chen et al., 2024). Beyond these studies, the role of PSME3 in differentiation remains uninvestigated. Additionally, due to its diverse functions in cellular physiology, it remains a ripe target for research.

To better understand the role of PSME3 in differentiation, we sought to investigate its function in the development of muscle tissue. The functional, contractile unit of skeletal muscle is the muscle fiber, which is embedded in a network of connective tissue (Sousa-Victor et al., 2022). The muscle fiber is syncytial, and contains many post-mitotic nuclei contained in a

common cytoplasm filled with myofibrils, which are in turn composed of many contractile sarcomeric subunits in series. As with any post-mitotic tissue, maintenance over time is a major challenge, and the daily stressors placed upon the mechanically active cells make them no exception. To combat regular damage, embedded in the surrounding basal lamina is a population of reserve stem cells, known in their quiescent state as satellite cells.

In response to damage to the muscle fiber, satellite cells exit their niche and reenter the cell cycle (and now are termed myoblasts), coincident with expression of the E-box binding protein Myogenic Differentiation (MyoD) (Zammit, 2017). MyoD drives expression of many proteins including the transcription factor myogenin, which coordinates with MyoD to drive cell cycle exit and subsequent terminal differentiation, while a portion of the population retains its stem cell potential and enters once more a quiescent state, such that the stem cell population is maintained.

We chose to study the muscle, in part, because an amenable cell model is readily available: the C2C12 myoblast cell line. C2C12 cells are a subclone of the parental strain C2, which was originally isolated from the thigh muscle of a 2-month-old female C3H mouse donor 70 h after a crush injury (Blau et al., 1983; Yaffe and Saxel, 1977). C2C12 cells express MyoD and divide rapidly in culture until they reach confluency. In conjunction with a withdrawal of serum, the cells will then begin to express myogenin, exit the cell cycle, and spontaneously form myotubes, which resemble those found within the muscle tissue in a living animal. In our study, we find an important role for PSME3 in the development of myotubes by C2C12 cells. In the search for a mechanism, we uncover an interesting interaction of PSME3 with two proteins during differentiation: the RNAPII interactor Regulation of Nuclear Pre-MRNA Domain Containing 1A (RPRD1A) and nuclear distribution C (NudC), a co-chaperone of the Hsp70/90

system. We discuss the existing body of knowledge concerning these two proteins in the following sections.

1.5 RPRD1A

RPRD1A (also known as p15-related sequence, or p15RS) and the closely related protein RPRD1B (also known as cell cycle-related and expression elevated protein in tumor, or CREPT) are regulators of the RNAPII complex that are likely mammalian orthologues of the ancestral protein Rtt103 in budding yeast (Li et al., 2021). These proteins share approximately 80% of their sequence with one another, and both possess a C-terminal coiled-coil terminus (CCT) important for dimerization. Both RPRD1A and RPRD1B are expected to form dimers, a process which enhances their affinity for the RNAPII CTD (Ni et al., 2014). RPRD1A and RPRD1B may also heterodimerize with one another, though the biological function of the heterodimer remains unclear. Additionally, both RPRD1A and RPRD1B possess a C-terminal domain (CTD)-interacting domain (CID) at their N-terminal region, which allows for association of the proteins with the long C-terminal tail of Rpb1, the largest subunit of RNAPII (Li et al., 2021).

Rpb1 is a member of and possesses the major catalytic activity of RNAPII, and is endowed with a long CTD, composed in mammals of 52 repeats, 21 of which adhere to an approximate consensus sequence of $Y_1S_2P_3T_4S_5P_6S_7$, and 31 of which diverge therefrom (Chapman et al., 2008). These residues undergo extensive modification during transcription, and serve to recruit various effector proteins, such as histone modifiers and chromatin remodelers throughout initiation, elongation, and termination, as well as processing enzymes required for 5’ capping, splicing, and polyadenylation (Spain and Govind, 2011).

While a full review of the tremendous body of research on elucidating these modifications is beyond the scope of this work, I will construct here a simple model that will suffice for our purposes. In general, as RNAPII progresses from the promoter through the gene

body, phosphorylation of Ser5 is gradually exchanged for that of Ser2 (Hsin and Manley, 2012). Additionally, Lys7, which may be found in eight of the non-consensus repeats, is mono- and dimethylated near promoters. These marks are gradually exchanged for Lys7-Ac in the gene body (Dias et al., 2015). Lys7-Ac is found in 80% of actively transcribed genes where it peaks +500 bp downstream of the transcriptional start site (TSS) (Schröder et al., 2013), and mutation of all eight lysine residues in the Rpb1 CTD results in broad defects in gene expression (Simonti et al., 2015).

In the most recently proposed model, acetylation of Lys7 recruits RPRD1A and RPRD1B via their CIDs to the CTD of Rpb1 shortly after the initiation of transcription (Ali et al., 2019). RPRD1A/B function as scaffolds for the recruitment of RPAP2 (Ni et al., 2014), a phosphatase that targets Ser5P for dephosphorylation, as well as HDAC1, which targets Lys7-Ac for deacetylation. The concomitant emergence of Ser2P as levels of Lys7-Ac are reduced likely serves to maintain RPRD1A/B recruitment throughout transcriptional elongation (Ali et al., 2019; Ni et al., 2014). Thus, while enriched in the promoter, RPRD1A/B can be found throughout the entire gene body of actively transcribed genes (Lu et al., 2012; Ni et al., 2011). While depletion of RPRD1B in NIH3T3 cells results in a very modest change in gene expression (Ali et al., 2019), its loss in regenerating intestinal crypt cells of mice results in marked changes in gene expression (Yang et al., 2021).

A separate suite of functions in regulating Wnt signaling have been attributed to RPRD1A and RPRD1B, but which has yet to be married to a biochemical description of RNAPII CTD binding (Li et al., 2021). Wnt signaling results in the nuclear accumulation of beta catenin where it frees T cell-specific factor (TCF) from its inhibitors which can then recruit histone acetylase p300 to activate the expression of target genes (Clevers, 2006; Daniels and Weis,

2005). In the absence of Wnt signaling, RPRD1A associates with TCF at the promoter to prevent its formation of a complex with beta catenin and additionally recruits HDAC2 to deacetylate the target gene (Liu et al., 2015). Once stabilized by Wnt signaling, beta catenin can sequester RPRD1A away from the promoter region, allowing TCF to activate gene expression (Wu et al., 2010). Of note, homodimerization is required for the inhibitory effect of RPRD1A on Wnt signaling, suggesting that this function may involve less cooperation between the two proteins than regulation of RNAPII's CTD (Fan et al., 2018). Indeed, RPRD1B appears to have a role opposed to RPRD1A in the context of beta catenin signaling, Wnt stimulation induces the recruitment of RPRD1B to the promoters of Wnt target genes where it stabilizes the TCF and beta catenin complex and enhances its association with the promoter, facilitating the recruitment of chromatin modifiers such as p300 (Zhang et al., 2014).

1.6 NUDC

NUDC was originally identified through a screen in the filamentous fungus *A. nidulans*, where it was found to be responsible for the migration of nuclei into the mycelium after mitosis (Osmani et al., 1990). Subsequent functional studies revealed that point mutation L279P of NudC resulted in the decrease of a putative client protein lissencephaly protein 1 (LIS1), a protein known to regulate the activity of the dynein motor. It became clear from this study that NudC acts to stabilize LIS1 through interacting with HSP90 and serving as a co-chaperone (Zhu et al., 2010).

Protein folding is a complex, active process mediated by many proteins, of which Hsp90 is only one part. Indeed, while Hsp90 is central to the processing of many protein clients, it normally mediates only the final stages of folding (Morán Luengo et al., 2018; Rosenzweig et al., 2019). Earlier steps are mediated by the more promiscuous Hsp70, which in turn both receives its cargo from and has its folding activity stimulated by the class of co-chaperones

known as Hsp40s (Rosenzweig et al., 2019, 2017). As might be expected, a major issue in protein folding is the proper transfer of cargo from one chaperone complex to the next. The Hsp70-Hsp90 organizing protein (Hop) is a well-studied co-chaperone known to facilitate the transfer of proteins between Hsp70 and Hsp90 under certain contexts (Wegele et al., 2006). However, it appears to only be necessary for the folding of a small subset of proteins, suggesting the presence of other transfer proteins (Sahasrabudhe et al., 2017). Indeed, NudC fulfills the same function, and does so through interaction sites independent of that used by Hop (Biebl et al., 2022).

While an interaction with the Hsp90 complex would position NudC to regulate a wide range of cellular functions, the number of roles attributed to NudC are still limited. Indeed, because of its original association with LIS1 and the dynein system, many studies of NudC concern themselves with this function. NudC has since been shown to interact with both dynein and dynactin and be important for both anterograde transport on microtubules and cell migration (Aumais et al., 2001; Islam et al., 2020; Yamada et al., 2010). It additionally appears to be important at other microtubule structures, including the microtubule organizing center (MTOC) where it plays an important role in chromosome segregation (Aumais et al., 2001; Zhou et al., 2003), and at the primary cilium where NudC regulates ciliary length and number (Zhang et al., 2016). Other studies have examined its function outside of the context of microtubules, where it has been found to play an organizing role in the actin cytoskeleton as well. NudC localizes to the leading edge of migrating RPE-1 cells where it stabilizes cofilin 1 and filamin A, and its loss results in reduced rates of cell migration (Liu et al., 2021; Zhang et al., 2016).

The proteasome and chaperone system share similarities not only for their central role in maintaining proteostasis but also face similar challenges in altering the secondary structures of

their client proteins. As such, one might easily imagine interactions between these systems. For example, proteins that are improperly folded by the chaperone system would require prompt degradation by the proteasome (Esser et al., 2004). Unsurprisingly, the involvement of the chaperone system in protein degradation is widespread, and the Hsp70/90 system has been shown to be necessary for the degradation of misfolded proteins in many contexts (Abildgaard et al., 2020; Jawed et al., 2022).

Many proteins are known to mediate the release of unfolded cargo from chaperones such as Hsp70, though direct mediators between the chaperone and proteasome system remain less well-studied (Abildgaard et al., 2020). Of interest, however, is the Bcl2-associated athanogene (BAG) family of proteins, as well as the protein carboxyl terminus of HSC70-interacting protein (CHIP). CHIP may interact directly with Hsp70 and ubiquitinate its cargo (McDonough and Patterson, 2003). BAG-1 then binds the Hsp70/cargo/CHIP complex through its C-terminal BAG domain and, through its N-terminal UBL domain, associate with the 19s particle of the 26s proteasome (Abildgaard et al., 2020). This binding event leads to release of the cargo by stimulating nucleotide exchange of Hsp70 and the cargo's degradation by the proteasome. The closely related protein BAG-6 likely does not interact with Hsp70 but rather acts as a chaperone in a separate complex for proteins destined for membrane insertion (Ganji et al., 2018). If the cargo is unfit for such a purpose, it is ubiquitinated, and the BAG-6 complex directly associates with the 19s particle of the proteasome to release its cargo for degradation (Minami et al., 2010).

Interestingly, BAG-2 has been found alongside PSME3 in cytoplasmic condensates under conditions of cellular stress (Carrettiero et al., 2022). BAG-2 mediates nucleotide exchange of Hsp70, similarly to BAG-1 (Qin et al., 2016). However, unlike BAG-1, BAG-2 inhibits the ubiquitination activity of CHIP, which has unknown consequences for protein degradation. The

discovery of these proteins in association with both PSME3 and the 20s proteasome indicate that the interactions between the proteasome and chaperone system may not be mediated by the 19s particle alone. How NudC situates itself among these interactions remains uninvestigated.

Rationale and Hypotheses

PSME3 is a non-canonical regulatory cap of the proteasome with well-established importance in aging, tumorigenesis, and cell signaling. Several facets of its activities remain investigated, however, and remain ripe areas of research. Despite PSME3's capacity to organize diverse nuclear structures such as heterochromatin, nuclear speckles, and Cajal bodies, little evidence has been collected on whether these have a functional consequence for the cell. Indeed, studies of gene expression are inconclusive due to a lack of untargeted assays, and whether PSME3 serves a similar function in transcription as the canonical proteasome remains unknown. Furthermore, despite being regarded as a regulatory cap of the 20s proteasome, only a small fraction of the total cellular PSME3 population forms such an association. Indeed, recent studies have demonstrated that PSME3 performs several proteasome-independent functions through unknown mechanisms. Given the rate at which new functions are ascribed to PSME3, and the apparent diversity of means by which it achieves them, it is important to both enrich our image of PSME3 activity and to reconcile existing differences within the field.

Our work seeks to achieve just that. To investigate new areas of PSME3 function, we utilize the C2C12 myoblast cell line, which can be differentiated *in vitro* into post-mitotic, syncytial myotubes. This allows us to investigate PSME3 activity not only in cells under physiological conditions, but also those of dynamic reorganization. In this study, we examined the localization, function, and interaction partners of PSME3 in C2C12 myoblasts prior to differentiation, as well as at days 0, 1, 2, and 3 of differentiation. We hypothesized that PSME3

would occupy several euchromatic regions in the chromatin and might thereby possess generalized gene-regulatory functions.

In **Chapter 2**, we test the association of PSME3 with the chromatin in undifferentiated C2C12 myoblasts, as well as those after 2 days of differentiation that have formed nascent myotubes. We further identify novel PSME3 binding partners through immunoprecipitation and test the impact of PSME3 depletion on gene expression over differentiation.

In **Chapter 3**, we investigate the impact of PSME3 loss on both cell migration rates and myogenesis and seek to understand the mechanism by which these functions are performed.

In **Chapter 4**, we synthesize our findings and discuss potential mechanisms for regulation of myogenesis by PSME3, as well as identify several experiments that will help resolve the remaining puzzles.

Chapter 2 PSME3 Dynamically Associates with Active Genes During Myogenesis

2.1 Abstract

Cellular differentiation requires large-scale changes in nuclear organization to accommodate an accompanying change in gene expression (Bitman-Lotan and Orian 2021; Dixon et al. 2015). PSME3 has been shown to both associate with and mediate the compaction of constitutively heterochromatic regions. Despite this global role in genome organization, scant evidence exists of a similarly global role for PSME3 in gene regulation. Here, we perform the first global, unbiased examination of chromatin binding by PSME3, which we show to bind extensively to highly active promoters in undifferentiated cells. Further, we identify the RNAPII-modifier RPRD1A as an PSME3 interacting partner, through which its association with chromatin may be mediated. Finally, we show that loss of PSME3 has no global effect on gene expression and is dispensable for this component of the differentiation process.

2.2 Introduction

The acquisition of cellular identity through differentiation requires the coordinated restructuring of diverse cellular systems. Even the differentiation of myoblasts, a relatively limited type of stem cell, into myofibers involves the altered expression of thousands of genes (Zheng et al., 2023). How such changes are brought about and sustained remains an active area of study.

The role of the proteasome in regulating gene expression has long been recognized. Indeed, a component of the proteasome, Sug1 (also known as PSMC5), was originally believed to be a component of the RNAPII holoenzyme due to its association with highly active gene regions (Geng and Tansey, 2012). Subsequent studies revealed a generalized role for the proteasome in transcription factor processing, transcriptional initiation, and histone displacement ahead of RNAPII (Geng et al., 2012; Rubin et al., 1996). Many of these functions have been attributed to the ability of the proteasome to recognize and degrade ubiquitinated proteins, as mediated by the proteasomal regulatory cap complex, termed the 19s subunit. This complex both recognizes ubiquitin and unfolds target proteins for

translocation into the proteolytic 20s core for degradation. However, alternative regulatory caps, such as PSME3, have been shown to possess similarly important roles in nuclear dynamics (Cascio, 2021).

PSME3 has been shown to degrade several important regulators of the cell cycle including p16, p19, and p21, transcriptional regulators such as c-Myc, Klf2, SMURF2, and LATS1/2, and to indirectly mediate degradation of p53 regulator MDM2 (Chen et al., 2018; S. Li et al., 2015; Li et al., 2007; Nie et al., 2010; Sun et al., 2016; Wang et al., 2018; Zhang and Zhang, 2008). Because of these functions, loss of PSME3 is associated with G1 arrest in cultured cells (Chen et al., 2017; Masson et al., 2001) as well as impaired growth rates of mice lacking PSME3 (Barton et al., 2004; Murata et al., 1999). Conversely, PSME3 is often overexpressed in various cancer cell lines, which results in increased replication rates, metastatic potential, and reduced rates of apoptosis (Lei et al., 2020; Mao et al., 2008). In addition, organization of diverse nuclear structures such as the nuclear speckle (Baldin et al., 2008), Cajal body (Cioce et al., 2006; Jonik-Nowak et al., 2018), promyelocytic leukemia body (Zannini et al., 2009), as well as densely packed heterochromatin (Fesquet et al., 2021) have been linked to PSME3 function. Though PSME3 is often understood to work through the degradation of target proteins in conjunction with the core 20s proteasome, several of its functions occur in the absence of such an association, as only a small fraction of cellular PSME3 is associated with the proteasome (Cascio, 2021; Fabre et al., 2014; Welk et al., 2016). Though the mechanism for these interactions remains unclear, PSME3 can induce mitotic arrest, regulate p53 levels, and maintain global heterochromatin compaction in conjunction with HP1β even when prevented from interacting with the proteasome (Fesquet et al., 2021).

Despite the extensive functions that PSME3 performs in the regulation of nuclear dynamics, a comprehensive study of both its DNA binding capacity and its role in global gene expression have yet to be performed. There exist, however, some limited pieces of evidence that suggest the extent of PSME3's activity. First, PSME3 was found to associate with all four constitutively heterochromatic regions, and only one of four actively transcribed genes as tested by ChIP-qPCR (Fesquet et al., 2021). Second, loss of PSME3 was found to have no effect on bulk incorporation of 5-FU, indicating it has no effect on global rates of transcription (Baldin et al., 2008), though PSME3 has been shown to affect expression of

individual genes when overexpressed in cancer cells as measured by qPCR (Bhatti et al., 2019; Tong et al., 2020; Wang et al., 2015; Yi et al., 2017). An unbiased and comprehensive examination of these two behaviors would be of great interest for better understanding PSME3 function.

In C2C12 myoblasts, withdrawal of serum induces the fusion of mononucleated myoblasts into syncytial myotubes that can support spontaneous contraction, which we use to interrogate multiple stages of differentiation. In this study, we find that PSME3 binds to highly active promoter regions at the chromatin in undifferentiated C2C12 cells. PSME3-bound regions are almost exclusively co-positive with active promoter marker H3K4me3, and PSME3 is found at roughly 20% of all H3K4me3 sites. Strikingly, PSME3 becomes undetectable at the chromatin by the second day of differentiation, suggesting a dynamic regulation of its binding. Co-precipitation experiments revealed an association with the RNAPII regulator RPRD1A, which may facilitate the interaction with RNAPII. However, this interaction lacks an apparent function in differentiating cells, as loss of PSME3 has no global effect on gene expression as measured at several points across differentiation.

2.3 Results

PSME3 Binds to Highly Active Promoters Prior to Differentiation

Previous studies have established a role for PSME3 in maintaining the integrity of a variety of nuclear structures (Baldin et al., 2008; Cioce et al., 2006; Fesquet et al., 2021). In particular, PSME3 was found to associate with heterochromatic regions to maintain their compacted state. However, an unbiased study of PSME3's chromatin binding activity has yet to be performed. We therefore sought to extend this work by investigating binding of PSME3 to genomic regions across differentiation.

To test whether PSME3 associates with chromatin in C2C12 myoblasts, we performed Cleavage Under Targets & Release Using Nuclease (CUT&RUN) against the endogenous population of PSME3. Surprisingly, we found that PSME3 associates extensively with the chromatin at over 5,000 distinct regions in cycling myoblasts (Figure 2.1 A and B). A large majority of these peaks were found to be co-positive for the active promoter mark H3K4me3. Furthermore, an analysis of PSME3 binding sites revealed an even stronger preference of PSME3 for promoter-proximal regions (<= 1kb) than H3K4me3,

largely at the expense of binding to gene bodies or intergenic regions (Figure 2.1 C). Genomic regions positive for PSME3 were subjected to motif analysis to identify putative PSME3 binding sites (Figure 2.1 D). Among these binding sites, three highly enriched sequences were discovered, the first of which is identical to a fraction of the GC box sequence (Kedar et al., 1991). Additionally, RNA sequencing was performed on dividing C2C12 myoblasts, and the results were correlated with the peaks discovered by CUT&RUN. We found that, of all transcriptionally active promoters, those bound by PSME3 are on average roughly 50% more active than those that lack PSME3 (Figure 2.1 E). Taken together, PSME3 possesses broad DNA binding abilities with a particular preference for highly active gene promoter regions.

Figure 2.1: PSME3 Binds to Highly Active Promoters Prior to Differentiation. **A**) CUT&RUN was performed in cycling C2C12 cells using antibodies targeting PSME3 or H3K4me3 to measure their position on the chromatin. Three biological replicates were performed and represented here together. **B**) Peaks were called using MACS2 for both PSME3 and H3K4me3, and their coincidence was measured. **C**) Both PSME3 and H3K4me3 CUT&RUN peaks were annotated with ChIPseeker for the type of region in which they reside. **D**) PSME3-bound sequences were subjected to motif analysis by MEME-ChIP. The top three enriched binding motifs are shown here. **E**) RNA sequencing was performed on cycling C2C12 cells. Genes that possess a PSME3 peak were separated from those that did not, and expression levels were analyzed. Three biological replicates per condition; analyzed with Welch two sample t-test; displayed here as a median and quartile plot with the mean indicated by a red point.

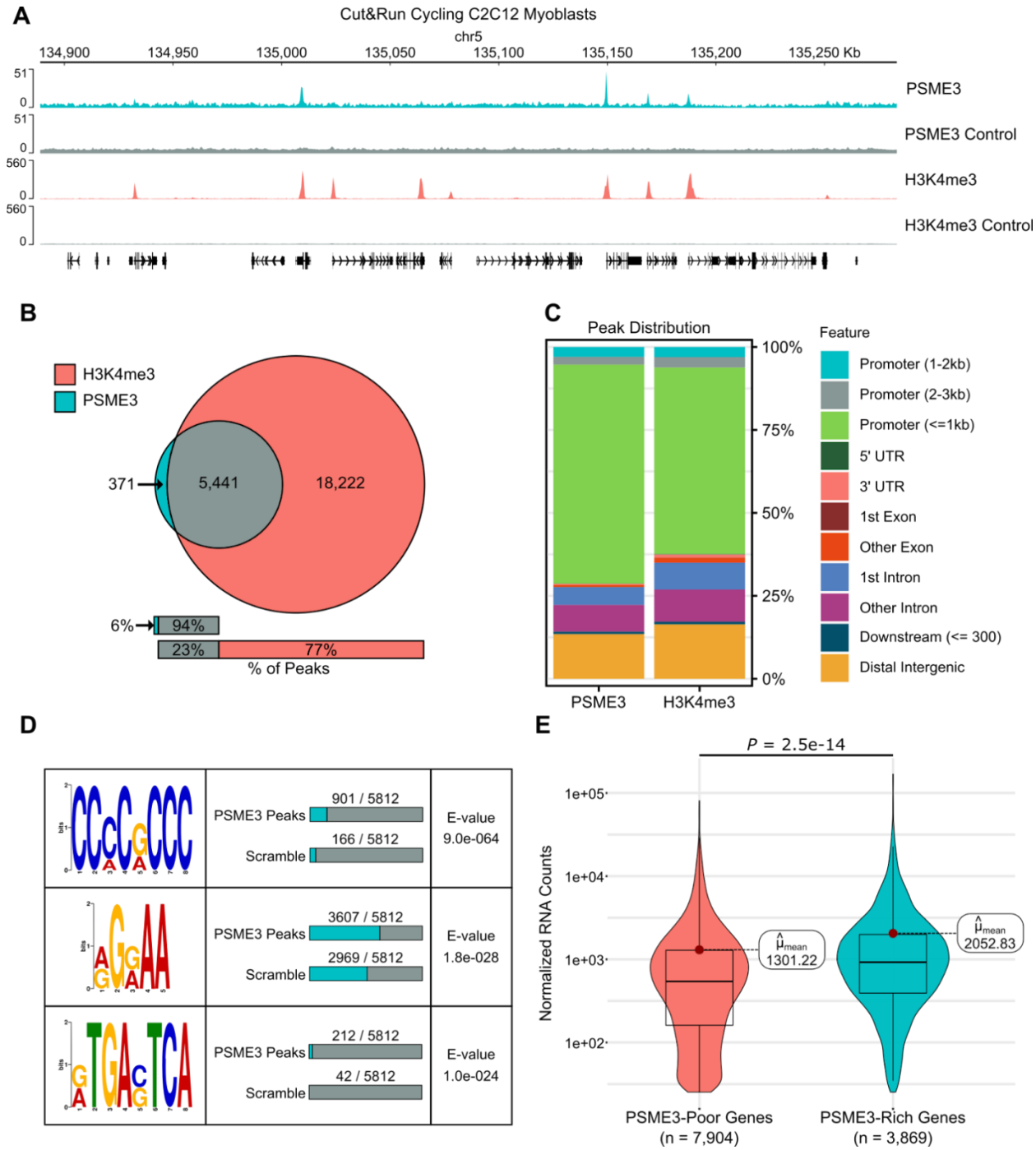
A
Cut&Run Cycling C2C12 Myoblasts
chr5
134,900
134,950
135,000
135,050
135,100
135,150
135,200
135,250 Kb
PSME3
PSME3 Control
H3K4me3
H3K4me3 Control
B
H3K4me3
PSME3
371
5,441
18,222
6%
94%
23%
77%
% of Peaks
C
Peak Distribution
100%
75%
50%
25%
0%
PSME3
H3K4me3
Feature
Promoter (1-2kb)
Promoter (2-3kb)
Promoter (<=1kb)
5' UTR
3' UTR
1st Exon
Other Exon
1st Intron
Other Intron
Downstream (<= 300)
Distal Intergenic
D
PSME3 Peaks
901 / 5812
Scramble
166 / 5812
E-value
9.0e-064
PSME3 Peaks
3607 / 5812
Scramble
2969 / 5812
E-value
1.8e-028
PSME3 Peaks
212 / 5812
Scramble
42 / 5812
E-value
1.0e-024
E
P = 2.5e-14
Normalized RNA Counts
1e+05
1e+04
1e+03
1e+02
μ̂mean
1301.22
μ̂mean
2052.83
PSME3-Poor Genes
(n = 7,904)
PSME3-Rich Genes
(n = 3,869)

PSME3 is Undetectable at the DNA Following the Onset of Differentiation

Differentiation involves rapid changes in the gene expression program, which is mediated by a similar reorganization of genome organization. To determine whether PSME3 exchanges its binding sites as differentiation progresses, we performed CUT&RUN in myoblasts that had differentiated for two days. In contrast with cycling cells, these differentiating cells show an almost complete absence of PSME3 peaks, as measured by CUT&RUN (Figure 2.2 A). Even when subjected to mild formaldehyde fixation, a treatment known to reduce the lability of transient chromatin interactions, scarcely any increase in the number of PSME3 peaks was observed in cells assayed, analyzed either fresh or after freezing (Figure 2.2 B). In summary, PSME3 binds selectively to highly active promoters in myoblasts, but becomes undetectable by the second day of myotube formation.

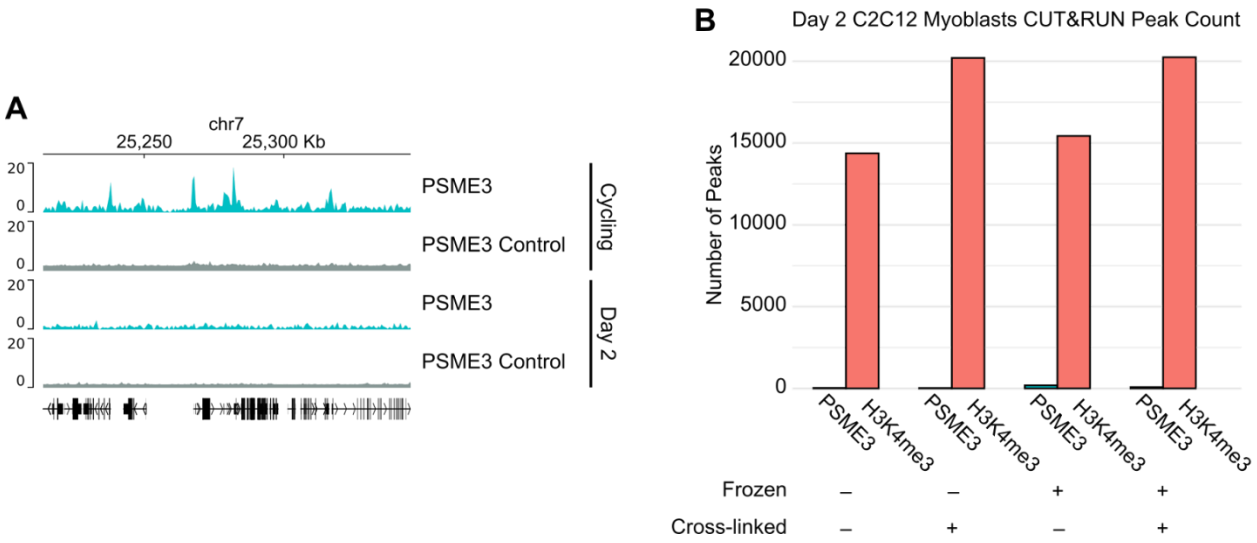

Figure 2.2: PSME3 is Undetectable at the DNA Following the Onset of Differentiation. **A**) CUT&RUN was performed in Day 2 differentiated C2C12 cells using an antibody targeting PSME3. Each track is the result of a single replicate, and the cycling replicate is drawn from those represented in panel (**A**) of Figure 2.1. **B**) CUT&RUN was performed using antibodies targeting PSME3 and H3K4me3 in Day 2 C2C12 cells under various cellular preparation conditions. Cells were either assayed fresh after being collected or were first cryopreserved at -80C. Further, cells were either assayed in their native state or after mild cross-linking with formaldehyde. A single replicate was performed for each condition, all from a single biological sample.

PSME3 Interacts in Situ with HP1

Studies of the DNA-binding activity of PSME3 are relatively sparse. One such paper demonstrated that PSME3 interacts with HP1β to mediate compaction of heterochromatin (Fesquet et al., 2021). They further showed through ChIP-qPCR that PSME3 associates predominantly with heavily compacted microsatellite regions, however the single euchromatic region investigated showed some mild enrichment for PSME3. The approach I have used, CUT&RUN, because of its reliance on sequencing technology, is unable to assess the binding of PSME3 to repetitive regions of the genome, by which microsatellite regions are characterized. Given the lack of overlap between the results of my work and this study, I sought to measure the degree of interaction of PSME3 with HP1β in our system.

To do so, I took advantage of an experimental system called the Proximity Ligation Assay (PLA), in which antibodies bound to two proteins of interest seed fluorescent RNA polymerization, provided that the target proteins are separated by less than 40 nanometers. These points of polymerization, and therefore proximity, can be visualized through confocal microscopy. A PLA study using an antibody targeting PSME3 and all variants of HP1 revealed a specific interaction specifically in the nucleus of dividing C2C12 cells (Figure 2.3 A), an observation which was reinforced by quantification of the number of punctae in the cell nucleus where both proteins reside (Figure 2.3 B). Though no firm conclusions can be drawn, our observations of PSME3's association with heavily transcribed, euchromatic regions in dividing myoblasts do not exclude the possibility that PSME3 also associates with and participates in the compaction of heterochromatic regions.

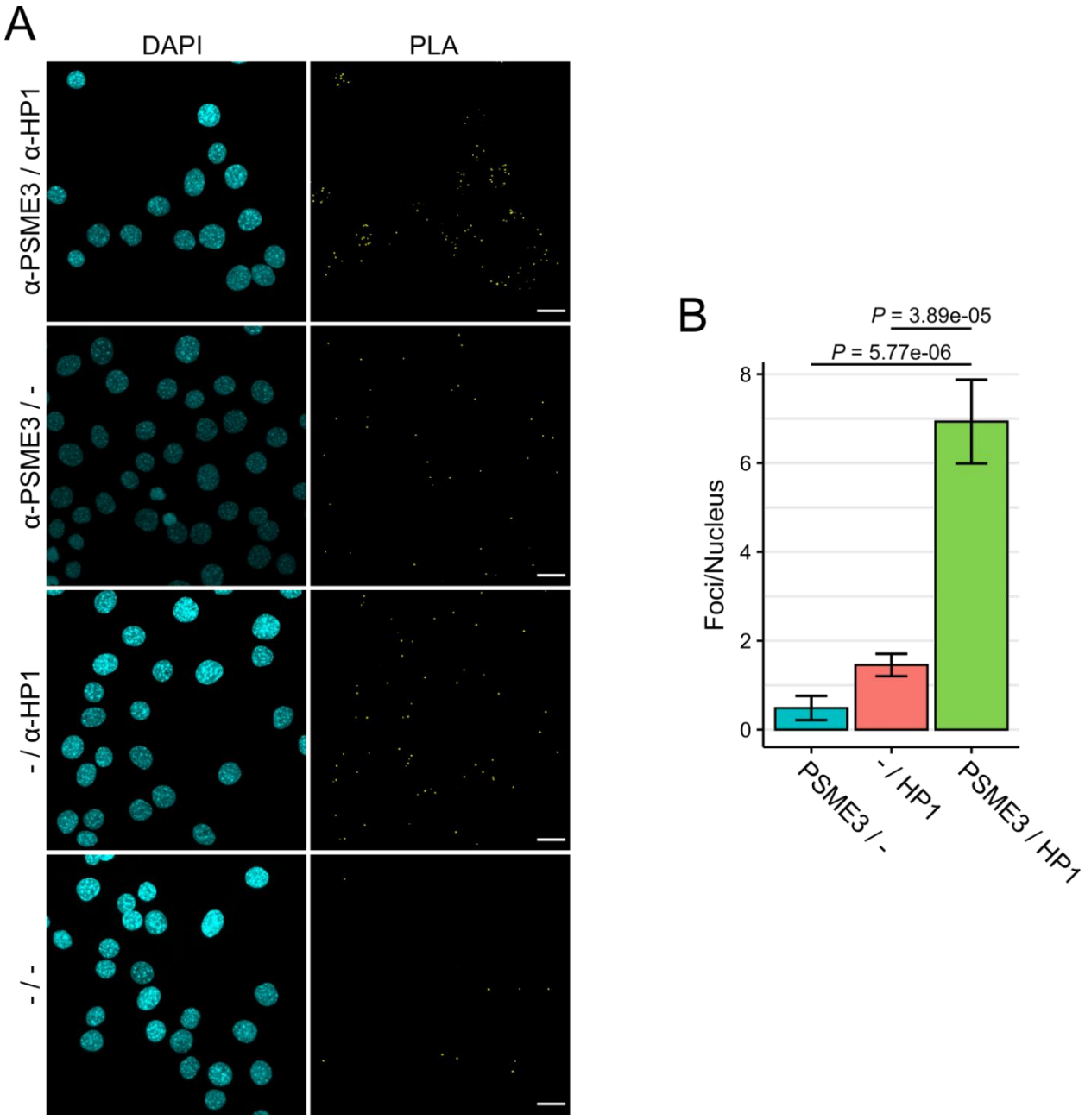

Figure 2.3: PSME3 Interacts in Situ with HP1. **A**) Cycling C2C12 cells were subject to proximity ligation assay (PLA) using primary antibodies targeting either PSME3 or HP1. The scale bar is 20 microns in length. **B**) The number of punctae contained within nuclei were quantified and analyzed with Welch two sample t-test. One replicate was performed with $n > 15$ nuclei per condition.

PSME3 Interacts with RNAPII Regulator RPRD1A

To understand what function PSME3 might be serving at the chromatin, we performed co-immunoprecipitation on endogenous PSME3 to identify potential interaction partners (Figure 2.4 A). Among the enriched binding partners was PSME3-interacting protein PSME3IP1, a known PSME3 interactor (Jonik-Nowak et al., 2018), and RPRD1A (Figure 2.4 A and B). RPRD1A regulates the dephosphorylation of S5 of RNAPII's CTD to facilitate progression of the polymerase from the promoter into the gene body (Ali et al., 2019; Ni et al., 2014). Given that S5P is found on polymerases poised to begin transcription and can recruit methyltransferases to deposit H3K4me3 marks on active promoters (Bae et al., 2020), we hypothesized RPRD1A was a potential mediator for PSME3's chromatin binding activity.

To verify this interaction *in situ*, we performed a proximity ligation assay (PLA) targeting PSME3 and RPRD1A. Cycling C2C12 cultures were transfected with a plasmid expressing FLAG-PSME3, and the colocalization of FLAG-PSME3 with endogenous RPRD1A was assessed (Figure 2.4 C). Cells expressing FLAG-PSME3 showed a high level of PLA signal, while those that were not transfected showed little to no signal. Omission of either antibody similarly abolished the signal (Figure 2.4 C), indicating signal specificity. These results suggest that PSME3 stably interacts with RPRD1A, which, by virtue of its ability to interact with RNA polymerase early in the transcription process, may be responsible for the localization of PSME3 to promoter regions.

Figure 2.4: PSME3 Interacts with RNAPII Regulator RPRD1A. **A**) PSME3 was precipitated from C2C12 cells while cycling and at days 0 and 1 of differentiation using a PSME3- or RPRD1A-specific antibody (one replicate per time point, combined for the purposes of analysis). Label-free quantitative mass spectrometry was performed on the PSME3 co-precipitate across all three days. **B**) Efficiency of PSME3 and RPRD1A capture compared to the supernatant (SN) versus that performed with an IgG control was assessed by Western blot. **C**) Cycling C2C12 cells were subject to proximity ligation assay (PLA) using primary antibodies targeting either FLAG-PSME3 or RPRD1A. Scale bar is 20 microns in length.

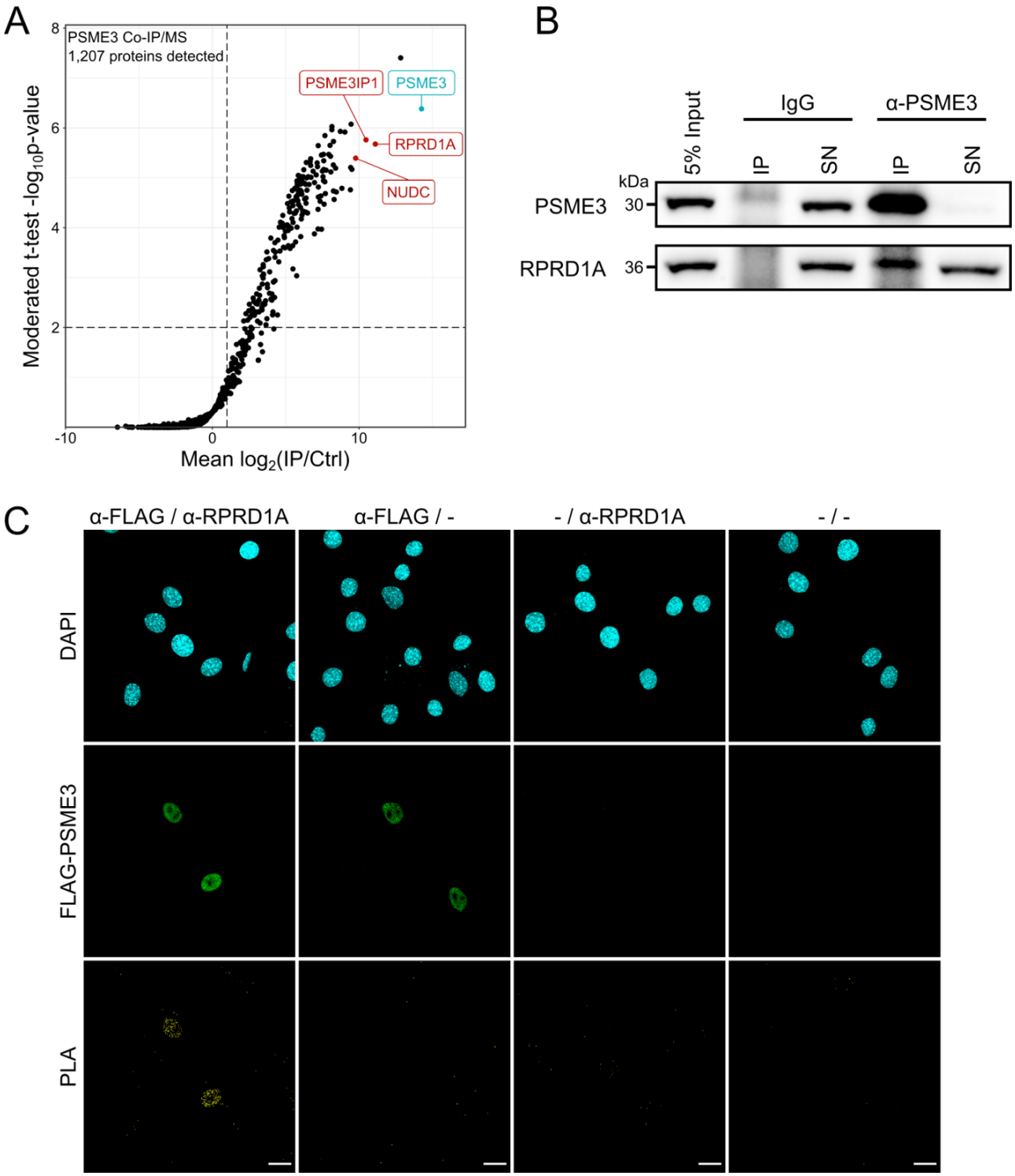
A
PSME3 Co-IP/MS
1,207 proteins detected
PSME3IP1
PSME3
RPRD1A
NUDC
Moderated t-test -log10p-value
Mean log2(IP/Ctrl)
B
5% Input
IgG
α-PSME3
IP
SN
IP
SN
kDa
PSME3
30
RPRD1A
36
C
α-FLAG / α-RPRD1A
α-FLAG / -
- / α-RPRD1A
- / -
DAPI
FLAG-PSME3
PLA

PSME3 Does Not Affect RPRD1A Levels or Localization

Due to PSME3's close association with RPRD1A, it is reasonable to suspect that it may be a regulator of RPRD1A activity. As PSME3 is known to be a component of the proteasome, we thought perhaps PSME3 may be responsible for degrading and thus regulating the levels of RPRD1A. To test this hypothesis, we depleted cells of PSME3 using siRNA and measured the levels of RPRD1A by Western blot over the course of differentiation (Figure 2.5 A). However, we observed no effect on RPRD1A levels at all timepoints measured.

The possibility remained that PSME3 regulates RPRD1A function instead of merely its level. RPRD1A has been shown to regulate the deposition of transcription-activating H3K27Ac marks through interaction with HDAC2 (Liu et al., 2015). To measure whether loss of PSME3 affected global H3K27Ac levels, we performed a Western blot across differentiation but saw a similar lack of change (Figure 2.5 A). While this does not rule out more localized, site-specific regulation of histone acetylation, it also provides no evidence thereof.

Finally, we considered that PSME3 may be a regulator not of the levels of RPRD1A, but its localization within the cell. To this end, we performed immunofluorescence staining on RPRD1A in day 3 differentiating cells that were depleted of PSME3 (Figure 2.5 B). We observed no change in RPRD1A localization at this time point.

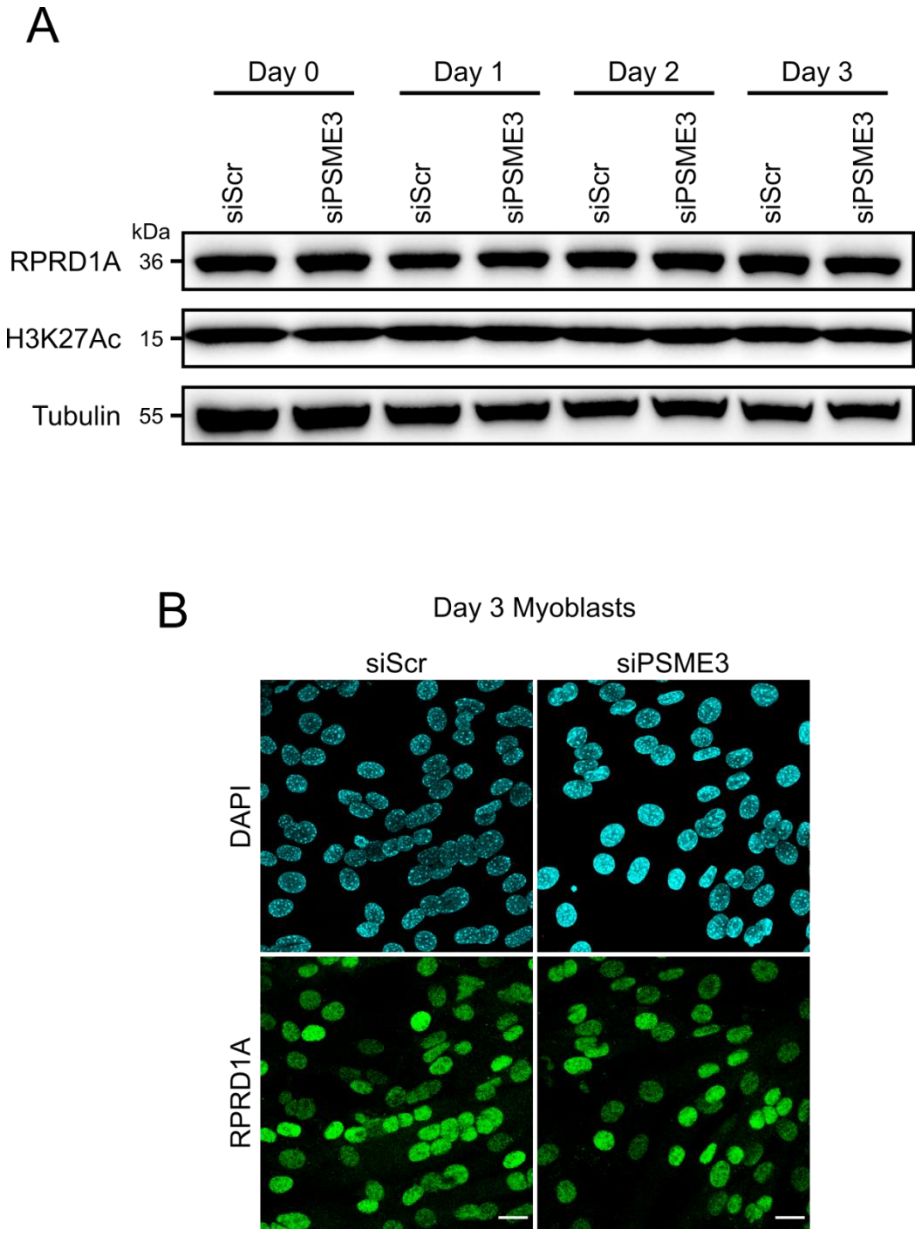

Figure 2.5: PSME3 Does Not Affect RPRD1A Levels or Localization. **A**) Dividing C2C12 cells were depleted of PSME3 through siRNA treatment and allowed to differentiate. Changed in the levels of RPRD1A and H3K27Ac were assessed. **B**) C2C12 cells that were differentiated for three days were stained with an antibody against RPRD1A to assess its localization. Scale bars are 20 microns in length.

PSME3 Does Not Regulate Global Expression in Differentiating C2C12 Cells

Though we observed no alterations in the levels or localization of PSME3 binding partner RPRD1A, it remains possible that PSME3 regulates other members of the RNAPII enzyme complex to regulate differentiation. Indeed, the dynamic binding pattern of PSME3 to the DNA over the course of differentiation, combined with its affinity for highly active gene regions, suggests that it may be involved in gene regulation. To assess this possibility, we subjected cells at various points of the differentiation process (cycling, day 0, and day 2) to RNA sequencing (Fig 2.6). Surprisingly, loss of PSME3 had no global effect on gene expression. The implications of this finding are discussed in the following section.

Taken together, we have characterized the DNA-binding patterns of PSME3. We observed an enrichment of PSME3 at highly active promoters in cycling cells, followed by a conspicuous absence in cells that have begun differentiation. This association with the DNA is likely mediated by an association with RPRD1A, which associates with RNAPII at sites of transcription. However, we observed no regulation of RPRD1A levels, function, or localization in the absence of PSME3, nor did we find evidence for a role for PSME3 in the global regulation of gene expression.

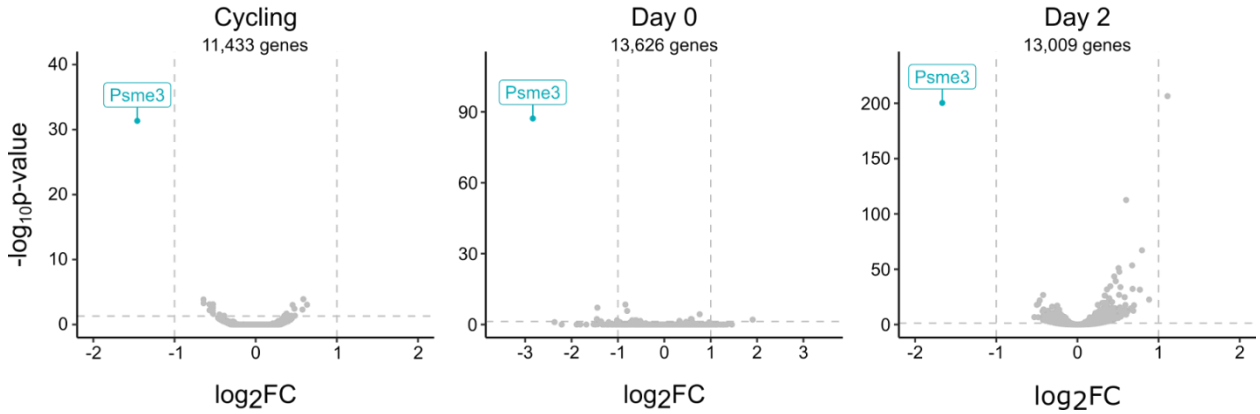

Figure 2.6: PSME3 Does Not Regulate Global Expression in Differentiating C2C12 Cells. C2C12 cells differentiating for the indicated duration were collected and subjected to RNA sequencing. Three biological replicates were collected for each time point.

2.4 Discussion

Our study provides the first unbiased study of PSME3 association with the DNA, discovers a new domain of PSME3 activity in its ability to bind highly active promoters, and identifies RPRD1A as a putative interaction partner. Though this study lacked the ability to replicate the results of earlier studies of PSME3 binding activity, while it does not contradict them, it suggests that PSME3 may have a more diverse set of functions than previously thought.

The finding that the proteasome associates with the chromatin is not entirely without precedent. The canonical 19s-containing proteasome has long been known to associate with the chromatin, where it is involved in diverse functions including transcription factor cycling and regulating the progression of RNA polymerase (McCann and Tansey, 2014). However, the finding that the non-canonical proteasome cap PSME3 interacts specifically with active promoters is a novel discovery. We believe that this interaction is mediated by an association with RPRD1A, a protein which binds to acetylated K7 of Pol II to facilitate dephosphorylation of S5P during the transition from transcriptional initiation to elongation (Ali et al., 2019; Ni et al., 2014) and has been shown to localize to the promoters of active genes (Liu et al., 2015). This aligns well with our finding that PSME3 mirrors H3K4me3 peaks in topology and localization and is enriched at the most transcriptionally active promoters. Our findings, combined with a recent study by Fesquet and colleagues (Fesquet et al., 2021) showing that PSME3 binds to and is crucial for maintaining heterochromatic regions, suggest that PSME3 may bind to a set of regions as diverse as the canonical proteasome, and perform additional still undocumented functions.

The observed interaction of PSME3 with RPRD1A would seem to provide an interesting mechanism by which PSME3 could regulate myoblast differentiation. PSME3 is known to attenuate the transcriptional response of macrophages to LPS (Sun et al., 2016), reduce the

activity of YAP in colon cancer tissue (Wang et al., 2018), and alter mRNA levels of E- and N-cadherins as well as vimentin in thyroid cancer cells, endometrial cancer cells, breast cancer cells, and lung cancer cells (Bhatti et al., 2019; Tong et al., 2020; Wang et al., 2015; Yi et al., 2017). Similar alterations in these genes would be expected to produce some effect during the differentiation process, which is heavily dependent on proper regulation of cell adhesion-related proteins. Similarly, RPRD1A is a known negative regulator of beta catenin signaling (Wu et al., 2010), proper activation of which is necessary for myotube development (Cui et al., 2019; Suzuki et al., 2018). We suspected that PSME3 may play a functional role in the regulation of RPRD1A binding or function, thus producing a change in gene expression and explaining the observed defect in differentiation.

We were surprised, therefore, to see such a weak effect on gene expression upon the depletion of PSME3. Although PSME3 has been shown in other systems to regulate gene expression, this is not a steadfast principle. For example, loss of PSME3 in HaCaT cells resulted in no changes in global transcriptional rates measured by 5-fluorouracil incorporation (Cioce et al., 2006), RNA levels of select genes were unaltered by PSME3 loss in U-2OS cells (Baldin et al., 2008) and splicing of several genes was unaffected by the disruption of the nuclear speckle caused by PSME3 loss (Baldin et al., 2008).

Such a lack of gene expression changes calls into question the physiological importance of the interaction between PSME3 and RPRD1A in cycling cells. One would hypothesize that if this interaction were important, loss of PSME3 would affect gene expression through altering RPRD1A activity. This hypothesis rests on two assumptions: first, that RPRD1A function is altered in the absence of PSME3; second, that changes in RPRD1A function are sufficient to alter gene expression in our system. We performed no experiments to test whether the post-

translational modification state of RNAPII is altered in cells lacking PSME3, so no conclusions may be made about the first point. As for the second, there is a paucity of evidence as to whether a loss of RPRD1A function would result in a change in gene expression. We may only make inferences based on evidence collected for its sister protein RPRD1B. As discussed in the first chapter of this dissertation, depletion of RPRD1B in NIH3T3 cells results in a very modest change in gene expression (Ali et al., 2019), a finding that closely resembles the results obtained in the present study. On the other hand, loss of RPRD1B in regenerating intestinal crypt cells of mice results in widespread, drastic changes in gene expression (Yang et al., 2021). If we were to assume these findings may be extended to RPRD1A, then one could suggest that PSME3 is dispensable for gene expression in an *in vitro* monoculture system but perhaps becomes more crucial in the complex developmental milieu of a regenerating organ. Existing evidence supports little more speculation on this point.

Why PSME3 should then occupy highly active promoter regions despite having no role in their regulation is unclear. The most parsimonious explanation posits that it plays no role whatsoever, and its presence may be an evolutionary artifact. However, it also bears considering that PSME3 may be primed to perform some function that is not engaged during differentiation, but in a separate set of circumstances entirely. For example, it is well-established that double strand DNA breaks (DSBs) cause a global degradation of RNA polymerase II complexes in a proteasome-dependent manner (Steurer et al., 2022). Loss of PSME3 has been found to sensitize cells to radiomimetic treatment and prevent timely repair at DSB sites (Levy-Barda et al., 2011). Thus, it remains possible that PSME3 might play a role in degrading Pol II in the case of DNA damage.

It should be noted that the presence of poly-ubiquitin chains found on Pol II prior to degradation argue for degradation by 26s proteasome rather than by the ubiquitin binding-incapable PSME3. However, the formation of this poly-ubiquitin chain is necessary for the function of the VCP complex, which was recently shown to extract Pol II at the promoter for proteasomal degradation (Bodnar and Rapoport, 2017) and may therefore be unimportant for recognition by the proteasome itself. A similar mechanism is employed for the degradation of p53, which is mediated by the recruitment of ubiquitin ligase MDM2 by PSME3 prior to p53 degradation by the 26s proteasome (Zhang and Zhang, 2008). In such a case, PSME3 activity is critical even though it does not cap the proteasome that effects target degradation. Alternatively, PSME3 has been shown to respond to other cellular insults, such as hyperosmotic stress (Carrettiero et al., 2022), and so such changes may be sufficient to elicit possible transcriptional regulation activity.

One might be inclined to argue, after observing the data presented in Figure 2.6 of the second day of differentiation, that there is indeed a change in gene expression upon loss of PSME3, however minor it might be. While indeed this may be the case, as we shall see in the next chapter, PSME3 depletion has no small effect on cellular physiology, which occurs as early as day 0 of differentiation. While this does not preclude the possibility of gene dysregulation by PSME3 only after an extended period of differentiation, we find it more likely that these minor alterations in gene expression represent compensatory responses to the other changes that the cells display at an earlier point in time. These changes will be discussed presently.

Chapters 2 and 3, in part, have been submitted to and are under review for publication at Life Science Alliance. The dissertation author was the primary researcher and author of this paper and is accompanied by Ukrae H. Cho and Martin W. Hetzer.

Chapter 3 PSME3 Associates with NUDC and Regulates Migration and Differentiation

3.1 Abstract

Reorganization of the cytoplasm, particularly the cytoskeleton in many cell types, is critical for the differentiation process. PSME3 has been demonstrated to regulate cell motility in diverse types of cancer cells, though its ability to do so in non-diseased tissue, and in developing tissue, remains uninvestigated. Here, we identify the HSP90 co-chaperone NUDC as a novel interacting partner of PSME3. Loss of PSME3 results in the increase of cell-adhesion-related protein targets of NUDC and an increase in cell migration rates. Further, we show that loss of PSME3 impairs myogenesis in a cell-intrinsic and proteasome-independent mechanism. These findings establish a new function for PSME3 and provide a new link between the chaperone and proteasome-adjacent system.

3.2 Introduction

The acquisition of cellular identity through differentiation requires the coordinated restructuring of diverse cellular systems. Particular demands are placed on differentiating myoblast cells, which must complete a gauntlet of biophysical feats. To form a functional myotube, mononucleated myoblasts must migrate to and recognize competent fusion partners, form proper cell adhesion contacts, extensively align their membranes, form fusion pores, and combine their cellular contents in a way that does not compromise the integrity of either cell (Bodnar and Rapoport, 2017; Simionescu and Pavlath, 2011).

Critical to this process is the proper regulation of the relevant effector proteins, which occurs both at the transcriptional and post-translational levels. PSME3 is a non-canonical regulatory cap of the proteasome, and its increased expression has been associated in many cancer cell lines with an increase in cell migration proteins and an invasive phenotype (Bhatti et al., 2019; Tong et al., 2020; Wang et al., 2015; Yi et al., 2017). A unifying mechanism has yet to

be identified, though in at least some cases, the change in migration-related protein abundance is the result of changes in gene expression profiles.

Because of PSME3's role in the regulation of cell migration, one would expect PSME3 to influence the rate of myoblast differentiation. Indeed, an alteration in the abundance of various migration-related proteins is sufficient to impair myogenesis (Lehka and Rędowicz, 2020). Further, PSME3 has been demonstrated to play important roles in the regulation of cell cycle regulators p16, p19, and p21, as well as transcriptional regulators such as c-Myc, Klf2, SMURF2, and LATS1/2 (Chen et al., 2018; S. Li et al., 2015; Li et al., 2007; Nie et al., 2010; Sun et al., 2016; Wang et al., 2018).

Despite the diverse functions that PSME3 performs in systems critical for differentiation, few studies examined its role in the acquisition of cellular identity. Indeed, it has recently been discovered that mice lacking PSME3 show deficits in the function of multiple systems because of impaired cellular differentiation. Loss of PSME3 impairs T cell maturation and triggers the differentiation of Th17 cells by altering the cell-surface protein profile of dendritic cells (Zhou et al., 2020). Additionally, suppressed PSME3 expression biases bone marrow stromal cells towards an adipogenic rather than osteogenic fate, and mice lacking PSME3 display corresponding bone-healing defects (Chen et al., 2024). Because of these findings, we hypothesized that PSME3 may be important for the differentiation of other cell types, such as those found in the muscular system.

To investigate this possibility, we used C2C12 myoblasts to interrogate the capacity of PSME3 to regulate differentiation. We find that, unexpectedly, the normally cytoplasmic NUDC displays a striking level of nuclear localization in myoblast cells, overlapping with that of PSME3. Indeed, the two proteins display a physical interaction as verified by PLA, though loss

of PSME3 has no effect on NUDC levels or localization. Further, loss of PSME3 results in an increase in cell adhesion- and migration-related proteins. As a result, myoblasts lacking PSME3 display an increase in cell migration capacity and impaired myogenesis, a process which PSME3 regulates in a cell-intrinsic, proteasome-independent manner.

3.3 Results

PSME3 and NUDC Overlap in Localization

As seen in section 2.3.4, an immunoprecipitate prepared with an antibody raised against PSME3 contained not only RPRD1A as a novel interaction partner, but also the protein NUDC (Figure 2.4). This protein drew our attention, as, while depleting cells of PSME3, we noticed they displayed a greater tendency to adhere to the cell culture plate, suggesting a change in cell-adhesion. NUDC was recently identified as a co-chaperone of HSP90 and has been documented to regulate cell migration through the stabilization of several cytoskeletal proteins, including cofilin and filamin A (Liu et al., 2021; Zhang et al., 2016). Because of the importance of cell-adhesion and its related properties for myoblast differentiation, we sought to investigate this interaction.

We were, however, surprised to observe an interaction as measured by immunoprecipitation, as NUDC has previously been documented to possess a primarily cytoplasmic localization (Islam et al., 2020; Zhang et al., 2016; Zhou et al., 2003; Zhu et al., 2010). That said, PSME3 has been known to relocalize from the nucleus to the cytoplasm under certain contexts (Carrettiero et al., 2022; Kobayashi et al., 2013; Pecori et al., 2021). To determine whether the two proteins possess spatial overlap in our system, we first performed live imaging on cycling C2C12 cells that were transfected with constructs expressing PSME3 with either an N- or C-terminal GFP tag (Figure 3.1 A), revealing PSME3's presence in the nucleus. Further, we found that NUDC displayed a strong signal across both cytoplasm and nucleus,

where it coincided with PSME3 staining (Figure 3.1 B), indicating that the two proteins are indeed well-positioned to interact.

To verify that the addition of a tag did not affect the localization of PSME3, cycling C2C12 cells treated with siRNA were stained with an antibody targeting the endogenous population of PSME3 (the same antibody used for the CUT&RUN experiments in Chapter 2). While a low level of cytoplasmic staining was visible, this signal was not affected by siRNA depletion of PSME3, suggesting that this is non-specific staining (Figure 3.1 C). Instead, the strong nuclear signal was predominantly depleted, indicating that PSME3 is largely nuclear in our system.

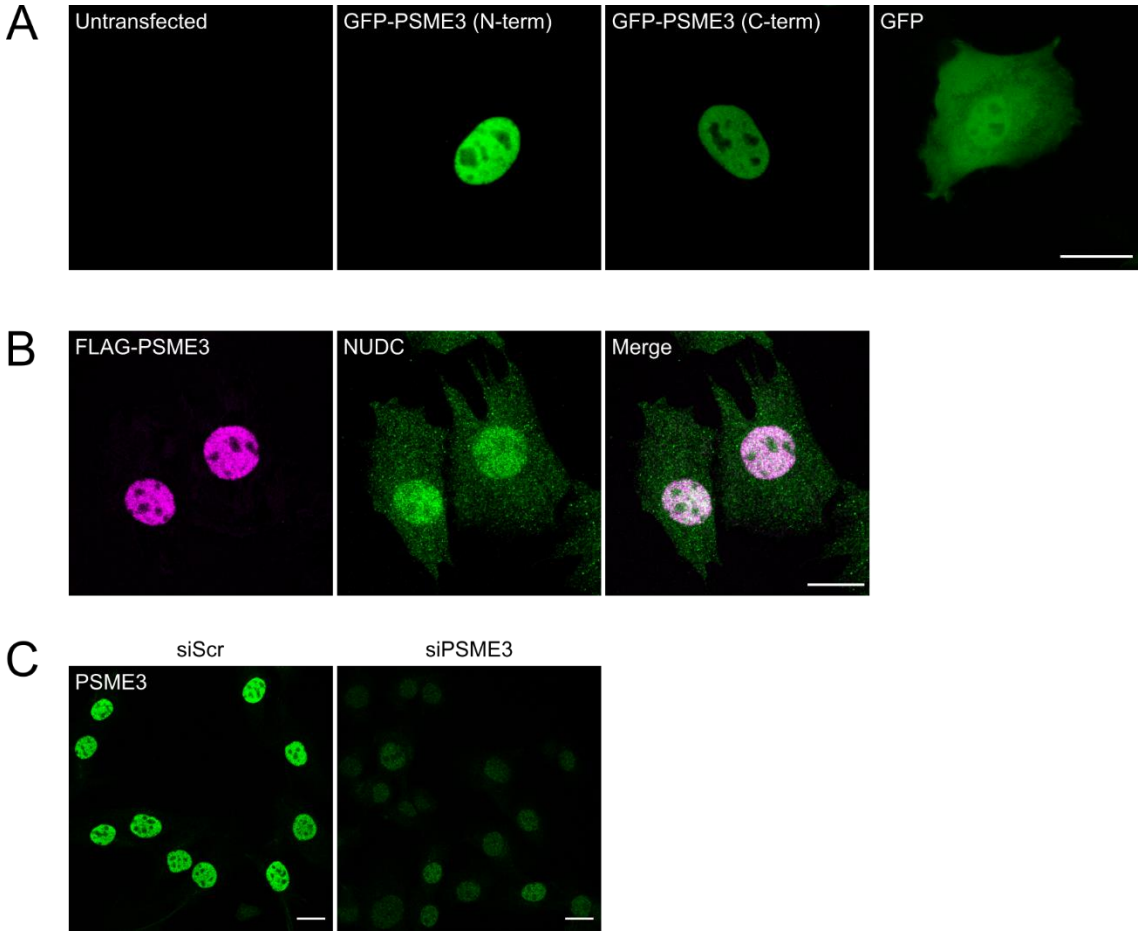

Figure 3.1: PSME3 and NUDC Overlap in Localization. **A**) Cycling C2C12 cells were transfected with constructs expressing PSME3 tagged with GFP either at its N- or C-terminal, or with a construct expressing free GFP. Cells were imaged live and unstained; the scale bar is 20 microns in length. **B**) C2C12 cells expressing FLAG-tagged PSME3 were stained with antibodies against FLAG or endogenous NUDC; scale bar is 20 microns in length. **C**) Cycling C2C12 cells treated with siRNA were stained with an antibody against endogenous PSME3; scale bar is 20 microns in length.

PSME3 and NUDC Physically Interact

To verify the interaction between PSME3 and NUDC we observed by mass spectrometry, we performed PLA. Cycling C2C12 cultures were transfected with a plasmid expressing FLAG-PSME3, and the colocalization of FLAG-PSME3 with endogenous NUDC was assessed (Figure 3.2). Cells expressing FLAG-PSME3 showed a high level of PLA signal, while those that were not transfected showed little to no signal. Omission of either antibody similarly abolished the signal (Figure 3.2), indicating signal specificity.

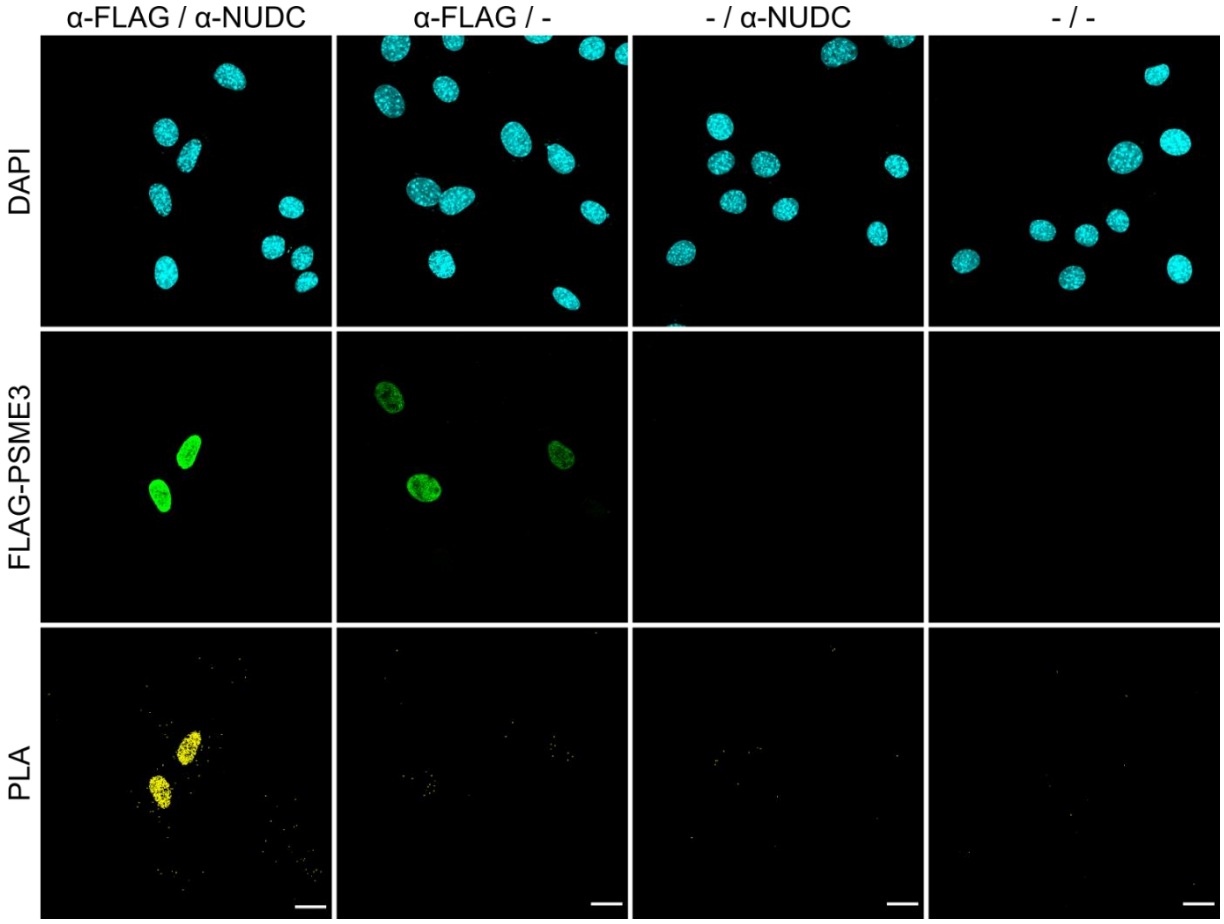

Figure 3.2: PSME3 and NUDC Physically Interact. Cycling C2C12 cells were subject to proximity ligation assay (PLA) using primary antibodies targeting either FLAG-PSME3 or RPRD1A. Scale bar is 20 microns in length.

PSME3 Regulates Cell Migration

Because NUDC is known to regulate the rate of migration of diverse cell types, and because we established a physical interaction between PSME3 and NUDC, we asked whether PSME3 itself influences cell migration. To this end, we grew cells lacking PSME3 to full confluency (Day 0 cells) and scratched the monolayer with a pipette tip. The cells were immediately switched to differentiation medium (sub-confluent, non-differentiating cells were found to be non-motile; data not shown) and allowed to migrate to fill the gap over a 20-hour period (Figure 3.3 A). Cells lacking PSME3 showed an elevated rate of migration of roughly 40%, indicating that PSME3 plays a striking role in regulating the cell motility (Figure 3.3 B).

To measure any accompanying changes in cytoskeletal organization, we stained migrating cells with the filamentous actin marker phalloidin (Figure 3.3 C). A cursory examination revealed no obvious differences at a population level, though a more in-depth quantification may reveal changes in actin organization resulting from PSME3 depletion.

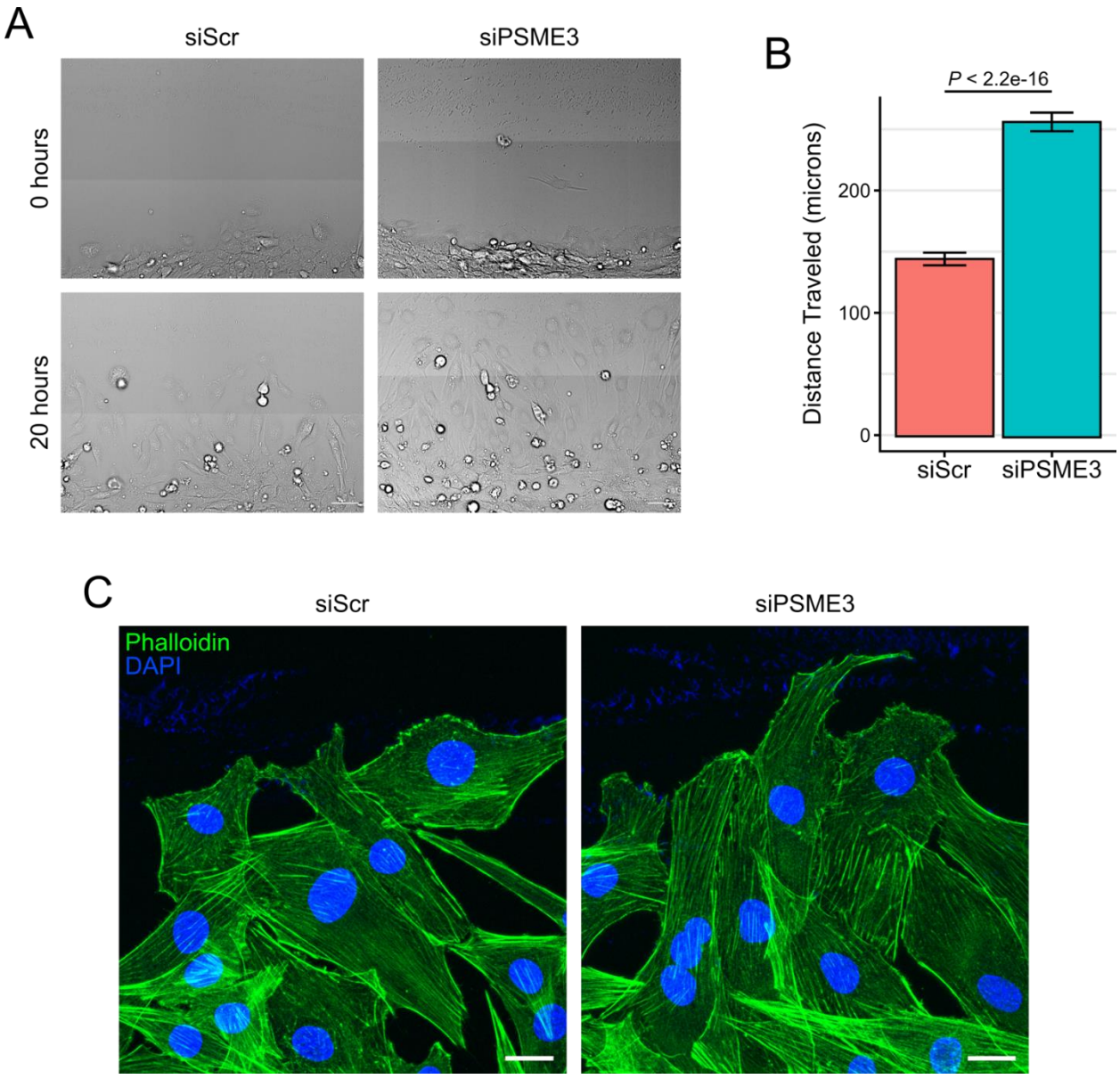

Figure 3.3: PSME3 and NUDC Overlap in Localization. **A**) Day 0 confluent C2C12 cells were scratched and allowed to migrate for 20 hours while continuously undergoing brightfield imaging. **B**) Quantification of the distance traveled over 20 hours by individual migrating cells treated with either scrambled siRNA or that targeting PSME3. Data was collected with three biological replicates each with two technical replicates of $n = 15$ each and analyzed Welch two sample t-test; error bars show the standard error of the mean. **C**) Day 0 confluent C2C12 cells were allowed to migrate for six hours after a scratch before being fixed and stained with fluorescent phalloidin.

Loss of PSME3 Does Not Affect NUDC Levels or Localization

Given the demonstrated possibility of a functional interaction between PSME3 and NUDC, we sought to understand what sort of effects loss of PSME3 would have on NUDC. We first performed a simple measurement of NUDC levels in Day 0 cells lacking PSME3 (Figure 3.4 A). We observed neither a change in NUDC abundance nor molecular weight (as might occur during a post-translational modification) when PSME3 was depleted.

NUDC has previously been shown to localize to the leading edge of migrating cells where it stabilizes actin cytoskeleton remodeling proteins (Zhang et al., 2016). To determine whether loss of PSME3 produces any changes in NUDC localization in migrating cells, we scratched confluent Day 0 myoblasts and allowed them to migrate for six hours before fixation and immunofluorescent staining for NUDC (Figure 3.3 B). We observed neither a localization of NUDC at the leading edge in control conditions, and a lack of change in its cellular distribution when PSME3 is depleted. Finally, we tested whether other known functions of NUDC were altered upon loss of PSME3. NUDC depletion of RPE-1 cells or in the developing zebrafish embryo results in increased primary cilium length and number (Zhang et al., 2016).

To determine whether the primary cilium is disrupted in C2C12 cells following PSME3 depletion, we stained fully confluent myoblasts which had been cultured in differentiation medium for six hours for primary cilium markers acetylated tubulin (the constituent tubulin of the primary cilium) and γ-tubulin (a marker of tubulin nucleation) (Figure 3.4 C) (Ishikawa and Marshall, 2011; Shankar et al., 2022). We find that loss of PSME3 has no apparent effect on the length or number of primary cilia in fully confluent cells (migrating cells were similarly tested as well and no difference was observed, data not shown).

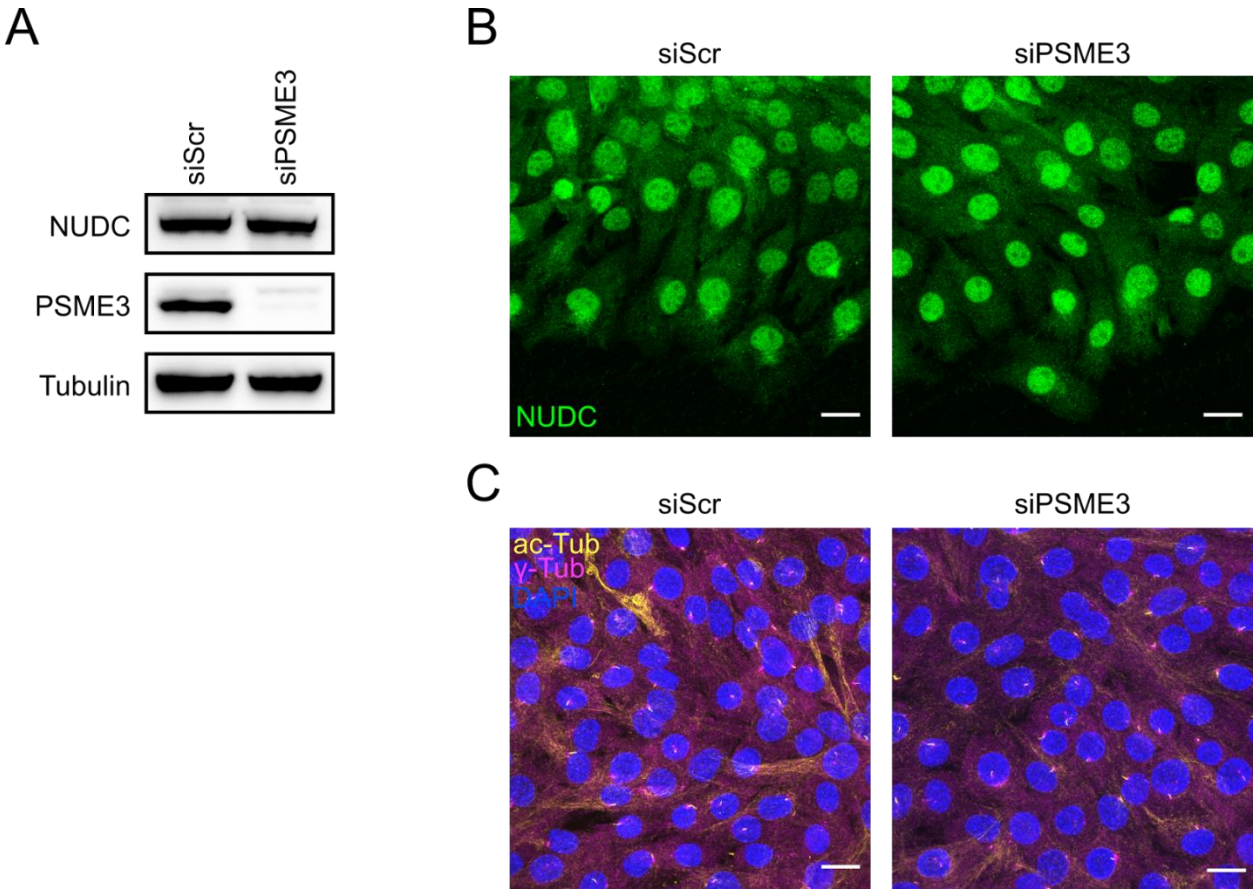

Figure 3.4: Loss of PSME3 Does Not Affect NUDC Levels or Localization. A) Day 0 confluent C2C12 cells were collected, lysed, and subjected to immunoblot. B) Day 0 confluent C2C12 cells were allowed to migrate for six hours after a scratch before being fixed and stained with an antibody raised against NUDC. C) Day 0 confluent C2C12 cells were allowed to differentiate for six hours before being fixed and stained with acetylated tubulin (ac-Tub) and γ-tubulin (γ-Tub).

Loss of PSME3 Increases the Abundance of Cell-Adhesion Proteins

To determine the molecular basis for the increased rates of cell migration, we performed proteomics on migrating cells depleted of PSME3. In line with the known targets that NUDC stabilizes, we observed an increase in the abundance of proteins involved in migration and cell-adhesion, including the E-cadherin regulator Adenomatous Polyposis Coli (APC) and Integrin Beta-3 (ITGB3) (Figure 3.5 A and C). Interestingly, loss of PSME3 appears to have a strong effect on the abundance of mitochondrial proteins as well, as it reduced the abundance of several components of the electron transport chain when depleted (Figure 3.5 B).

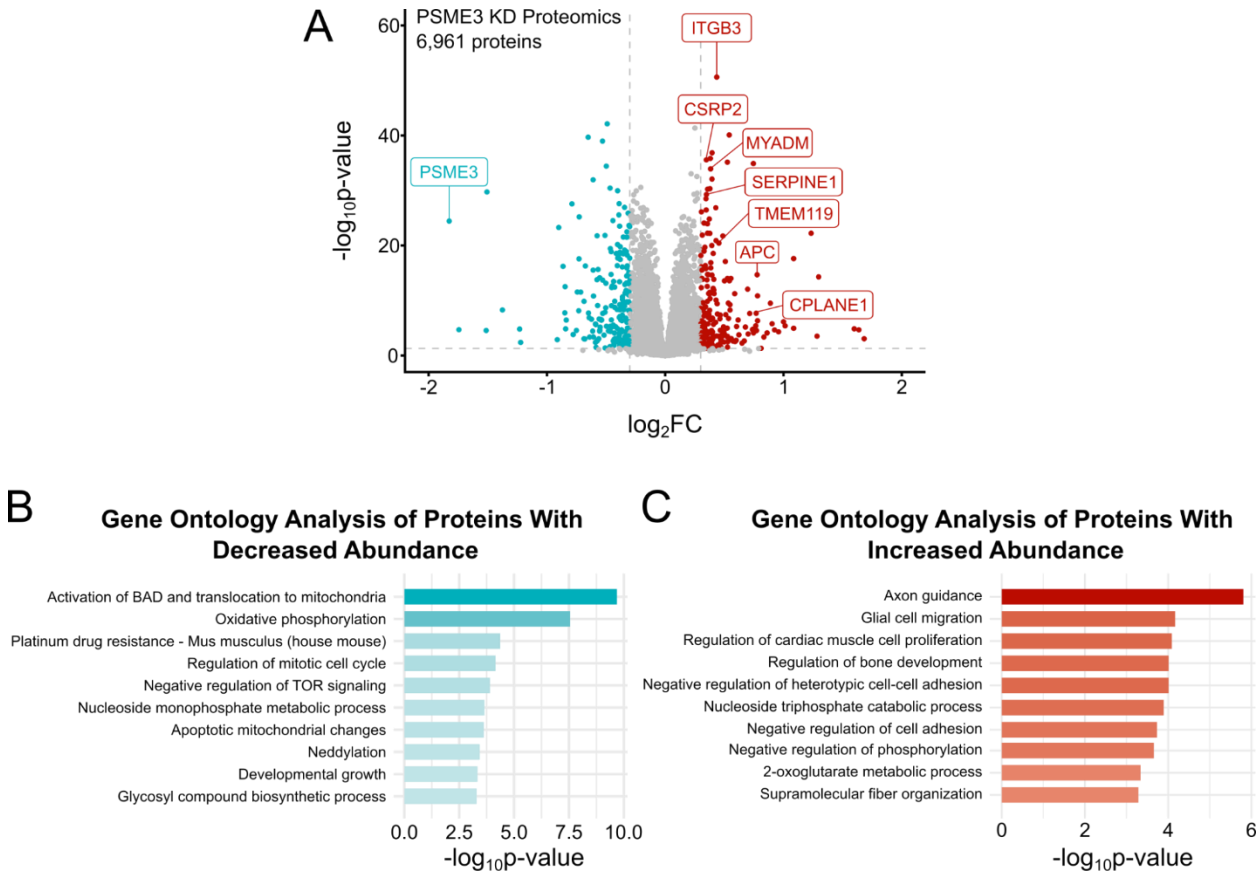

Figure 3.5: Loss of PSME3 Increases the Abundance of Cell-Adhesion Proteins. **A**) Day 0 confluent C2C12 cells treated with either scrambled or PSME3-targeting siRNA were subjected to label-free proteomics. The changes in protein abundance are plotted here with decreased-abundance proteins in blue and increased-abundance proteins in red, with several select species involved in cell migration receiving a label. Three biological replicates were used. Gene ontology analysis of decreased- (**B**) and increased-abundance proteins (**C**); the top ten categories are shown.

Loss of PSME3 Impairs Myotube Formation

We reasoned that if loss of PSME3 altered levels of cell migration, it may also be critical for the differentiation of C2C12 myoblasts, which are particularly sensitive to changes in cytoskeleton function due to the heavy demands imposed by membrane apposition and cell fusion. To this end, we depleted C2C12 myoblast cells of PSME3 through siRNA treatment prior to serum withdrawal and subsequent differentiation (Figure 3.6 A and B). siRNA-treated myoblasts were allowed to differentiate for two days before fixation and staining with antibodies against myogenin, a myogenic transcription factor, and myosin heavy chain (MHC), a major contractile protein found in differentiated myotubes. Widefield imaging revealed a clear deficit in differentiation (Figure 3.6 C). Cultures lacking PSME3 produced myotubes with fewer nuclei (Figure 3.6 D) and possessed a lower fusion index (Figure 3.6 E), defined as the percentage of nuclei contained within MHC-positive myotubes.

Figure 3.6: Depletion of PSME3 Impairs Myotube Formation. **A**) Cycling C2C12 cells were treated with siRNA prior to growth to confluency and serum deprivation, which together induce differentiation and myotube formation. **B**) C2C12 cells were treated with scrambled or PSME3-targeting siRNA and collected at Day 0, 1, or 2 of differentiation; target protein levels were assessed by Western blot. **C**) C2C12 cells depleted of PSME3 were induced to differentiate for two days and were subjected to immunofluorescence using antibodies targeting MHC and myogenin; scale bar is 200 microns in length. **D**) Immunostained cultures were analyzed for the number of nuclei contained in each MHC-positive cell. Data includes three biological replicates each with two technical replicates of $n = 250$ cells and was analyzed by Welch two sample t-test, displayed here with a graph showing median and quartiles. **E**) Immunostained cultures were analyzed for the percentage of all DAPI-positive nuclei that are contained within MHC-positive cells. Data includes three biological replicates each with two technical replicates of roughly $n =$ 20,000 cells; two sample t-test of proportions.

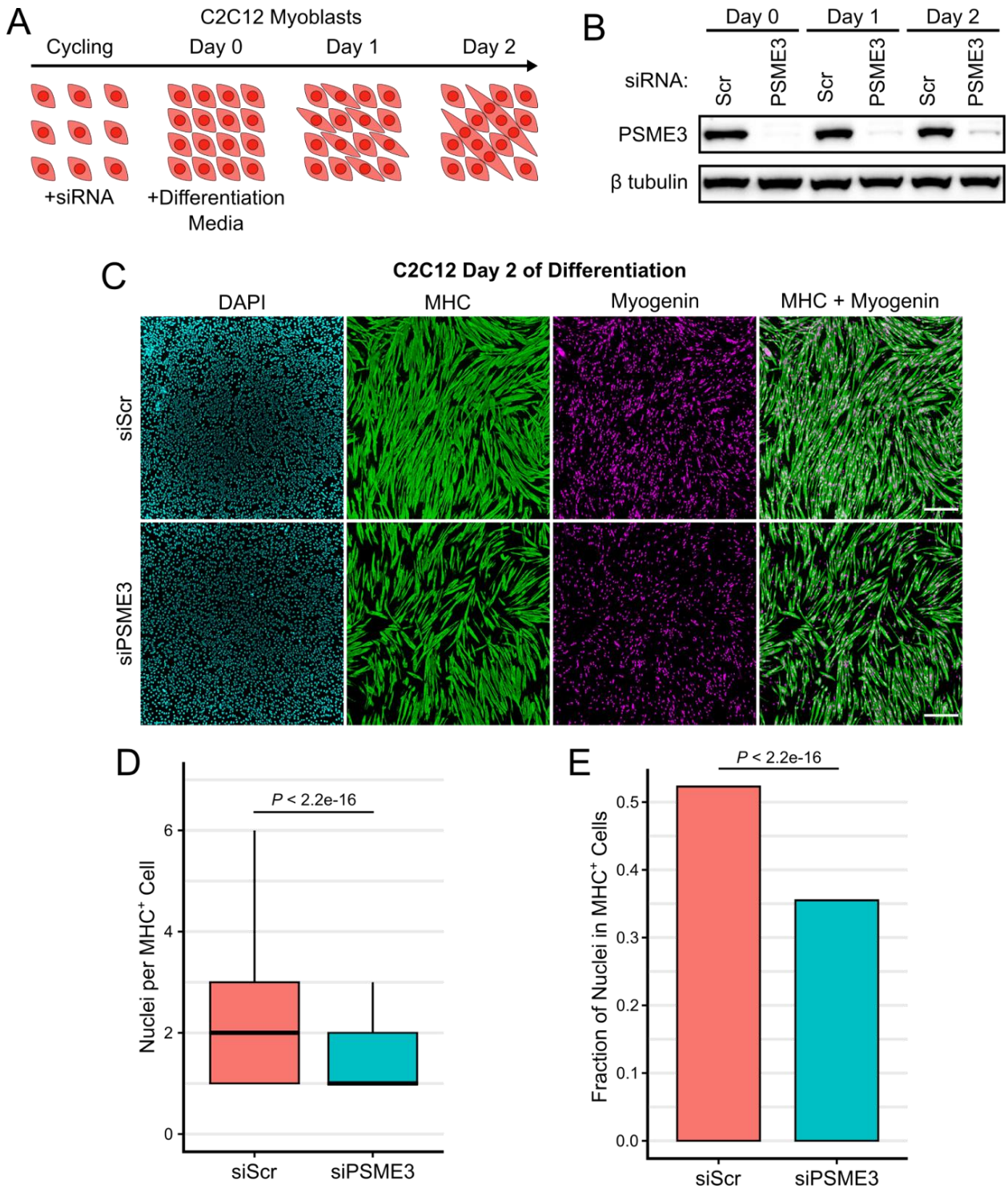
A
C2C12 Myoblasts
Cycling
Day 0
Day 1
Day 2
+siRNA
+Differentiation Media
B
Day 0
Day 1
Day 2
siRNA:
Scr
PSME3
Scr
PSME3
Scr
PSME3
PSME3
β tubulin
C
C2C12 Day 2 of Differentiation
DAPI
MHC
Myogenin
MHC + Myogenin
siScr
siPSME3
D
P < 2.2e-16
Nuclei per MHC+ Cell
0
2
4
6
siScr
siPSME3
E
P < 2.2e-16
Fraction of Nuclei in MHC+ Cells
0.0
0.1
0.2
0.3
0.4
0.5
siScr
siPSME3

PSME3 Regulate Myogenesis Through a Proteasome-Independent Mechanism

To determine if the effect of PSME3 on myogenesis is dependent on an interaction with the proteasome, we stably expressed FLAG-tagged PSME3 either in its full length or with a deletion of the terminal fourteen amino acids, which renders it unable to associate with the 20s proteasome (Figure 3.7 B) (Fesquet et al., 2021; Förster et al., 2005; Ma et al., 1993; Zannini et al., 2008; Zhang and Zhang, 2008). We found that expression of either the full-length or C-terminal deletion mutant was sufficient to rescue the myogenesis phenotype caused by depletion of endogenous PSME3, indicating that PSME3 regulates myoblast differentiation through a proteasome-independent mechanism (Figure 3.7 A-C).

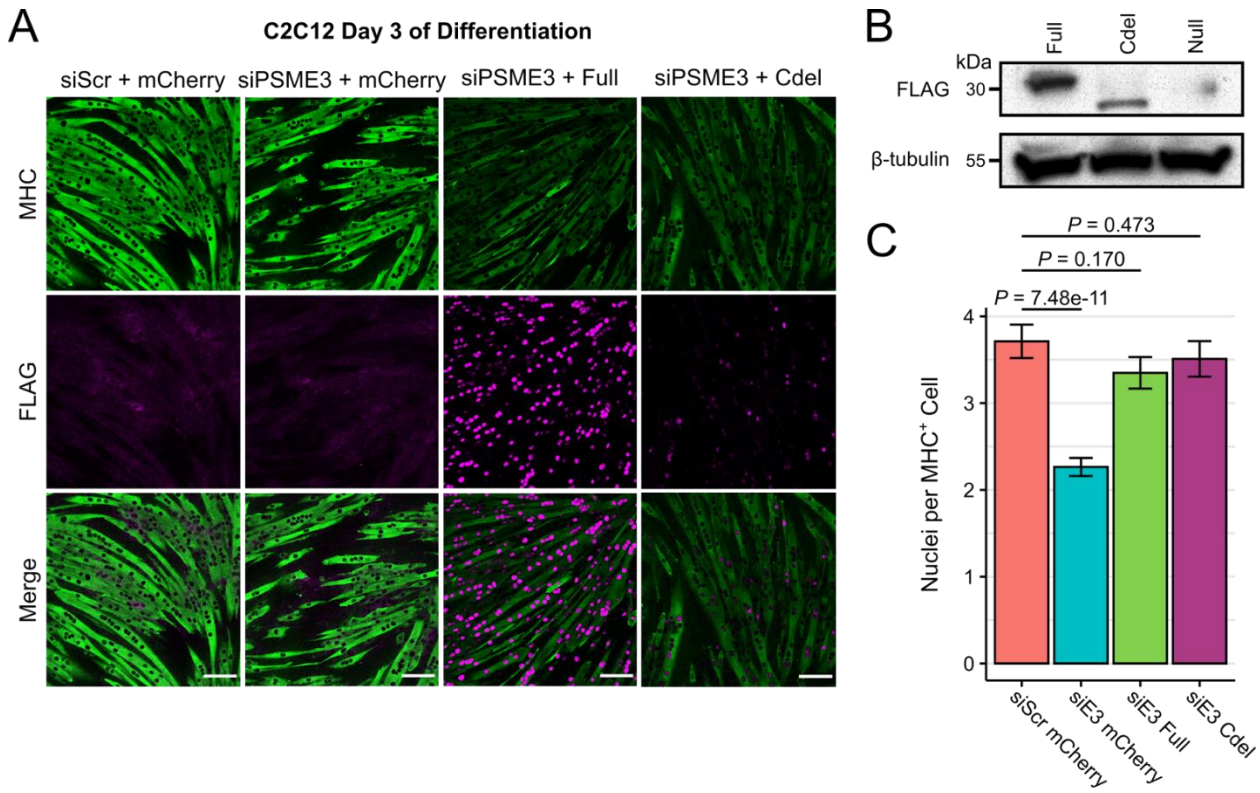

Figure 3.7: Depletion of PSME3 Results in a Proteasome-Independent Differentiation Deficit. **A**) Cells were stably transduced with a retroviral construct expressing mCherry, FLAG-tagged PSME3 (Full), or a truncated FLAG-tagged C-terminal deletion PSME3 mutant (Cdel). Cells were then depleted of endogenous PSME3 by treatment with siRNA and allowed to differentiate for three days before staining. The scale bars are 100 microns in length. **B**) Expression of FLAG constructs in undifferentiated myoblasts. **C**) The number of nuclei contained within each MHC-positive myotube was quantified across conditions and analyzed by the Welch two sample t-test; two biological replicates with each condition with $n > 200$ myotubes; error bars display the standard error of the mean.

PSME3 Regulate Myogenesis Through a Cell-Intrinsic Mechanism

Though there were no global alterations in gene expression when PSME3 was depleted, we observed a modest increase in several collagen transcripts on the second day of differentiation (Figure 2.6). To confirm that the observed differentiation phenotype is the result of a cell-intrinsic effect and not an alteration in the extracellular matrix, we created a mixed culture system of cells treated with scrambled siRNA or that targeting PSME3 and labeled them with a red or blue dye, respectively. If the differentiation phenotype is due to a cell-extrinsic effect, the presence of control cells should improve the differentiation efficiency of those lacking PSME3. However, when the mixed population was induced to differentiate for three days, we instead observed a selective exclusion of cells lacking PSME3 from mature myotubes (Figure 3.8 A and B). Taken together, these results indicate that PSME3 is necessary for myoblast differentiation in a cell-intrinsic manner.

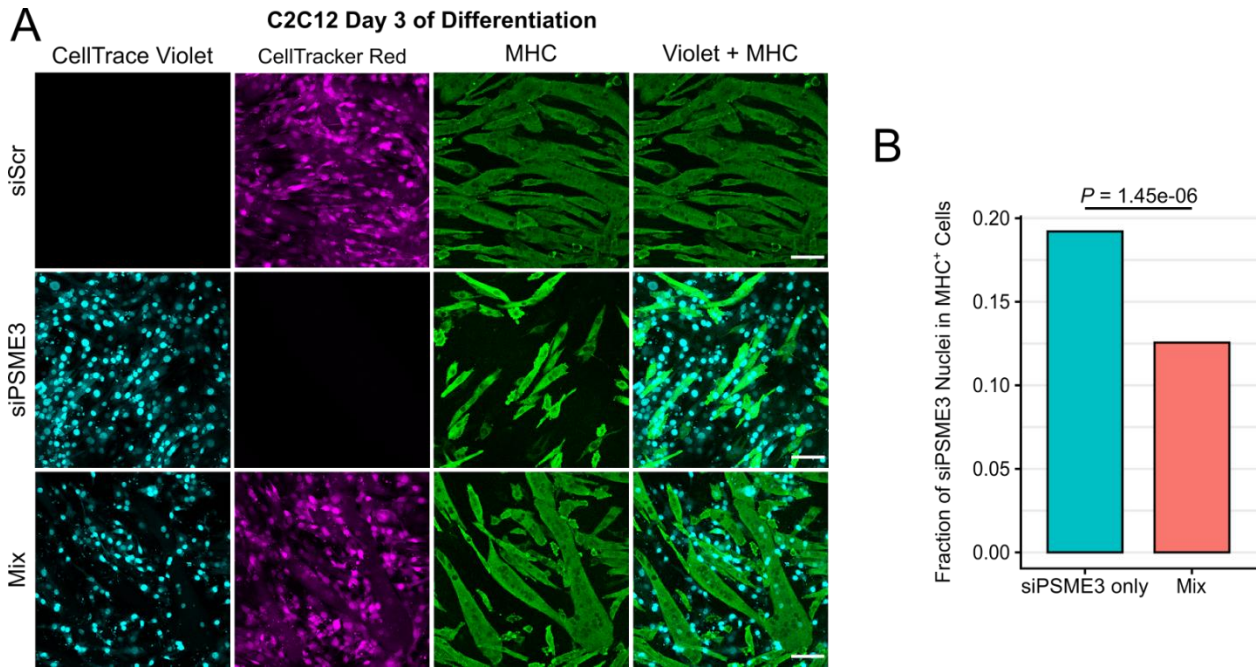

Figure 3.8: Depletion of PSME3 Results in a Cell-Intrinsic Differentiation Deficit. **A**) Cells transfected with scrambled siRNA or that targeting PSME3 were labeled red or blue, respectively. These cells were induced to differentiate for three days before fixation and staining with an antibody against MHC before imaging. The scale bar is 50 microns. **B**) Quantification of number of siPSME3 (blue) nuclei contained within MHC-positive cells when in the absence or presence of siScr-treated cells; one biological replicate with n = 1,155 and n = 2,145 Violet-stained nuclei in the mixed and siPSME3-only conditions, respectively; analyzed by two sample t-test of proportions.

3.4 Discussion

Our study identifies NUDC, the HSP90 co-chaperone, as a new nuclear binding partner of PSME3. We further demonstrate that PSME3 regulates the abundance of cell-adhesion and migration related proteins, such that loss of PSME3 results in an increase in cell motility. While we could not dissect the nature of the interaction between PSME3 and NUDC, nor could we identify any changes in NUDC function in the absence of PSME3, we showed that a depletion of PSME3 was sufficient to result in a cell-intrinsic deficit in myogenesis, a function PSME3 performs without interaction with the core proteasome.

The observation that PSME3 regulates the rates of cell migration is not a novel one. Indeed, overexpression of PSME3 in cancer cells appears to uniformly increase cell migration and invasiveness, in many cases through altered expression of E-cadherins, N-cadherins, vimentin and other markers of EMT (Bhatti et al., 2019; Chen et al., 2018; Guo et al., 2017; Liu et al., 2018, 2014; Tong et al., 2020; Wang et al., 2015; Yi et al., 2017). Curiously, however, PSME3 has the opposite effect in C2C12 myoblasts. Loss of PSME3, rather than reducing the rate of migration as observed in cancer cells, instead markedly increases it. The layers of regulation that differ between myoblasts and previously studied cancer cells are completely unknown, and whether the molecular targets of PSME3 are similar between the two cell types is also unclear.

Similarly puzzling results are to be found in the list of proteins downregulated by the depletion of PSME3 (Figure 3.5 B). Most highly enriched in this group are members of the mitochondrial respiratory chain, responsible for oxidative production of ATP. This finding recalls the similarly remarkable enrichment of mitochondrial structural proteins, including several members of the MICOS complex, observed in the PSME3 immunoprecipitate described in Chapter 2 (Figure 2.4 A). Loss of the MICOS complex can result in disorganization of the

inner folds of the mitochondrial membrane and improper distribution of respiratory chain components across the membrane (Friedman et al., 2015). The significance of this finding is unclear. While it is well-established that myogenesis requires great changes in mitochondrial function and number and this phenotype is simply a prodrome of impaired myogenesis (Wagatsuma and Sakuma, 2013), it is also possible that an altered mitochondrial network may be contributing to the changes in cell migration alongside the changes observed in cytoskeleton-regulatory proteins (Chen et al., 2023). These changes hardly occur in isolation, and the influences between cell metabolism and cell migration with respect to the extracellular environment flow in both directions (Zanotelli et al., 2021).

We note in our experiments, however, that alterations in the extracellular matrix do not appear to be responsible for the changes, at least, in myogenesis. While cell migration was not measured, it appears that changes intrinsic to the cell itself are primarily responsible for the impaired formation of myotubes rather than alterations in the extracellular environment. Indeed, not only did we fail to observe an improved ability of PSME3-depleted myoblasts to form myotubes in the presence of healthy cells, but we also observed their selective exclusion, such that PSME3-depleted cells were even less capable of forming myotubes in the presence of those that were healthy. One explanation is that the PSME3-depleted population is heterogeneous (a near certainty, given the stochastic nature of transfections), such that, because of inefficient PSME3 knockdown or some other effect, some cells are intrinsically more capable of forming myotubes than others. These exceptionally fusion-competent cells may, in the absence of more facile fusion partners, remain available for long periods of time, allowing less-capable cells sufficient time to fuse and form myotubes. However, when healthy cells are available, these competent cells are more quickly able to find a fusion partner, and thus the normal PSME3-

depleted cell is left without other cells to associate with. This is merely a hypothesis vulnerable to empirical challenges; the mechanisms of myoblast fusion in vertebrates remain obscure, and it remains possible that other mechanisms are at play (Petrany and Millay, 2019).

While an interaction with NUDC is functionally consistent with an alteration in the rates of cell migration, how exactly PSME3 would interact with NUDC to achieve this function, and particularly how the spatial organization of such a system would be arranged, is a standing question that requires the synthesis of several findings and will therefore be addressed in the following section.

Chapters 2 and 3, in part, have been submitted to and are under review for publication at Life Science Alliance. The dissertation author was the primary researcher and author of this paper and is accompanied by Ukrae H. Cho and Martin W. Hetzer.

Chapter 4 Discussion and Future Directions

In this study, we provide several new insights into PSME3 function, particularly as it relates to its role in differentiation. In the second chapter, we provide the first unbiased, global study of PSME3 binding to the chromatin, and find it to associate with roughly 20% of all active promoters, and that these select promoters are on average about 50% more active than their PSME3-poor counterparts. We show that this association is dynamic and dissipates by the second day of differentiation. We identify the RNAPII modifying protein RPRD1A as an interaction partner likely mediator of the chromatin-binding activity of PSME3. However, contrary to our expectations, loss of PSME3 has no effect on gene expression at any measured time point during differentiation.

In the third chapter, we focus on a second newly identified PSME3 interacting partner, the HSP90 co-chaperone NUDC. We show that, consistent with a functional interaction with NUDC, that PSME3 negatively regulates cell migration rates, as well as the abundance of a suite of cell-adhesion and -migration proteins. Loss of PSME3 therefore impaired myogenesis, as myoblasts lacking PSME3 formed fewer and smaller myotubes relative to healthy cells. Finally, we demonstrated that PSME3 acts independently of the proteasome to mediate myogenesis, and such an effect is intrinsic to each cell rather than the result of an alteration in the extracellular environment.

Let us first focus on this final finding: that loss of PSME3 results in the increased abundance of cell-adhesion proteins and an impairment of myogenesis. The most parsimonious explanation based on these two pieces of data would be that PSME3 regulates protein stability through an interaction with the proteasome. This PSME3-containing proteasome would directly degrade target proteins, namely those cell adhesion proteins seen to be upregulated upon loss of

PSME3 and thereby regulate cell migration and differentiation. However, two major pieces of data argue against this possibility, which we will discuss in turn and in depth.

First, we provide abundant evidence in Chapter 3 that PSME3 is solely nuclear. As such, it would be expected to possess no overlap in localization through which it might degrade its target proteins, which are largely cytoplasmic and located to the cell periphery. We show that PSME3 is found largely in the nucleus through imaging in live cells with GFP tagging, further through FLAG-tagging, and finally with staining by an endogenous antibody. It should be granted, however, that several pieces of evidence suggest PSME3 may not be solely nuclear. First, we observed enrichment of several cytoplasmic proteins in the PSME3 immunoprecipitate, including several structural components of mitochondrial membranes (Figure 2.4 A). This might be written off as contamination and non-specific signal were it not also for the serendipitous loss of respiratory chain proteins upon PSME3 depletion (Figure 3.5). Without further evidence of mitochondrial dysfunction, however, no further conclusions can be made. Second, we observed in a minority of cells examined through the live imaging experiments that PSME3 may display a low-abundance association with the centrosome. To what sort of regulation this localization may be subject is unclear and may depend on the state of the cell cycle, as often PSME3 was present at the centrosome when two were present (that is, after the centrosome's replication and prior to mitosis).

One should note that NUDC possesses a general cytoplasmic localization, so it is therefore conceivable that the two proteins may overlap at the centrosome and interact there. It is further possible, yet does not appear immediately plausible, that this small amount of PSME3 conditionally localized to the cytoplasm might regulate the abundance of myriad cytoplasmic proteins on a large scale. One would expect a larger population of protein to be required for such

a function. It is, admittedly, conceivable that such a population of PSME3, invisible to our antibodies and tagging methods, may be found in the cytoplasm without our knowledge. Such would be the case if an alternative splicing variant of PSME3 were found to be highly expressed in our system. However, RNA seq analysis revealed that the major isoform, that which was utilized for GFP- and FLAG-tagging experiments and was targeted by the antibodies used in our experiments, was that which was most highly expressed (Table 4.1). However, a second splicing variant which lacks the exons necessary for detection by the antibodies used in this study is expressed at low levels. It is also depleted by siRNA treatment, and so it cannot be ruled out that this may be the variant of PSME3 relevant for myogenesis.

Table 4.1: A list of detected PSME3 splicing isoforms in C2C12 cells.cycling C2C12 cells. Data is derived from the same three replicates presented in Figure 2.6. The splicing variant detected by all antibodies used in this study, as well as that which was used for all tagging and overexpression experiments, is highlighted in green. In yellow is a lesser splicing isoform that may evade detection by the antibodies used.

Transcript name	**Number of Exons**	**Length (bp)**	**siScr FPKM**	**siPSME3 FPKM**	**Fraction Remaining After Knockdown**
ENSMUST00000142640.7	7	714	0.1	0.04	0.40
ENSMUST00000019470.13	11	2664	32.28	8.02	0.25
ENSMUST00000151385.1	9	674	0.22	0.02	0.10
ENSMUST00000127998.1	6	524	0.19	0.21	1.12
ENSMUST00000131170.1	6	2216	3.58	0.23	0.07

We will discuss explanations for the regulation of myogenesis alternative to protein degradation shortly, but we should first consider the second piece of evidence against such a hypothesis. In Chapter 3, we depleted cells of endogenous PSME3 and induced re-expression of either the full-length copy of PSME3 or that lacking the C-terminal domain necessary for 20s association. We found that the expression of either form of PSME3 was sufficient to restore myotube fusion to its normal levels, suggesting that 20s association (and therefore protein degradation) is dispensable for PSME3-mediated myogenesis. However, several points are worth considering to this end.

First, depletion of endogenous PSME3 was performed with siRNA and was therefore not as complete as a knockout experiment may have been. Unfortunately, performing transgenics in C2C12 cells is technically challenging, as the cells are highly sensitive to passage number. As such, the number of cycles required for selection and expansion would result in cells being so old that myogenesis would be impaired simply by virtue of their replicative age.

Second, as is visible in Figure 3.7, the re-expression of the truncated form of PSME3 was marred by low expression rates. Further, because PSME3 does not co-precipitate with the proteasome in our system (Figure 2.4 A) we had little means to determine whether an interaction between PSME3 and the core proteasome was truly impaired. As discussed earlier, the body of biochemical knowledge pertaining to PSME3 is small. While it is known that a homoheptamer composed of only subunits lacking the C-terminal domain are unable to associate with the 20s core (Zhang and Zhang, 2008), whether complexes containing only one or two mutant copies are similarly affected is unclear. Additionally, what level of PSME3 activity may be required for myogenesis is unknown. As such, a system where lowly-expressed endogenous copies may combine with lowly-expressed mutant copies in any combination is less than ideal. It remains

possible that expression of the C-terminal deletion mutant was able to rescue the phenotype not because PSME3 acts independently of the proteasome, but because it produced mixed PSME3 homoheptamers that could still associate with the proteasome at the level necessary for myogenesis.

An improved experimental scheme to assess PSME3's independence of the proteasome for myogenesis will be discussed in the next section. Let us for the moment, however, accept the data at face value. If PSME3 is not mediating myogenesis through protein degradation, then it need not be situated immediately near its target proteins. Instead, for the purpose of further discussion, we can grant that the functionally relevant population of PSME3 resides in the nucleus, as the bulk of our data suggests. As a result, we need a functional intermediary to bridge PSME3 function in the nucleus with alterations in the abundance of its target proteins in the cytoplasm.

In Chapter 2, we demonstrate that PSME3 binds extensively to highly active promoters in association with RNAPII-regulator RPRD1A. This provided a seductive explanation: perhaps PSME3 regulates the expression of these cell-adhesion genes, such that depletion of PSME3 increases their expression, increases cell migration rates, and thereby impairs differentiation. However, an extensive analysis of gene expression across differentiation lent no evidence to this hypothesis. Indeed, at Day 0 when PSME3-depleted cells already display elevated levels of cell-adhesion-related proteins and an increased migration rate, no mRNA transcript other than PSME3 itself is altered. While a modest change in gene splicing was observed (data not shown), no global defects were observed, and none of the identified isoforms were consistently altered across differentiation, nor would they seem to have any ability to influence these processes.

Bereft of satisfying evidence for gene expression driving the deficits in myogenesis, we turn instead to another highly enriched binding partner of PSME3: NUDC. NUDC is known to be a major player in the chaperone network, a family of proteins with which PSME3 already has demonstrated associations (see the discussions in Chapter 1 on BAG-family proteins). Further, NUDC is known to regulate the post-translational stability of target proteins, specifically those found at the leading edge of migrating cells. Though NUDC is normally considered to be a cytoplasmic protein, we find that it is uniquely situated in both the nucleus and cytoplasm in C2C12 cells, positioning it well to interact with PSME3.

NUDC may thus bridge the gap that the transcription hypothesis failed to span. PSME3 may interact with NUDC within the nucleus to alter its activity in some manner, such that were this altered protein to exit the nucleus (as one would expect there to be some flow between the nuclear and cytoplasmic populations), its ability to aid in the folding of client proteins might be changed. In this way, one could imagine that PSME3 could influence the abundance of cell-adhesion proteins without ever having to leave the nucleus. Though the nature of this "modification" of NUDC is unclear, PSME3's only documented intrinsic function is to act as a chaperone and mediator of protein-protein associations (Cascio, 2021; Zhang and Zhang, 2008). It's possible that this interaction either changes the folding state of NUDC or leads it to associate with binding partners or modifiers that might alter NUDC's activity. This process might be similar to the ubiquitination event that PSME3 elicits by recruiting MDM2 to p53 to promote its degradation (Zhang and Zhang, 2008).

The substantiation of this hypothesis relies on evidence of a functional interaction between PSME3 and NUDC. Unfortunately, none availed themselves over the course of this study. We sought to demonstrate such an interaction by measuring the functional output of

NUDC in the absence of PSME3. However, in PSME3-depleted cells, the number and length of primary cilia, phenotypes known to be regulated by NUDC in retinal epithelial cells, were unaffected. Further, depletion of PSME3 had no effect on NUDC localization or abundance. The only links between PSME3 and NUDC were the physical associations demonstrated by co-IP and PLA, and the documented importance in other cell types for NUDC in cell migration.

As such, the nature of the interaction between PSME3 and NUDC regarding myogenesis remains unknown. In the absence of clear evidence of changes in NUDC function in the absence of PSME3, and for the other reasons listed above, the possibility of protein degradation as a mechanism must be seriously considered, as well as other uninvestigated mechanisms, including mRNA export from the nucleus or activities associated with the ribosome.

Nevertheless, we leave the importance of PSME3 for C2C12 myoblast differentiation well established. We believe that these findings represent a major step forward to understanding PSME3 function and, while they do not resolve many of the standing mysteries surrounding the protein, they will be of interest not only to those who are interested in PSME3 but will be of broad use for their application to the study of chromatin organization and cellular differentiation.

Before we discuss ways in which this study might be improved and other experiments that may resolve some of the difficulties, we will pause briefly to consider the discovery that PSME3 associates extensively with the chromatin in dividing C2C12 cells. Though it appears to bear no physiological importance for myogenesis, the finding is possibly the most striking of those made by the present study, not least for the unexpectedly widespread nature of this interaction. Even more surprising, and equally disappointing from this writer's perspective, was the lack of gene expression changes upon depletion of PSME3. As the results discussed in Chapter 3 fail to shed any further light on this puzzle, a thorough discussion of the nature and

purpose of this interaction is relegated to Chapter 2 Section 4; any further attempts to this end threaten to turn from speculation to fantasy.

Only one additional point bears mentioning in this regard: the apparent heterogeneity of PSME3 activities across experimental contexts. Table 1.1 lists degradation targets of PSME3 and includes, among several other proteins, a slew of transcription factors. These proteins are well-established targets of PSME3 in their respective systems and yet appear unaffected by PSME3 depletion in our experiments. This is not for lack of resolution within our work, as we possess several means by which to measure any disruptions in their function. A stabilization of major transcription factors such as c-Myc, NF-κB, and p53 in the absence of PSME3 should result in measurable changes in gene expression, which we failed to observe. This result alone should not be considered decisive, but similar findings were obtained through proteomics performed on cells lacking PSME3. Indeed, among the proteins upregulated upon PSME3 depletion, not one was a documented degradation target of PSME3. Whether PSME3 possesses any proteolytic functions at all in our system, or instead is simply degrading heretofore uncharacterized targets, is unclear and requires further investigation.

What one may concede without too great a risk is that PSME3 possesses divergent functions dependent on the cellular context. What is true of PSME3 in macrophages or intestinal crypt cells may not be true of PSME3 in C2C12 cells. Indeed, in all published instances, PSME3 was positively correlated with cell migration rates in diverse forms of cancer (Bhatti et al., 2019; Tong et al., 2020; Wang et al., 2015; Yi et al., 2017). In our system, the opposite effect was observed; loss of PSME3 resulted in a marked increase in cell migration rates. Even among cells of the same type, PSME3 may display divergent behaviors. In one lineage of C2C12 cells, we observed a dynamic relocalization of PSME3 from the nucleus to the cytoplasm exclusively in

mature myotubes while it remained cytoplasmic in quiescent satellite cells. However, when a fresh vial was obtained from the cell bank, its descendent cells displayed a uniformly nuclear localization of PSME3 across differentiation.

While no mechanistic insights can be obtained from these observations alone, it suggests that there is much more to learn about the diversity of modification states and interaction partners that PSME3 may possess that allow it to perform so inconstantly. Further, it highlights the need for consistent experimental practices when studying this particularly elusive protein. In the following section, we will discuss precisely what these future studies might be, and through what means PSME3's function might be better understood.

Future Directions

While we demonstrate that a proteasome-binding deficient form of PSME3 is sufficient to restore myogenesis to a normal level in the absence of endogenous PSME3, this experiment involved several less-than-ideal alterations to the cells that may have resulted in results unrepresentative of true cellular physiology. Included among these flaws was the use of a null rather than a dominant negative mutant in an overexpression system. A more ideal experiment would have used the dominant negative N151Y mutation (discussed in Chapter 1), overexpression of which should be sufficient to poison even complexes formed with the endogenous PSME3 copies, no knockdown required. Provided the expression level of this mutant protein was high enough, then one would be more confident that the proteasome-binding activity of PSME3 were truly being impaired. This would have provided a clearer picture of the necessity of PSME3's interaction with the core proteasome in the context of myogenesis.

Additionally, an extensive examination of the function of the chaperone system in the absence of PSME3, with particular attention paid to HSP90/70 efficiency, would be fruitful in revealing the interaction of PSME3 with the protein folding network. Further, positive evidence

that PSME3 functionally interacts with NUDC would strengthen the hypothesis that PSME3 acts independently of the proteasome. Such data may be collected through various means with varyingly satisfying results. One could repeat the same assay that was originally used to identify NUDC as an HSP90 co-chaperone, where HSP90-dependent signaling through the glucocorticoid receptor in transgenic cells results in mCherry expression (Biebl et al., 2022). Loss of PSME3 in such a context may be expected to produce a change in mCherry expression upon glucocorticoid stimulation if PSME3 interacts productively with NUDC. Alternatively, several cell-free *in vitro* protein folding assays with purified HSP90, NUDC, and PSME3 might shed some light on the direct biochemical necessity of PSME3 on NUDC function (Banerjee et al., 2021).

A simpler approach, though, may be to first verify that loss of NUDC in C2C12 cells results in a change in cell migration rates. As this study has leaned heavily on previous findings that NUDC regulates cytoskeletal dynamics, it would be useful to demonstrate that it holds a similar role in our system as well. Further, understanding the effects of a concurrent depletion of PSME3 and NUDC would be particularly important. If NUDC is a positive regulator of cell migration rates as previously demonstrated, then it would suggest that PSME3 and NUDC have an antagonistic relationship in this context. Whether depletion of both NUDC and PSME3 restores cells to a normal rate of migration would be interesting to determine.

Finally regarding NUDC, an investigation of the regions of each protein necessary for an interaction would be enlightening and could be achieved through expression of various deletion mutants of each protein. We would suggest that the homolog-specific insert region of PSME3 (discussed in Chapter 1) is the most likely candidate for this interaction, as it has previously been shown to mediate non-proteolytic protein interactions, as in the case of p53 and MDM2 (Zhang

and Zhang, 2008). What regions of NUDC might be necessary for the interaction are unclear. Additionally, a similar study performed with PSME3 and its interactor RPRD1A would be similarly productive.

As for PSME3's DNA binding activity, it would naturally be useful to investigate other cell types. Given the seemingly labile interaction PSME3 appears to display with the chromatin over the course of differentiation, understanding the contexts under which PSME3 associates with the DNA would seem important, and might be revealed using cells of different lineages. Performing CUT&RUN in cycling myoblasts treated with other conditions known to affect PSME3 function, such as DNA damage or cell cycle inhibitors, may alter its DNA-binding profile as well in an interesting manner.

Lastly, it is important to understand the contribution of PSME3 to myogenesis in a more relevant cell type. C2C12 cells are immortalized and significantly more difficult to differentiate than primary myoblasts obtained directly from a living animal, hinting at important physiological differences between the two cell types. Further, C2C12 cells will only migrate after forming a monolayer, and are hardly mobile when plated in isolation (data not shown). In contrast, primary myoblasts are motile regardless of confluency and will quickly fuse with any available binding partner. This indicates that primary myoblasts, the cells that are responsible for forming muscle in the organism, subject their cytoskeleton to a different system of regulation that may either preclude or potentiate contributions of PSME3. Whether PSME3 is equally important for migration and myogenesis in primary myoblasts and in the developing animal as in cultured C2C12 cells remains unclear, and merits further investigation.

Chapter 5 Materials and Methods

Plasmids

Constructs were created by insertion of PSME3 into pcDNA3.1(+)-C-eGFP or pcDNA3.1(+)-N-eGFP for live imaging, and pcDNA3.1(+)-N-DYK or pcDNA3.1(+)-C-DYK for FLAG-tagged experiments. PSME3 sequence (accession NM_011192.4) was obtained from GenScript.

Antibodies

The following antibodies were used: PSME3 (rabbit polyclonal, BML-PW8190, Enzo Life Sciences, 1:6,000 IF, 1:200 CUT&RUN) (rabbit polyclonal, 38-3800, Thermo Fisher Scientific, 1:125 WB, 1:25 IP); β-Tubulin (rabbit monoclonal 9F3, #2128, Cell Signaling Technology; 1:1,000 Western blot); Myosin 4 (mouse monoclonal MF20, 14-6503-82, Thermo Fisher Scientific; 1:100 IF); Myogenin (mouse monoclonal F5D, 14-5643-82, Thermo Fisher Scientific, 1:250 IF); FLAG (mouse monoclonal M2, F1804, Sigma-Aldrich, 1:500 IF and PLA, 1:1,000 Western Blot); RPRD1A (rabbit polyclonal, HPA040602, Sigma-Aldrich, 1:50 PLA, 1:250 Western Blot); NUDC (rabbit polyclonal, 10681-1-AP, Proteintech, 1:25 IF and PLA); H3K4me3 (rabbit monoclonal C42D8, #9751, Cell Signaling Technology, 1:50 CUT&RUN).

Cell culture and transfection

C2C12 cells obtained from the American Type Culture Collection (ATCC) were cultured in DMEM with 20% FBS. Cells were allowed two passages (four days) after thawing before being subjected to any experiments. No cells over passage nine were used for any experiment.

For transfection with siRNA, cycling C2C12 cells were reverse transfected on two consecutive days with Lipofectamine RNAiMAX transfection reagent (Thermo Fisher Scientific) and either SMARTpool siRNA from Horizon Discovery targeting PSME3 (L-062727-01-0005) or a non-targeting control pool (DH-D-001810-10-20) in OptiMEM. Cells were allowed to recover for two days before being collected or induced to differentiate. For differentiation into

myotubes, cells were grown to full confluency, washed once with PBS, and switched to DMEM with 2% horse serum, designated as Day 0. Differentiation media was refreshed every 48 hours.

For transfection with plasmids, cells were grown to 80% confluency and were treated with a mixture of Lipofectamine 2000 (Thermo Fisher Scientific, 11668019) and the plasmid of interest. Cells were passaged on the following day and examined on the day thereafter for expression.

Immunofluorescence and proximity ligation assay

Two methods were used for immunofluorescence. In the first method, cells were fixed with 4% formaldehyde in PBS for five minutes at room temperature. They were then incubated with a blocking/permeabilization buffer containing 0.1% Triton X-100, 0.02% SDS, and 10 mg/mL BSA in PBS. The cells were incubated in primary antibody in the blocking solution for ninety minutes, followed by three washes in PBS, an incubation with fluorescent secondary antibodies in the blocking solution, then an additional three washes in PBS before mounting in Everbrite Mounting Medium with DAPI (Biotium, 23002). This method was used for all imaging experiments that did not involve staining for NUDC.

In the second method, fixation was performed by incubation with 4% formaldehyde in PBS for five minutes at room temperature, followed by eight minutes in cold 100% methanol at -20°C. The blocking/permeabilization buffer was composed of 0.1% saponin with 10 mg/mL BSA, which was also used as a diluent for the primary and secondary antibody. This method is otherwise identical to the first method and was used exclusively for experiments requiring staining of NUDC.

The proximity ligation assay was performed with the DuoLink In Situ Orange Starter Kit (Sigma-Aldrich, DUO92102-KT) according to the manufacturer's instructions with the following exceptions: permeabilization/blocking and primary antibody dilution/incubation was performed

with the buffers and according to the principles described in the immediately preceding paragraphs. Negative controls included several wells in which one or both primary antibodies were omitted, while all other components remained.

Imaging of mature myotubes as well as cell migration was performed with a Nikon Ti2-E Widefield Fluorescence Microscope using a 20x objective, while all other imaging experiments utilized a Leica SP8 Laser Confocal Microscope using a 63x oil immersion objective. All imaging experiments were performed in µ-Slide 8 Well ibiTreat IBIDI chambers.

Retrovirus production

The coding sequence of PSME3 was FLAG-tagged and cloned into the pQCXIB vector, with which 80% confluent HEK293T cells were transfected along with the pCL-Ampho retrovirus packaging vector in equal proportions. The media was changed at 24 hours after transfection and virus-containing conditioned media was collected an additional 24 hours thereafter. After being passed through a 0.45 micron filter, the conditioned media was combined 1:1 with fresh growth media and incubated with C2C12 cells for 24 hours before exchange with fresh growth media. At 48 hours after infection, cells were selected with 1-2 ug/mL of puromycin until cell death ceased and control cells had uniformly perished. For knockdown experiments, siRNA targeting the 3'-UTR was used to deplete the endogenous copy of PSME3 while sparing the tagged variants.

Cell mixing

Cells were treated with siRNA as described above, and on the day prior to differentiation were stained with either CellTracker Deep Red Dye (1mM solution at 1:250; Thermo Fisher Scientific, C34565) or CellTrace Violet Dye (5mM at 1:500; Thermo Fisher Scientific, C34571) according to the manufacturer's instructions and as previously described (Zhang et al., 2017). After staining, cells were counted and either plated in isolation, or in a 1:1 mixture.

Differentiation was induced on the following day, and incorporation into myotubes was assessed on day 3 after fixing and staining for MHC. Due to the level of cell death normally observed during differentiation, blue nuclei indicating cells lacking PSME3 were counted by hand. The fraction contained in MHC-positive structures was quantified and compared between the separate conditions.

Image analysis

The number of myogenin-positive nuclei within each MHC-positive structure was performed manually in ImageJ (Schindelin et al., 2012). The total fraction of nuclei contained within MHC-positive structures was performed by thresholding the MHC channel to create a binary image, followed by watershedding to fill in the gaps within the cell. DAPI-positive nuclei were similarly converted to a binary image, and the MHC image was used as a mask to subtract nuclei not contained within. The total number of nuclei remaining were quantified using the Analyze Particles function of ImageJ.

Cell migration was measured manually by displacement of the center of the nucleus over two-hour intervals. The sum of these displacements over ten such intervals (20 hours total) was summed for each individual cell. Cells were selected at hour zero only if they were clearly visible, and were discarded if, during the course of the measurement, they divided or died.

Immunoblotting

Cells were collected by trypsinization and counted. 200 uL of RIPA buffer (50mM Tris-HCl pH 7.5, 150mM NaCl, 1% Triton X-100, 0.5% sodium deoxycholate, 0.1% SDS, and 1x Pierce Protease Inhibitor Tablet (Thermo Fisher Scientific, A32963)) was added per 1e6 cells, which were incubated for 30 minutes at 4°C with rotation. Lysates were then briefly sonicated (three five second pulses at approximately 1 Watt) before being clarified by centrifugation for 8 minutes at 10,000 RPM at 4°C on a tabletop centrifuge. 4x Sample Loading Buffer (Biorad,

1610747) with beta mercaptoethanol was added to the lysates, which were then incubated at 95℃ for five minutes.

Samples were loaded into 4-12% gradient gels (Bolt™ Bis-Tris Plus Mini Protein Gels, Thermo Fisher Scientific, NW04122BOX) and run in Bolt MOPS SDS (Thermo Fisher Scientific, B000102). Proteins were transferred using the Biorad Trans-Blot Turbo Transfer System and were blocked in TBS-T plus 5% milk for one hour before being incubated overnight with primary antibodies in the same solution. Membranes were washed three times in TBS-T before probing with secondary antibodies conjugated with HRP targeting either mouse (Thermo Fisher Scientific, 31430) or rabbit (Thermo Fisher, G-21234). Membranes were incubated with SuperSignal West Pico PLUS Chemiluminescent Substrate (Thermo Fisher Scientific, 34580) before imaging.

Immunoprecipitation

Cells were collected by trypsinization, washed once with PBS, and lysed for 30 minutes at 4℃ with rotation in an immunoprecipitation (IP) buffer containing 20 mM Tris-HCl pH 7.5, 100mM NaCl, 1% NP40, 1mM EDTA, and 1x Pierce Protease Inhibitor Tablet (Thermo Fisher Scientific, A32963). 200 uL of IP buffer was used per 1e6 cells, and 2.5e6 cells were used for each immunoprecipitation. Cells were clarified by centrifugation for 8 minutes at 10,000 RPM at 4℃ on a tabletop centrifuge. Primary antibodies were added directly into the clarified supernatant at 2.8 ug per 1e6 cells, with an isotype IgG (Biotechne, AB-105-C) used as a control. This solution was incubated overnight at 4℃ with rotation. The following morning, 50 uL of Protein A Dynabeads (Thermo Fisher Scientific, 10008D) was added directly to the solution, which was then incubated for two hours at 4℃ with rotation. Beads were removed from solution with a magnet and washed three times by resuspension with 200 uL of IP buffer. Beads were then collected in 100 uL of IP buffer and transferred to a clean tube before being resuspended in

3x Sample Loading Buffer (Biorad, 1610747) with beta mercaptoethanol and incubated for five minutes at 95℃. The supernatant was collected and frozen on dry ice before being stored at -80℃. Efficacy of the precipitation was assessed via immunoblot as described above, but using a protein A-HRP conjugate (Millipore, 18-160) instead of the usual secondary antibodies to avoid detection of eluted IgG.

CUT&RUN

CUT&RUN was performed using the kit provided by Cell Signaling Technology (#86652) according to the manufacturer's instructions, but with the following modifications. Three hundred thousand cells were used per condition. Further, incubation was performed not overnight at 4℃ as the manufacturer recommends, but rather for 30 minutes at room temperature to limit the level of cell death. Cells, unfixed, were frozen prior to assaying in 10% DMSO in FBS unless otherwise indicated.

Libraries were prepared using the NEBNext Ultra™ II DNA Library Prep Kit for Illumina (E7645L) with primers from the NEBNext Multiplex Oligos for Illumina (Dual Index Primers Set 1, E7600S) according to the manufacturer's instructions. Prepared libraries were sent to Novogene for sequencing. Raw reads were cleaned with Trim Galore and aligned with Bowtie2, whereafter peaks were called with MACS2 (Babraham, 2016; Langmead and Salzberg, 2012; Zhang et al., 2008).

RNA Sequencing

Cells were collected directly from the plate by washing once with PBS followed by addition of Trizol reagent (Thermo Fisher Scientific, 15596026). The samples were incubated in the plate for three minutes at room temperature prior to freezing in dry ice and long-term storage at -80℃. RNA was isolated from the sample using a chloroform extraction followed by purification with the RNeasy kit from Qiagen. Samples were submitted to Novogene for library

preparation and sequencing. RNA reads were aligned with RNA STAR and comparative gene expression analysis was performed with DESeq2 (Dobin et al., 2013; Love et al., 2014).

Mass Spectrometry Sample preparation

Samples in 3x Laemmli buffer were first cleaned up by SP3 using a commercial kit (PreOmics GmbH, 50 mg of beads per sample), then processed using the iST kit (PreOmics GmbH) according to the manufacturer's instructions. Tryptic digestion was stopped after 1 h and cleaned-up samples were vacuum dried. Finally, samples were re-dissolved by 10 min sonication in the iST kit's LC LOAD buffer.

LC-MS/MS analysis

Samples were analyzed by LC-MS/MS on a nanoElute 2 nano-HPLC (Bruker Daltonics) coupled with a timsTOF HT (Bruker Daltonics), concentrated over a "Thermo Trap Cartridge 5mm", then bound to a PepSep XTREME column (1.5 µm C18-coated particles, 25 cm * 150 µm ID, Bruker P/N 1893476) heated at 50°C and eluted over the following 90 min gradient: solvent A, MS-grade H_2O + 0.1% formic acid; solvent B, 100% acetonitrile + 0.1% formic acid; constant 0.60 nL/min flow; B percentage: 0 min, 2%; 90 min, 30%, followed immediately by a 8 min plateau at 95%. MS method: M/Z range = 99.993933-1700 Th, ion mobility range = 0.6-1.6 1/K0; transfer time = 60 µs, pre-pulse storage time = 12 µs, enable high sensitivity modus = off, ion polarity = Positive, scan mode = MS/MS (Pasef); TIMS parameters: ramp time = 100 ms, accumulation time = 100 ms; PASEF parameters: ms/ms scans = 10, total cycle time = 1.167166 s, charge range = 0-5, intensity threshold for scheduling = 2000, scheduling target intensity = 15000, exclusion release time = 0.4 min, reconsider precursor switch = on, current/previous intensity ratio = 4, exclusion window mass width = 0.015 m/z, exclusion window v·s/cm² width = 0.015 V*s/cm².

LC-MS/MS Data analysis

Raw files were searched in FragPipe version 20.0 against a *Mus musculus* proteome sourced from UniprotKB. Fixed cysteine modification was set to +57.02146 (Cysteine). Variable modifications were set to +15.9949 (Methionine), +42.0106 (protein N-term), +79.96633 (STY) and -17.0265 (Gln -> pyroGlu). Peptide identifications were validated using Percolator. Results were filtered in Philosopher at protein level at FDR 1%. MS1-level peptide quantitation was performed using IonQuant with match-between-runs turned on.

FragPipe's output was re-processed using in-house R scripts, starting from the psm.tsv tables. MS1 intensities were re-normalized to the median. The long format psm.tsv table was consolidated into a wide format peptidoforms table, summing up quantitative values where necessary. Missing values were imputed using two different strategies: i) the KNN (K-Nearest Neighbours) method for Missing-At-Random values within sample groups, and ii) the QRICL (Quantile Regression Imputation of Left-Censored data) method for Missing-Not-At-Random values. Peptidoform intensity values were re-normalized as follows: 1 and 2. Peptidoform-level ratios were then calculated. Protein groups were inferred from observed peptides, and quantified using an in-house algorithm which: i) computes a mean protein-level profile across samples using individual, normalized peptidoform profiles ("relative quantitation" step), ii) following the best-flyer hypothesis, normalizes this profile to the mean intensity level of the most intense peptidoform ("unscaled absolute quantitation" step); for protein groups with at least 3 unique peptidoforms, only unique ones were used, otherwise razor peptidoforms were also included; Phosphopeptidoforms and their unmodified counterparts were excluded from the calculations. Estimated expression values were log10-converted and re-normalized using the Levenberg-Marquardt procedure. Average log10 expression values were tested for significance using a one-sided moderated t-test per samples group (limma). Significance thresholds were calculated using

the Benjamini-Hochberg procedure for False Discovery Rate values of 10%, 20% and 30%. FRegulated protein groups were defined as those with a significant P-value and a log2 ratio greater than 1 for immunoprecipitation experiments, and a log2 ratio greater than 0.3 for proteomics experiments. GO terms enrichment analysis was performed using Metascape Gene Annotation & Analysis Resource (Zhou et al., 2019).

References

Abildgaard AB, Gersing SK, Larsen-Ledet S, Nielsen SV, Stein A, Lindorff-Larsen K, Hartmann-Petersen R. 2020. Co-Chaperones in Targeting and Delivery of Misfolded Proteins to the 26S Proteasome. *Biomolecules* **10**. doi:10.3390/biom10081141

Ali I, Ruiz DG, Ni Z, Johnson JR, Zhang H, Li P-C, Khalid MM, Conrad RJ, Guo X, Min J, Greenblatt J, Jacobson M, Krogan NJ, Ott M. 2019. Crosstalk between RNA Pol II C-Terminal Domain Acetylation and Phosphorylation via RPRD Proteins. *Mol Cell* **74**:1164-1174.e4. doi:10.1016/j.molcel.2019.04.008

Ashok A, Ashwathnarayan A, Bhaskar S, Shekar S, Kalathur G, Prasanna J, Kumar A. 2024. Inhibition of proteasome activity facilitates definitive endodermal specification of pluripotent stem cells by influencing YAP signalling. *Life Sci* **358**:123160. doi:10.1016/j.lfs.2024.123160

Auld KL, Brown CR, Casolari JM, Komili S, Silver PA. 2006. Genomic association of the proteasome demonstrates overlapping gene regulatory activity with transcription factor substrates. *Mol Cell* **21**:861–871. doi:10.1016/j.molcel.2006.02.020

Aumais JP, Tunstead JR, McNeil RS, Schaar BT, McConnell SK, Lin SH, Clark GD, Yu-Lee LY. 2001. NudC associates with Lis1 and the dynein motor at the leading pole of neurons. *J Neurosci* **21**:RC187. doi:10.1523/JNEUROSCI.21-24-j0002.2001

Bae HJ, Dubarry M, Jeon J, Soares LM, Dargemont C, Kim J, Geli V, Buratowski S. 2020. The Set1 N-terminal domain and Swd2 interact with RNA polymerase II CTD to recruit COMPASS. *Nat Commun* **11**:2181. doi:10.1038/s41467-020-16082-2

Baldin V, Militello M, Thomas Y, Doucet C, Fic W, Boireau S, Jariel-Encontre I, Piechaczyk M, Bertrand E, Tazi J, Coux O. 2008. A novel role for PA28gamma-proteasome in nuclear speckle organization and SR protein trafficking. *Mol Biol Cell* **19**:1706–1716. doi:10.1091/mbc.e07-07-0637

Banerjee M, Hatial I, Keegan BM, Blagg BSJ. 2021. Assay design and development strategies for finding Hsp90 inhibitors and their role in human diseases. *Pharmacol Ther* **221**:107747. doi:10.1016/j.pharmthera.2020.107747

Bard JAM, Goodall EA, Greene ER, Jonsson E, Dong KC, Martin A. 2018. Structure and function of the 26S proteasome. *Annu Rev Biochem* **87**:697–724. doi:10.1146/annurev-biochem-062917-011931

Barton LF, Runnels HA, Schell TD, Cho Y, Gibbons R, Tevethia SS, Deepe GS, Monaco JJ. 2004. Immune defects in 28-kDa proteasome activator gamma-deficient mice. *J Immunol* **172**:3948–3954. doi:10.4049/jimmunol.172.6.3948

Bax M, McKenna J, Do-Ha D, Stevens CH, Higginbottom S, Balez R, Cabral-da-Silva MEC, Farrawell NE, Engel M, Poronnik P, Yerbury JJ, Saunders DN, Ooi L. 2019. The ubiquitin proteasome system is a key regulator of pluripotent stem cell survival and motor neuron differentiation. *Cells* **8**. doi:10.3390/cells8060581

Ben-Nissan G, Sharon M. 2014. Regulating the 20S proteasome ubiquitin-independent

degradation pathway. *Biomolecules* **4**:862–884. doi:10.3390/biom4030862

Bethesda (MD): National Library of Medicine (US), National Center for Biotechnology Information. 1988. Psme3 proteaseome (prosome, macropain) activator subunit 3 (PA28 gamma, Ki) [Mus musculus (house mouse)]Gene ID: 19192. https://www.ncbi.nlm.nih.gov/gene/19192

Bhatti MZ, Pan L, Wang T, Shi P, Li L. 2019. REGγ potentiates TGF-β/Smad signal dependent epithelial-mesenchymal transition in thyroid cancer cells. *Cell Signal* **64**:109412. doi:10.1016/j.cellsig.2019.109412

Biebl MM, Delhommel F, Faust O, Zak KM, Agam G, Guo X, Mühlhofer M, Dahiya V, Hillebrand D, Popowicz GM, Kampmann M, Lamb DC, Rosenzweig R, Sattler M, Buchner J. 2022. NudC guides client transfer between the Hsp40/70 and Hsp90 chaperone systems. *Mol Cell* **82**:555-569.e7. doi:10.1016/j.molcel.2021.12.031

Bitman-Lotan E, Orian A. 2021. Nuclear organization and regulation of the differentiated state. Cell Mol Life Sci 78:3141–3158. doi:10.1007/s00018-020-03731-4

Blau HM, Chiu CP, Webster C. 1983. Cytoplasmic activation of human nuclear genes in stable heterocaryons. *Cell* **32**:1171–1180. doi:10.1016/0092-8674(83)90300-8

Bodnar N, Rapoport T. 2017. Toward an understanding of the Cdc48/p97 ATPase. [version 1; peer review: 4 approved]. *F1000Res* **6**:1318. doi:10.12688/f1000research.11683.1

Boulpicante M, Darrigrand R, Pierson A, Salgues V, Rouillon M, Gaudineau B, Khaled M, Cattaneo A, Bachi A, Cascio P, Apcher S. 2020. Tumors escape immunosurveillance by overexpressing the proteasome activator PSME3. *Oncoimmunology* **9**:1761205. doi:10.1080/2162402X.2020.1761205

Brooks P, Fuertes G, Murray RZ, Bose S, Knecht E, Rechsteiner MC, Hendil KB, Tanaka K, Dyson J, Rivett J. 2000. Subcellular localization of proteasomes and their regulatory complexes in mammalian cells. *Biochem J* **346 Pt 1**:155–161. doi:10.1042/bj3460155

Carrettiero DC, Almeida MC, Longhini AP, Rauch JN, Han D, Zhang X, Najafi S, Gestwicki JE, Kosik KS. 2022. Stress routes clients to the proteasome via a BAG2 ubiquitin-independent degradation condensate. *Nat Commun* **13**:3074. doi:10.1038/s41467-022-30751-4

Cascio P. 2021. Pa28γ: new insights on an ancient proteasome activator. *Biomolecules* **11**. doi:10.3390/biom11020228

Cascio P. 2014. PA28αβ: the enigmatic magic ring of the proteasome? *Biomolecules* **4**:566–584. doi:10.3390/biom4020566

Catic A, Suh CY, Hill CT, Daheron L, Henkel T, Orford KW, Dombkowski DM, Liu T, Liu XS, Scadden DT. 2013. Genome-wide map of nuclear protein degradation shows NCoR1 turnover as a key to mitochondrial gene regulation. *Cell* **155**:1380–1395. doi:10.1016/j.cell.2013.11.016

Chapman RD, Heidemann M, Hintermair C, Eick D. 2008. Molecular evolution of the RNA

polymerase II CTD. *Trends Genet* **24**:289–296. doi:10.1016/j.tig.2008.03.010

Chaves S, Baskerville C, Yu V, Reed SI. 2010. Cks1, Cdk1, and the 19S proteasome collaborate to regulate gene induction-dependent nucleosome eviction in yeast. *Mol Cell Biol* **30**:5284–5294. doi:10.1128/MCB.00952-10

Chen D-D, Hao J, Shen C-H, Deng X-M, Yun C-H. 2022. Atomic resolution Cryo-EM structure of human proteasome activator PA28γ. *Int J Biol Macromol* **219**:500–507. doi:10.1016/j.ijbiomac.2022.07.246

Chen H, Gao X, Sun Z, Wang Q, Zuo D, Pan L, Li Kun, Chen J, Chen G, Hu K, Li Ke, Shah AS, Huang T, Muhammad Zeeshan B, Tong L, Jiao C, Liu J, Chen T, Yao L, Dang Y, Li L. 2017. REGγ accelerates melanoma formation by regulating Wnt/β-catenin signalling pathway. *Exp Dermatol* **26**:1118–1124. doi:10.1111/exd.13394

Chen J, Wang Y, Xu C, Chen K, Zhao Q, Wang S, Yin Y, Peng C, Ding Z, Cong Y. 2021. Cryo-EM of mammalian PA28αβ-iCP immunoproteasome reveals a distinct mechanism of proteasome activation by PA28αβ. *Nat Commun* **12**:739. doi:10.1038/s41467-021-21028-3

Chen Qian, Wu Z, Shi Y, Li Z, Yang J, Qu M, Zhang S, Wang Z, Ji N, Li J, Shen Y, Xie L, Chen Qianming. 2024. Loss of PA28γ exacerbates imbalanced differentiation of bone marrow stromal cells during bone formation and bone healing in mice. *J Bone Miner Res* **39**:326–340. doi:10.1093/jbmr/zjae012

Chen S, Wang Q, Wang L, Chen H, Gao X, Gong D, Ma J, Kubra S, Yao X, Li X, Li L, Zhai W, Zheng J. 2018. REGγ deficiency suppresses tumor progression via stabilizing CK1ε in renal cell carcinoma. *Cell Death Dis* **9**:627. doi:10.1038/s41419-018-0646-2

Chen W, Zhao H, Li Y. 2023. Mitochondrial dynamics in health and disease: mechanisms and potential targets. *Signal Transduct Target Ther* **8**:333. doi:10.1038/s41392-023-01547-9

Chen X, Barton LF, Chi Y, Clurman BE, Roberts JM. 2007. Ubiquitin-independent degradation of cell-cycle inhibitors by the REGgamma proteasome. *Mol Cell* **26**:843–852. doi:10.1016/j.molcel.2007.05.022

Cioce M, Boulon S, Matera AG, Lamond AI. 2006. UV-induced fragmentation of Cajal bodies. *J Cell Biol* **175**:401–413. doi:10.1083/jcb.200604099

Clevers H. 2006. Wnt/β-catenin signaling in development and disease. *Cell* **127**:469–480. doi:10.1016/j.cell.2006.10.018

Cui S, Li L, Yu RT, Downes M, Evans RM, Hulin J-A, Makarenkova HP, Meech R. 2019. β-Catenin is essential for differentiation of primary myoblasts via cooperation with MyoD and α-catenin. *Development* **146**. doi:10.1242/dev.167080

Daniels DL, Weis WI. 2005. Beta-catenin directly displaces Groucho/TLE repressors from Tcf/Lef in Wnt-mediated transcription activation. *Nat Struct Mol Biol* **12**:364–371. doi:10.1038/nsmb912

Dasuri K, Zhang L, Ebenezer P, Fernandez-Kim SO, Bruce-Keller AJ, Szweda LI, Keller JN. 2011. Proteasome alterations during adipose differentiation and aging: links to impaired adipocyte differentiation and development of oxidative stress. *Free Radic Biol Med* **51**:1727–1735. doi:10.1016/j.freeradbiomed.2011.08.001

Deshmukh FK, Ben-Nissan G, Olshina MA, Füzesi-Levi MG, Polkinghorn C, Arkind G, Leushkin Y, Fainer I, Fleishman SJ, Tawfik D, Sharon M. 2023. Allosteric regulation of the 20S proteasome by the Catalytic Core Regulators (CCRs) family. *Nat Commun* **14**:3126. doi:10.1038/s41467-023-38404-w

Dias JD, Rito T, Torlai Triglia E, Kukalev A, Ferrai C, Chotalia M, Brookes E, Kimura H, Pombo A. 2015. Methylation of RNA polymerase II non-consensus Lysine residues marks early transcription in mammalian cells. *eLife* **4**. doi:10.7554/eLife.11215

Dixon JR, Jung I, Selvaraj S, Shen Y, Antosiewicz-Bourget JE, Lee AY, Ye Z, Kim A, Rajagopal N, Xie W, Diao Y, Liang J, Zhao H, Lobanenkov VV, Ecker JR, Thomson JA, Ren B. 2015. Chromatin architecture reorganization during stem cell differentiation. Nature 518:331–336. doi:10.1038/nature14222

Dong S, Jia C, Zhang S, Fan G, Li Y, Shan P, Sun L, Xiao W, Li L, Zheng Y, Liu Jinqin, Wei H, Hu C, Zhang W, Chin YE, Zhai Q, Li Q, Liu Jian, Jia F, Mo Q, Wang C. 2013. The REGγ proteasome regulates hepatic lipid metabolism through inhibition of autophagy. *Cell Metab* **18**:380–391. doi:10.1016/j.cmet.2013.08.012

Esser C, Alberti S, Höhfeld J. 2004. Cooperation of molecular chaperones with the ubiquitin/proteasome system. *Biochim Biophys Acta* **1695**:171–188. doi:10.1016/j.bbamcr.2004.09.020

Ezhkova E, Tansey WP. 2004. Proteasomal ATPases link ubiquitylation of histone H2B to methylation of histone H3. *Mol Cell* **13**:435–442. doi:10.1016/s1097-2765(04)00026-7

Fabre B, Lambour T, Delobel J, Amalric F, Monsarrat B, Burlet-Schiltz O, Bousquet-Dubouch M-P. 2013. Subcellular distribution and dynamics of active proteasome complexes unraveled by a workflow combining in vivo complex cross-linking and quantitative proteomics. *Mol Cell Proteomics* **12**:687–699. doi:10.1074/mcp.M112.023317

Fabre B, Lambour T, Garrigues L, Ducoux-Petit M, Amalric F, Monsarrat B, Burlet-Schiltz O, Bousquet-Dubouch M-P. 2014. Label-free quantitative proteomics reveals the dynamics of proteasome complexes composition and stoichiometry in a wide range of human cell lines. *J Proteome Res* **13**:3027–3037. doi:10.1021/pr500193k

Fan J, Liu L, Liu Q, Cui Y, Yao B, Zhang M, Gao Y, Fu Y, Dai H, Pan J, Qiu Y, Liu CH, He F, Wang Y, Zhang L. 2019. CKIP-1 limits foam cell formation and inhibits atherosclerosis by promoting degradation of Oct-1 by REGγ. *Nat Commun* **10**:425. doi:10.1038/s41467-018-07895-3

Fan X, Zhao J, Ren F, Wang Y, Feng Y, Ding L, Zhao L, Shang Y, Li J, Ni J, Jia B, Liu Y, Chang Z. 2018. Dimerization of p15RS mediated by a leucine zipper-like motif is critical for its

inhibitory role on Wnt signaling. *J Biol Chem* **293**:7618–7628. doi:10.1074/jbc.RA118.001969

Ferdous A, Gonzalez F, Sun L, Kodadek T, Johnston SA. 2001. The 19S regulatory particle of the proteasome is required for efficient transcription elongation by RNA polymerase II. *Mol Cell* **7**:981–991. doi:10.1016/s1097-2765(01)00250-7

Fesquet D, Llères D, Grimaud C, Viganò C, Méchali F, Boulon S, Coux O, Bonne-Andrea C, Baldin V. 2021. The 20S proteasome activator PA28γ controls the compaction of chromatin. *J Cell Sci* **134**. doi:10.1242/jcs.257717

Förster A, Masters EI, Whitby FG, Robinson H, Hill CP. 2005. The 1.9 A structure of a proteasome-11S activator complex and implications for proteasome-PAN/PA700 interactions. *Mol Cell* **18**:589–599. doi:10.1016/j.molcel.2005.04.016

Fort P, Kajava AV, Delsuc F, Coux O. 2015. Evolution of proteasome regulators in eukaryotes. *Genome Biol Evol* **7**:1363–1379. doi:10.1093/gbe/evv068

Frayssinhes J-YA, Cerruti F, Laulin J, Cattaneo A, Bachi A, Apcher S, Coux O, Cascio P. 2021. PA28γ-20S proteasome is a proteolytic complex committed to degrade unfolded proteins. *Cell Mol Life Sci* **79**:45. doi:10.1007/s00018-021-04045-9

Friedman JR, Mourier A, Yamada J, McCaffery JM, Nunnari J. 2015. MICOS coordinates with respiratory complexes and lipids to establish mitochondrial inner membrane architecture. *eLife* **4**. doi:10.7554/eLife.07739

Ganji R, Mukkavalli S, Somanji F, Raman M. 2018. The VCP-UBXN1 Complex Mediates Triage of Ubiquitylated Cytosolic Proteins Bound to the BAG6 Complex. *Mol Cell Biol* **38**. doi:10.1128/MCB.00154-18

Gao X, Chen H, Liu J, Shen S, Wang Q, Clement TM, Deskin BJ, Chen C, Zhao D, Wang L, Guo L, Ma X, Zhang B, Xu Y, Li X, Li L. 2019. The REGγ-Proteasome Regulates Spermatogenesis Partially by P53-PLZF Signaling. *Stem Cell Reports* **13**:559–571. doi:10.1016/j.stemcr.2019.07.010

Gao X, Wang Q, Yuan L, Jiao C, Yu Y, Wang X, Xu P, Ma Y, Wu Y, Wu Z, Li L, Xiao J, Dang Y. 2021. REGγ regulates hair cycle by activating Lgr5 positive hair follicle stem cells. *J Dermatol Sci* **102**:101–108. doi:10.1016/j.jdermsci.2021.04.002

Geng F, Tansey WP. 2012. Similar temporal and spatial recruitment of native 19S and 20S proteasome subunits to transcriptionally active chromatin. *Proc Natl Acad Sci USA* **109**:6060–6065. doi:10.1073/pnas.1200854109

Geng F, Wenzel S, Tansey WP. 2012. Ubiquitin and proteasomes in transcription. *Annu Rev Biochem* **81**:177–201. doi:10.1146/annurev-biochem-052110-120012

Gillette TG, Gonzalez F, Delahodde A, Johnston SA, Kodadek T. 2004. Physical and functional association of RNA polymerase II and the proteasome. *Proc Natl Acad Sci USA* **101**:5904–5909. doi:10.1073/pnas.0305411101

Guo J, Hao J, Jiang H, Jin J, Wu H, Jin Z, Li Z. 2017. Proteasome activator subunit 3 promotes pancreatic cancer growth via c-Myc-glycolysis signaling axis. *Cancer Lett* **386**:161–167. doi:10.1016/j.canlet.2016.08.018

Hagemann C, Patel R, Blank JL. 2003. MEKK3 interacts with the PA28 gamma regulatory subunit of the proteasome. *Biochem J* **373**:71–79. doi:10.1042/BJ20021758

Hsin J-P, Manley JL. 2012. The RNA polymerase II CTD coordinates transcription and RNA processing. *Genes Dev* **26**:2119–2137. doi:10.1101/gad.200303.112

Huang L, Haratake K, Miyahara H, Chiba T. 2016. Proteasome activators, PA28γ and PA200, play indispensable roles in male fertility. *Sci Rep* **6**:23171. doi:10.1038/srep23171

Ishikawa H, Marshall WF. 2011. Ciliogenesis: building the cell's antenna. *Nat Rev Mol Cell Biol* **12**:222–234. doi:10.1038/nrm3085

Islam MA, Choi HJ, Dash R, Sharif SR, Oktaviani DF, Seog D-H, Moon IS. 2020. N-Acetyl-D-Glucosamine Kinase Interacts with NudC and Lis1 in Dynein Motor Complex and Promotes Cell Migration. *Int J Mol Sci* **22**. doi:10.3390/ijms22010129

Jawed A, Ho C-T, Grousl T, Shrivastava A, Ruppert T, Bukau B, Mogk A. 2022. Balanced activities of Hsp70 and the ubiquitin proteasome system underlie cellular protein homeostasis. *Front Mol Biosci* **9**:1106477. doi:10.3389/fmolb.2022.1106477

Jiang T-X, Ma S, Han X, Luo Z-Y, Zhu Q-Q, Chiba T, Xie W, Lin K, Qiu X-B. 2021. Proteasome activator PA200 maintains stability of histone marks during transcription and aging. *Theranostics* **11**:1458–1472. doi:10.7150/thno.48744

Jiao C, Li L, Zhang P, Zhang L, Li K, Fang R, Yuan L, Shi K, Pan L, Guo Q, Gao X, Chen G, Xu S, Wang Q, Zuo D, Wu W, Qiao S, Wang X, Moses R, Xiao J, Li X. 2020. REGγ ablation impedes dedifferentiation of anaplastic thyroid carcinoma and accentuates radio-therapeutic response by regulating the Smad7-TGF-β pathway. *Cell Death Differ* **27**:497–508. doi:10.1038/s41418-019-0367-9

Jonik-Nowak B, Menneteau T, Fesquet D, Baldin V, Bonne-Andrea C, Méchali F, Fabre B, Boisguerin P, de Rossi S, Henriquet C, Pugnière M, Ducoux-Petit M, Burlet-Schiltz O, Lamond AI, Fort P, Boulon S, Bousquet M-P, Coux O. 2018. PIP30/FAM192A is a novel regulator of the nuclear proteasome activator PA28γ. *Proc Natl Acad Sci USA* **115**:E6477–E6486. doi:10.1073/pnas.1722299115

Kanai K, Aramata S, Katakami S, Yasuda K, Kataoka K. 2011. Proteasome activator PA28{gamma} stimulates degradation of GSK3-phosphorylated insulin transcription activator MAFA. *J Mol Endocrinol* **47**:119–127. doi:10.1530/JME-11-0044

Kedar PS, Widen SG, Englander EW, Fornace AJ, Wilson SH. 1991. The ATF/CREB transcription factor-binding site in the polymerase beta promoter mediates the positive effect of N-methyl-N'-nitro-N-nitrosoguanidine on transcription. *Proc Natl Acad Sci USA* **88**:3729–3733. doi:10.1073/pnas.88.9.3729

Kim YJ, Björklund S, Li Y, Sayre MH, Kornberg RD. 1994. A multiprotein mediator of transcriptional activation and its interaction with the C-terminal repeat domain of RNA polymerase II. *Cell* **77**:599–608. doi:10.1016/0092-8674(94)90221-6

Kincaid EZ, Che JW, York I, Escobar H, Reyes-Vargas E, Delgado JC, Welsh RM, Karow ML, Murphy AJ, Valenzuela DM, Yancopoulos GD, Rock KL. 2011. Mice completely lacking immunoproteasomes show major changes in antigen presentation. *Nat Immunol* **13**:129–135. doi:10.1038/ni.2203

Knowlton JR, Johnston SC, Whitby FG, Realini C, Zhang Z, Rechsteiner M, Hill CP. 1997. Structure of the proteasome activator REGalpha (PA28alpha). *Nature* **390**:639–643. doi:10.1038/37670

Kobayashi T, Wang J, Al-Ahmadie H, Abate-Shen C. 2013. ARF regulates the stability of p16 protein via REGγ-dependent proteasome degradation. *Mol Cancer Res* **11**:828–833. doi:10.1158/1541-7786.MCR-13-0207

Konstantinova IM, Tsimokha AS, Mittenberg AG. 2008. Role of proteasomes in cellular regulationInternational Review of Cell and Molecular Biology. Elsevier. pp. 59–124. doi:10.1016/S1937-6448(08)00602-3

Kosugi S, Hasebe M, Matsumura N, Takashima H, Miyamoto-Sato E, Tomita M, Yanagawa H. 2009. Six classes of nuclear localization signals specific to different binding grooves of importin alpha. *J Biol Chem* **284**:478–485. doi:10.1074/jbc.M807017200

Lehka L, Rędowicz MJ. 2020. Mechanisms regulating myoblast fusion: A multilevel interplay. *Semin Cell Dev Biol* **104**:81–92. doi:10.1016/j.semcdb.2020.02.004

Lei K, Bai H, Sun S, Xin C, Li J, Chen Q. 2020. Pa28γ, an accomplice to malignant cancer. *Front Oncol* **10**:584778. doi:10.3389/fonc.2020.584778

Leng X, Ji X, Hou Y, Settlage R, Jiang H. 2019. Roles of the proteasome and inhibitor of DNA binding 1 protein in myoblast differentiation. *FASEB J* **33**:7403–7416. doi:10.1096/fj.201800574RR

Levy-Barda A, Lerenthal Y, Davis AJ, Chung YM, Essers J, Shao Z, van Vliet N, Chen DJ, Hu MC-T, Kanaar R, Ziv Y, Shiloh Y. 2011. Involvement of the nuclear proteasome activator PA28γ in the cellular response to DNA double-strand breaks. *Cell Cycle* **10**:4300–4310. doi:10.4161/cc.10.24.18642

Lim S, Kwak J, Kim M, Lee D. 2013. Separation of a functional deubiquitylating module from the SAGA complex by the proteasome regulatory particle. *Nat Commun* **4**:2641. doi:10.1038/ncomms3641

Li J, Gao X, Ortega J, Nazif T, Joss L, Bogyo M, Steven AC, Rechsteiner M. 2001. Lysine 188 substitutions convert the pattern of proteasome activation by REGgamma to that of REGs alpha and beta. *EMBO J* **20**:3359–3369. doi:10.1093/emboj/20.13.3359

Li S, Jiang C, Pan J, Wang X, Jin J, Zhao L, Pan W, Liao G, Cai X, Li X, Xiao J, Jiang J, Wang P. 2015. Regulation of c-Myc protein stability by proteasome activator REGγ. *Cell Death Differ* **22**:1000–1011. doi:10.1038/cdd.2014.188

Li X, Amazit L, Long W, Lonard DM, Monaco JJ, O'Malley BW. 2007. Ubiquitin- and ATP-independent proteolytic turnover of p21 by the REGgamma-proteasome pathway. *Mol Cell* **26**:831–842. doi:10.1016/j.molcel.2007.05.028

Lipford JR, Smith GT, Chi Y, Deshaies RJ. 2005. A putative stimulatory role for activator turnover in gene expression. *Nature* **438**:113–116. doi:10.1038/nature04098

Liu C, Zhang Y, Li J, Wang Y, Ren F, Zhou Yifan, Wu Y, Feng Y, Zhou Yu, Su F, Jia B, Wang D, Chang Z. 2015. p15RS/RPRD1A (p15INK4b-related sequence/regulation of nuclear pre-mRNA domain-containing protein 1A) interacts with HDAC2 in inhibition of the Wnt/β-catenin signaling pathway. *J Biol Chem* **290**:9701–9713. doi:10.1074/jbc.M114.620872

Liu Jiang, Wang Ying, Li L, Zhou L, Wei H, Zhou Q, Liu Jian, Wang W, Ji L, Shan P, Wang Yan, Yang Y, Jung SY, Zhang P, Wang C, Long W, Zhang B, Li X. 2013. Site-specific acetylation of the proteasome activator REGγ directs its heptameric structure and functions. *J Biol Chem* **288**:16567–16578. doi:10.1074/jbc.M112.437129

Liu M, Xu Z, Zhang C, Yang C, Feng J, Lu Y, Zhang W, Chen W, Xu X, Sun X, Yang M, Liu W, Zhou T, Yang Y. 2021. Nudc L279P mutation destabilizes filamin A by inhibiting the hsp90 chaperoning pathway and suppresses cell migration. *Front Cell Dev Biol* **9**:671233. doi:10.3389/fcell.2021.671233

Liu S, Lai L, Zuo Q, Dai F, Wu L, Wang Y, Zhou Q, Liu Jian, Liu Jiang, Li L, Lin Q, Creighton CJ, Costello MG, Huang S, Jia C, Liao L, Luo H, Fu J, Liu M, Yi Z, Li X. 2014. PKA turnover by the REGγ-proteasome modulates FoxO1 cellular activity and VEGF-induced angiogenesis. *J Mol Cell Cardiol* **72**:28–38. doi:10.1016/j.yjmcc.2014.02.007

Li J, Rechsteiner M. 2001. Molecular dissection of the 11S REG (PA28) proteasome activators. *Biochimie* **83**:373–383. doi:10.1016/s0300-9084(01)01236-6

Li L, Zhao D, Wei H, Yao L, Dang Y, Amjad A, Xu J, Liu Jiang, Guo L, Li D, Li Z, Zuo D, Zhang Y, Liu Jian, Huang S, Jia C, Wang L, Wang Y, Xie Y, Luo J, Li X. 2013. REGγ deficiency promotes premature aging via the casein kinase 1 pathway. *Proc Natl Acad Sci USA* **110**:11005–11010. doi:10.1073/pnas.1308497110

Li X, Lonard DM, Jung SY, Malovannaya A, Feng Q, Qin J, Tsai SY, Tsai M-J, O'Malley BW. 2006. The SRC-3/AIB1 coactivator is degraded in a ubiquitin- and ATP-independent manner by the REGgamma proteasome. *Cell* **124**:381–392. doi:10.1016/j.cell.2005.11.037

Liu S, Zheng L-L, Zhu Y-M, Shen H-J, Zhong Q, Huang J, Li C, Liu Z, Yao M-D, Ou R-M, Zhang Q. 2018. Knockdown of REGγ inhibits the proliferation and migration and promotes the apoptosis of multiple myeloma cells by downregulating NF-κB signal pathway. *Hematology* **23**:277–283. doi:10.1080/10245332.2017.1385194

Li L, Dang Y, Zhang J, Yan W, Zhai W, Chen H, Li K, Tong L, Gao X, Amjad A, Ji L, Jing T, Jiang Z, Shi K, Yao L, Song D, Liu T, Yang X, Yang C, Cai X, Li X. 2015. REGγ is critical for skin carcinogenesis by modulating the Wnt/β-catenin pathway. *Nat Commun* **6**:6875. doi:10.1038/ncomms7875

Li M, Ma D, Chang Z. 2021. Current understanding of CREPT and p15RS, carboxy-terminal domain (CTD)-interacting proteins, in human cancers. *Oncogene* **40**:705–716. doi:10.1038/s41388-020-01544-0

Lu D, Wu Y, Wang Y, Ren F, Wang D, Su F, Zhang Y, Yang X, Jin G, Hao X, He D, Zhai Y, Irwin DM, Hu J, Sung JJY, Yu J, Jia B, Chang Z. 2012. CREPT accelerates tumorigenesis by regulating the transcription of cell-cycle-related genes. *Cancer Cell* **21**:92–104. doi:10.1016/j.ccr.2011.12.016

Majumder P, Baumeister W. 2019. Proteasomes: unfoldase-assisted protein degradation machines. *Biol Chem* **401**:183–199. doi:10.1515/hsz-2019-0344

Mandemaker IK, Geijer ME, Kik I, Bezstarosti K, Rijkers E, Raams A, Janssens RC, Lans H, Hoeijmakers JH, Demmers JA, Vermeulen W, Marteijn JA. 2018. DNA damage-induced replication stress results in PA200-proteasome-mediated degradation of acetylated histones. *EMBO Rep* **19**. doi:10.15252/embr.201745566

Manohar S, Jacob S, Wang J, Wiechecki KA, Koh HWL, Simões V, Choi H, Vogel C, Silva GM. 2019. Polyubiquitin chains linked by lysine residue 48 (K48) selectively target oxidized proteins in vivo. *Antioxid Redox Signal* **31**:1133–1149. doi:10.1089/ars.2019.7826

Mao I, Liu J, Li X, Luo H. 2008. REGgamma, a proteasome activator and beyond? *Cell Mol Life Sci* **65**:3971–3980. doi:10.1007/s00018-008-8291-z

Masson P, Andersson O, Petersen UM, Young P. 2001. Identification and characterization of a Drosophila nuclear proteasome regulator. A homolog of human 11 S REGgamma (PA28gamma). *J Biol Chem* **276**:1383–1390. doi:10.1074/jbc.M007379200

Ma CP, Willy PJ, Slaughter CA, DeMartino GN. 1993. PA28, an activator of the 20 S proteasome, is inactivated by proteolytic modification at its carboxyl terminus. *J Biol Chem* **268**:22514–22519. doi:10.1016/S0021-9258(18)41559-1

McCann TS, Tansey WP. 2014. Functions of the proteasome on chromatin. *Biomolecules* **4**:1026–1044. doi:10.3390/biom4041026

McDonough H, Patterson C. 2003. CHIP: a link between the chaperone and proteasome systems. *Cell Stress Chaperones* **8**:303–308. doi:10.1379/1466-1268(2003)008<0303:calbtc>2.0.co;2

Minami R, Hayakawa A, Kagawa H, Yanagi Y, Yokosawa H, Kawahara H. 2010. BAG-6 is essential for selective elimination of defective proteasomal substrates. *J Cell Biol* **190**:637–650. doi:10.1083/jcb.200908092

Moncsek A, Gruner M, Meyer H, Lehmann A, Kloetzel P-M, Stohwasser R. 2015. Evidence for

anti-apoptotic roles of proteasome activator 28γ via inhibiting caspase activity. *Apoptosis* **20**:1211–1228. doi:10.1007/s10495-015-1149-6

Morán Luengo T, Kityk R, Mayer MP, Rüdiger SGD. 2018. Hsp90 breaks the deadlock of the hsp70 chaperone system. *Mol Cell* **70**:545-552.e9. doi:10.1016/j.molcel.2018.03.028

Moriishi K, Mochizuki R, Moriya K, Miyamoto H, Mori Y, Abe T, Murata S, Tanaka K, Miyamura T, Suzuki T, Koike K, Matsuura Y. 2007. Critical role of PA28gamma in hepatitis C virus-associated steatogenesis and hepatocarcinogenesis. *Proc Natl Acad Sci USA* **104**:1661–1666. doi:10.1073/pnas.0607312104

Murata S, Kawahara H, Tohma S, Yamamoto K, Kasahara M, Nabeshima Y, Tanaka K, Chiba T. 1999. Growth retardation in mice lacking the proteasome activator PA28gamma. *J Biol Chem* **274**:38211–38215. doi:10.1074/jbc.274.53.38211

Nie J, Wu M, Wang J, Xing G, He F, Zhang L. 2010. REGgamma proteasome mediates degradation of the ubiquitin ligase Smurf1. *FEBS Lett* **584**:3021–3027. doi:10.1016/j.febslet.2010.05.034

Ni Z, Olsen JB, Guo X, Zhong G, Ruan ED, Marcon E, Young P, Guo H, Li J, Moffat J, Emili A, Greenblatt JF. 2011. Control of the RNA polymerase II phosphorylation state in promoter regions by CTD interaction domain-containing proteins RPRD1A and RPRD1B. *Transcription* **2**:237–242. doi:10.4161/trns.2.5.17803

Ni Z, Xu C, Guo X, Hunter GO, Kuznetsova OV, Tempel W, Marcon E, Zhong G, Guo H, Kuo W-HW, Li J, Young P, Olsen JB, Wan C, Loppnau P, El Bakkouri M, Senisterra GA, He H, Huang H, Sidhu SS, Greenblatt JF. 2014. RPRD1A and RPRD1B are human RNA polymerase II C-terminal domain scaffolds for Ser5 dephosphorylation. *Nat Struct Mol Biol* **21**:686–695. doi:10.1038/nsmb.2853

Noda C, Tanahashi N, Shimbara N, Hendil KB, Tanaka K. 2000. Tissue distribution of constitutive proteasomes, immunoproteasomes, and PA28 in rats. *Biochem Biophys Res Commun* **277**:348–354. doi:10.1006/bbrc.2000.3676

Osmani AH, Osmani SA, Morris NR. 1990. The molecular cloning and identification of a gene product specifically required for nuclear movement in Aspergillus nidulans. *J Cell Biol* **111**:543–551. doi:10.1083/jcb.111.2.543

Ostendorff HP, Peirano RI, Peters MA, Schlüter A, Bossenz M, Scheffner M, Bach I. 2002. Ubiquitination-dependent cofactor exchange on LIM homeodomain transcription factors. *Nature* **416**:99–103. doi:10.1038/416099a

Pan Y-R, Sun M, Wohlschlegel J, Reed SI. 2013. Cks1 enhances transcription efficiency at the GAL1 locus by linking the Paf1 complex to the 19S proteasome. *Eukaryotic Cell* **12**:1192–1201. doi:10.1128/EC.00151-13

Pecori F, Kondo N, Ogura C, Miura T, Kume M, Minamijima Y, Yamamoto K, Nishihara S. 2021. Site-specific O-GlcNAcylation of Psme3 maintains mouse stem cell pluripotency by

impairing P-body homeostasis. *Cell Rep* **36**:109361. doi:10.1016/j.celrep.2021.109361

Petrany MJ, Millay DP. 2019. Cell fusion: merging membranes and making muscle. *Trends Cell Biol* **29**:964–973. doi:10.1016/j.tcb.2019.09.002

Pinto MJ, Alves PL, Martins L, Pedro JR, Ryu HR, Jeon NL, Taylor AM, Almeida RD. 2016. The proteasome controls presynaptic differentiation through modulation of an on-site pool of polyubiquitinated conjugates. *J Cell Biol* **212**:789–801. doi:10.1083/jcb.201509039

Podenkova UI, Zubarev IV, Tomilin AN, Tsimokha AS. 2023. Ubiquitin-Proteasome System in the Regulation of Cell Pluripotency and Differentiation. *Cell and tissue biol* **17**:441–453. doi:10.1134/S1990519X23050103

Qian M-X, Pang Y, Liu CH, Haratake K, Du B-Y, Ji D-Y, Wang G-F, Zhu Q-Q, Song W, Yu Y, Zhang X-X, Huang H-T, Miao S, Chen L-B, Zhang Z-H, Liang Y-N, Liu S, Cha H, Yang D, Zhai Y, Qiu X-B. 2013. Acetylation-mediated proteasomal degradation of core histones during DNA repair and spermatogenesis. *Cell* **153**:1012–1024. doi:10.1016/j.cell.2013.04.032

Qin L, Guo J, Zheng Q, Zhang H. 2016. BAG2 structure, function and involvement in disease. *Cell Mol Biol Lett* **21**:18. doi:10.1186/s11658-016-0020-2

Raule M, Cerruti F, Benaroudj N, Migotti R, Kikuchi J, Bachi A, Navon A, Dittmar G, Cascio P. 2014. PA28αβ reduces size and increases hydrophilicity of 20S immunoproteasome peptide products. *Chem Biol* **21**:470–480. doi:10.1016/j.chembiol.2014.02.006

Realini C, Jensen CC, Zhang Z, Johnston SC, Knowlton JR, Hill CP, Rechsteiner M. 1997. Characterization of recombinant REGalpha, REGbeta, and REGgamma proteasome activators. *J Biol Chem* **272**:25483–25492. doi:10.1074/jbc.272.41.25483

Rechsteiner M, Realini C, Ustrell V. 2000. The proteasome activator 11 S REG (PA28) and class I antigen presentation. *Biochem J* **345 Pt 1**:1–15. doi:10.1042/bj3450001

Rosenzweig R, Nillegoda NB, Mayer MP, Bukau B. 2019. The Hsp70 chaperone network. *Nat Rev Mol Cell Biol* **20**:665–680. doi:10.1038/s41580-019-0133-3

Rosenzweig R, Sekhar A, Nagesh J, Kay LE. 2017. Promiscuous binding by Hsp70 results in conformational heterogeneity and fuzzy chaperone-substrate ensembles. *eLife* **6**. doi:10.7554/eLife.28030

Rousseau A, Bertolotti A. 2018. Regulation of proteasome assembly and activity in health and disease. *Nat Rev Mol Cell Biol* **19**:697–712. doi:10.1038/s41580-018-0040-z

Rubin DM, Coux O, Wefes I, Hengartner C, Young RA, Goldberg AL, Finley D. 1996. Identification of the gal4 suppressor Sug1 as a subunit of the yeast 26S proteasome. *Nature* **379**:655–657. doi:10.1038/379655a0

Sahasrabudhe P, Rohrberg J, Biebl MM, Rutz DA, Buchner J. 2017. The Plasticity of the Hsp90 Co-chaperone System. *Mol Cell* **67**:947-961.e5. doi:10.1016/j.molcel.2017.08.004

Savulescu AF, Glickman MH. 2011. Proteasome activator 200: the heat is on.. *Mol Cell Proteomics* **10**:R110.006890. doi:10.1074/mcp.R110.006890

Schröder S, Herker E, Itzen F, He D, Thomas S, Gilchrist DA, Kaehlcke K, Cho S, Pollard KS, Capra JA, Schnölzer M, Cole PA, Geyer M, Bruneau BG, Adelman K, Ott M. 2013. Acetylation of RNA polymerase II regulates growth-factor-induced gene transcription in mammalian cells. *Mol Cell* **52**:314–324. doi:10.1016/j.molcel.2013.10.009

Schröter F, Adjaye J. 2014. The proteasome complex and the maintenance of pluripotency: sustain the fate by mopping up? *Stem Cell Res Ther* **5**:24. doi:10.1186/scrt413

Shankar S, Hsu Z-T, Ezquerra A, Li C-C, Huang T-L, Coyaud E, Viais R, Grauffel C, Raught B, Lim C, Lüders J, Tsai S-Y, Hsia K-C. 2022. A γ-tubulin complex-dependent pathway suppresses ciliogenesis by promoting cilia disassembly. *Cell Rep* **41**:111642. doi:10.1016/j.celrep.2022.111642

Sijts EJAM, Kloetzel PM. 2011. The role of the proteasome in the generation of MHC class I ligands and immune responses. *Cell Mol Life Sci* **68**:1491–1502. doi:10.1007/s00018-011-0657-y

Simionescu A, Pavlath GK. 2011. Molecular mechanisms of myoblast fusion across species. *Adv Exp Med Biol* **713**:113–135. doi:10.1007/978-94-007-0763-4_8

Simonti CN, Pollard KS, Schröder S, He D, Bruneau BG, Ott M, Capra JA. 2015. Evolution of lysine acetylation in the RNA polymerase II C-terminal domain. *BMC Evol Biol* **15**:35. doi:10.1186/s12862-015-0327-z

Smith DM, Chang S-C, Park S, Finley D, Cheng Y, Goldberg AL. 2007. Docking of the proteasomal ATPases' carboxyl termini in the 20S proteasome's alpha ring opens the gate for substrate entry. *Mol Cell* **27**:731–744. doi:10.1016/j.molcel.2007.06.033

Son SH, Kim MY, Lim YS, Jin HC, Shin JH, Yi JK, Choi S, Park MA, Chae JH, Kang HC, Lee YJ, Uversky VN, Kim CG. 2023. SUMOylation-mediated PSME3-20S proteasomal degradation of transcription factor CP2c is crucial for cell cycle progression. *Sci Adv* **9**:eadd4969. doi:10.1126/sciadv.add4969

Sousa-Victor P, García-Prat L, Muñoz-Cánoves P. 2022. Control of satellite cell function in muscle regeneration and its disruption in ageing. *Nat Rev Mol Cell Biol* **23**:204–226. doi:10.1038/s41580-021-00421-2

Spain MM, Govind CK. 2011. A role for phosphorylated Pol II CTD in modulating transcription coupled histone dynamics. *Transcription* **2**:78–81. doi:10.4161/trns.2.2.14638

Stadtmueller BM, Hill CP. 2011. Proteasome activators. *Mol Cell* **41**:8–19. doi:10.1016/j.molcel.2010.12.020

Stavreva DA, Müller WG, Hager GL, Smith CL, McNally JG. 2004. Rapid glucocorticoid receptor exchange at a promoter is coupled to transcription and regulated by chaperones and

proteasomes. *Mol Cell Biol* **24**:2682–2697. doi:10.1128/MCB.24.7.2682-2697.2004

Steurer B, Janssens RC, Geijer ME, Aprile-Garcia F, Geverts B, Theil AF, Hummel B, van Royen ME, Evers B, Bernards R, Houtsmuller AB, Sawarkar R, Marteijn J. 2022. DNA damage-induced transcription stress triggers the genome-wide degradation of promoter-bound Pol II. *Nat Commun* **13**:3624. doi:10.1038/s41467-022-31329-w

Strober BJ, Elorbany R, Rhodes K, Krishnan N, Tayeb K, Battle A, Gilad Y. 2019. Dynamic genetic regulation of gene expression during cellular differentiation. *Science* **364**:1287–1290. doi:10.1126/science.aaw0040

Sugiyama M, Sahashi H, Kurimoto E, Takata S, Yagi H, Kanai K, Sakata E, Minami Y, Tanaka K, Kato K. 2013. Spatial arrangement and functional role of α subunits of proteasome activator PA28 in hetero-oligomeric form. *Biochem Biophys Res Commun* **432**:141–145. doi:10.1016/j.bbrc.2013.01.071

Sun J, Luan Y, Xiang D, Tan X, Chen H, Deng Q, Zhang J, Chen M, Huang H, Wang W, Niu T, Li W, Peng H, Li S, Li L, Tang W, Li X, Wu D, Wang P. 2016. The 11S Proteasome Subunit PSME3 Is a Positive Feedforward Regulator of NF-κB and Important for Host Defense against Bacterial Pathogens. *Cell Rep* **14**:737–749. doi:10.1016/j.celrep.2015.12.069

Suzuki A, Minamide R, Iwata J. 2018. WNT/β-catenin signaling plays a crucial role in myoblast fusion through regulation of nephrin expression during development. *Development* **145**. doi:10.1242/dev.168351

Swaffield JC, Bromberg JF, Johnston SA. 1992. Alterations in a yeast protein resembling HIV Tat-binding protein relieve requirement for an acidic activation domain in GAL4. *Nature* **357**:698–700. doi:10.1038/357698a0

Tanahashi N, Murakami Y, Minami Y, Shimbara N, Hendil KB, Tanaka K. 2000. Hybrid proteasomes. Induction by interferon-gamma and contribution to ATP-dependent proteolysis. *J Biol Chem* **275**:14336–14345. doi:10.1074/jbc.275.19.14336

Thomas T, Salcedo-Tacuma D, Smith DM. 2023. Structure, function, and allosteric regulation of the 20S proteasome by the 11S/PA28 family of proteasome activators. *Biomolecules* **13**. doi:10.3390/biom13091326

Thomas TA, Smith DM. 2022. Proteasome activator 28γ (PA28γ) allosterically activates trypsin-like proteolysis by binding to the α-ring of the 20S proteasome. *J Biol Chem* **298**:102140. doi:10.1016/j.jbc.2022.102140

Tong L, Shen S, Huang Q, Fu J, Wang T, Pan L, Zhang P, Chen G, Huang T, Li K, Liu Q, Xie S, Yang X, Moses RE, Li X, Li L. 2020. Proteasome-dependent degradation of Smad7 is critical for lung cancer metastasis. *Cell Death Differ* **27**:1795–1806. doi:10.1038/s41418-019-0459-6

Toste Rêgo A, da Fonseca PCA. 2019. Characterization of Fully Recombinant Human 20S and 20S-PA200 Proteasome Complexes. *Mol Cell* **76**:138-147.e5. doi:10.1016/j.molcel.2019.07.014

Ustrell V, Hoffman L, Pratt G, Rechsteiner M. 2002. PA200, a nuclear proteasome activator involved in DNA repair. *EMBO J* **21**:3516–3525. doi:10.1093/emboj/cdf333

Uyama M, Sato MM, Kawanami M, Tamura M. 2012. Regulation of osteoblastic differentiation by the proteasome inhibitor bortezomib. *Genes Cells* **17**:548–558. doi:10.1111/j.1365-2443.2012.01611.x

Wagatsuma A, Sakuma K. 2013. Mitochondria as a potential regulator of myogenesis. *ScientificWorldJournal* **2013**:593267. doi:10.1155/2013/593267

Wang H, Bao W, Jiang F, Che Q, Chen Z, Wang F, Tong H, Dai C, He X, Liao Y, Liu B, Sun J, Wan X. 2015. Mutant p53 (p53-R248Q) functions as an oncogene in promoting endometrial cancer by up-regulating REGγ. *Cancer Lett* **360**:269–279. doi:10.1016/j.canlet.2015.02.028

Wang Q, Gao X, Yu T, Yuan L, Dai J, Wang W, Chen G, Jiao C, Zhou W, Huang Q, Cui L, Zhang P, Moses RE, Yang J, Chen F, Fu J, Xiao J, Li L, Dang Y, Li X. 2018. REGγ Controls Hippo Signaling and Reciprocal NF-κB-YAP Regulation to Promote Colon Cancer. *Clin Cancer Res* **24**:2015–2025. doi:10.1158/1078-0432.CCR-17-2986

Wegele H, Wandinger SK, Schmid AB, Reinstein J, Buchner J. 2006. Substrate transfer from the chaperone Hsp70 to Hsp90. *J Mol Biol* **356**:802–811. doi:10.1016/j.jmb.2005.12.008

Welk V, Coux O, Kleene V, Abeza C, Trümbach D, Eickelberg O, Meiners S. 2016. Inhibition of proteasome activity induces formation of alternative proteasome complexes. *J Biol Chem* **291**:13147–13159. doi:10.1074/jbc.M116.717652

Whitby FG, Masters EI, Kramer L, Knowlton JR, Yao Y, Wang CC, Hill CP. 2000. Structural basis for the activation of 20S proteasomes by 11S regulators. *Nature* **408**:115–120. doi:10.1038/35040607

Wu Y, Wang L, Zhou P, Wang G, Zeng Y, Wang Y, Liu J, Zhang B, Liu S, Luo H, Li X. 2011. Regulation of REGγ cellular distribution and function by SUMO modification. *Cell Res* **21**:807–816. doi:10.1038/cr.2011.57

Wu Y, Zhang Y, Zhang H, Yang X, Wang Y, Ren F, Liu H, Zhai Y, Jia B, Yu J, Chang Z. 2010. p15RS attenuates Wnt/{beta}-catenin signaling by disrupting {beta}-catenin·TCF4 Interaction. *J Biol Chem* **285**:34621–34631. doi:10.1074/jbc.M110.148791

Xie SC, Metcalfe RD, Hanssen E, Yang T, Gillett DL, Leis AP, Morton CJ, Kuiper MJ, Parker MW, Spillman NJ, Wong W, Tsu C, Dick LR, Griffin MDW, Tilley L. 2019. The structure of the PA28-20S proteasome complex from Plasmodium falciparum and implications for proteostasis. *Nat Microbiol* **4**:1990–2000. doi:10.1038/s41564-019-0524-4

Xie T, Chen H, Shen S, Huang T, Huang B, Hu G, Li L, Xu Y. 2019. Proteasome activator REGγ promotes inflammation in Leydig cells via IkBε signaling. *Int J Mol Med* **43**:1961–1968. doi:10.3892/ijmm.2019.4115

Xie Y, Gao R, Gao Y, Dong Z, Ge J. 2023. 11S proteasome activator regγ promotes aortic

dissection by inhibiting RBM3 (RNA binding motif protein 3) pathway. *Hypertension* **80**:125–137. doi:10.1161/HYPERTENSIONAHA.122.19618

Xu J, Zhou L, Ji L, Chen F, Fortmann K, Zhang K, Liu Q, Li K, Wang W, Wang H, Xie W, Wang Q, Liu J, Zheng B, Zhang P, Huang S, Shi T, Zhang B, Dang Y, Chen J, Li X. 2016. The REGγ-proteasome forms a regulatory circuit with IκBε and NFκB in experimental colitis. *Nat Commun* **7**:10761. doi:10.1038/ncomms10761

Yaffe D, Saxel O. 1977. Serial passaging and differentiation of myogenic cells isolated from dystrophic mouse muscle. *Nature* **270**:725–727. doi:10.1038/270725a0

Yamada M, Toba S, Takitoh T, Yoshida Y, Mori D, Nakamura T, Iwane AH, Yanagida T, Imai H, Yu-Lee L-Y, Schroer T, Wynshaw-Boris A, Hirotsune S. 2010. mNUDC is required for plus-end-directed transport of cytoplasmic dynein and dynactins by kinesin-1. *EMBO J* **29**:517–531. doi:10.1038/emboj.2009.378

Yang L, Yang H, Chu Y, Song Y, Ding L, Zhu B, Zhai W, Wang X, Kuang Y, Ren F, Jia B, Wu W, Ye X, Wang Y, Chang Z. 2021. CREPT is required for murine stem cell maintenance during intestinal regeneration. *Nat Commun* **12**:270. doi:10.1038/s41467-020-20636-9

Yan Q, Sharma-Kuinkel BK, Deshmukh H, Tsalik EL, Cyr DD, Lucas J, Woods CW, Scott WK, Sempowski GD, Thaden JT, Rude TH, Ahn SH, Fowler VG. 2014. Dusp3 and Psme3 are associated with murine susceptibility to Staphylococcus aureus infection and human sepsis. *PLoS Pathog* **10**:e1004149. doi:10.1371/journal.ppat.1004149

Ying H, Furuya F, Zhao L, Araki O, West BL, Hanover JA, Willingham MC, Cheng S-Y. 2006. Aberrant accumulation of PTTG1 induced by a mutated thyroid hormone beta receptor inhibits mitotic progression. *J Clin Invest* **116**:2972–2984. doi:10.1172/JCI28598

Yi Z, Yang D, Liao X, Guo F, Wang Y, Wang X. 2017. PSME3 induces epithelial-mesenchymal transition with inducing the expression of CSC markers and immunosuppression in breast cancer. *Exp Cell Res* **358**:87–93. doi:10.1016/j.yexcr.2017.05.017

Yu G, Zhao Y, He J, Lonard DM, Mao C-A, Wang G, Li M, Li X. 2010. Comparative analysis of REG{gamma} expression in mouse and human tissues. *J Mol Cell Biol* **2**:192–198. doi:10.1093/jmcb/mjq009

Zammit PS. 2017. Function of the myogenic regulatory factors Myf5, MyoD, Myogenin and MRF4 in skeletal muscle, satellite cells and regenerative myogenesis. *Semin Cell Dev Biol* **72**:19–32. doi:10.1016/j.semcdb.2017.11.011

Zannini L, Buscemi G, Fontanella E, Lisanti S, Delia D. 2009. REGgamma/PA28gamma proteasome activator interacts with PML and Chk2 and affects PML nuclear bodies number. *Cell Cycle* **8**:2399–2407. doi:10.4161/cc.8.15.9084

Zannini L, Lecis D, Buscemi G, Carlessi L, Gasparini P, Fontanella E, Lisanti S, Barton L, Delia D. 2008. REGgamma proteasome activator is involved in the maintenance of chromosomal stability. *Cell Cycle* **7**:504–512. doi:10.4161/cc.7.4.5355

Zanotelli MR, Zhang J, Reinhart-King CA. 2021. Mechanoresponsive metabolism in cancer cell migration and metastasis. *Cell Metab* **33**:1307–1321. doi:10.1016/j.cmet.2021.04.002

Zhang C, Zhang W, Lu Y, Yan Xiaoyi, Yan Xiumin, Zhu X, Liu W, Yang Y, Zhou T. 2016. NudC regulates actin dynamics and ciliogenesis by stabilizing cofilin 1. *Cell Res* **26**:239–253. doi:10.1038/cr.2015.152

Zhang H, Tu J, Cao C, Yang T, Gao L. 2020. Proteasome activator PA28γ-dependent degradation of coronavirus disease (COVID-19) nucleocapsid protein. *Biochem Biophys Res Commun* **529**:251–256. doi:10.1016/j.bbrc.2020.06.058

Zhang Y, Liu C, Duan X, Ren F, Li S, Jin Z, Wang Y, Feng Y, Liu Z, Chang Z. 2014. CREPT/RPRD1B, a recently identified novel protein highly expressed in tumors, enhances the β-catenin·TCF4 transcriptional activity in response to Wnt signaling. *J Biol Chem* **289**:22589–22599. doi:10.1074/jbc.M114.560979

Zhang Z, Clawson A, Realini C, Jensen CC, Knowlton JR, Hill CP, Rechsteiner M. 1998. Identification of an activation region in the proteasome activator REGalpha. *Proc Natl Acad Sci USA* **95**:2807–2811. doi:10.1073/pnas.95.6.2807

Zhang Z, Zhang R. 2008. Proteasome activator PA28 gamma regulates p53 by enhancing its MDM2-mediated degradation. *EMBO J* **27**:852–864. doi:10.1038/emboj.2008.25

Zhang Z-H, Jiang T-X, Chen L-B, Zhou W, Liu Y, Gao F, Qiu X-B. 2020. Proteasome subunit α4s is essential for formation of spermatoproteasomes and histone degradation during meiotic DNA repair in spermatocytes. *J Biol Chem* **296**:100130. doi:10.1074/jbc.RA120.016485

Zheng Q, Hu R, Zhu C, Jing J, Lou M, Zhang S, Li S, Cao H, Zhang X, Ling Y. 2023. Identification of transition factors in myotube formation from proteome and transcriptome analyses. *J Integr Agric* **22**:3135–3147. doi:10.1016/j.jia.2023.08.001

Zhou L, Yao L, Zhang Q, Xie W, Wang X, Zhang H, Xu J, Lin Q, Li Q, Xuan Y, Ji L, Wang L, Wang Weicang, Wang Weichao, Shi T, Fang L, Zheng B, Li L, Liu S, Zhang B, Li X. 2020. REGγ controls Th17 cell differentiation and autoimmune inflammation by regulating dendritic cells. *Cell Mol Immunol* **17**:1136–1147. doi:10.1038/s41423-019-0287-0

Zhou T, Aumais JP, Liu X, Yu-Lee L-Y, Erikson RL. 2003. A role for Plk1 phosphorylation of NudC in cytokinesis. *Dev Cell* **5**:127–138. doi:10.1016/s1534-5807(03)00186-2

Zhu X, Li Y, Tian X, Jing Y, Wang Z, Yue L, Li J, Wu L, Zhou X, Yu Z, Zhang Y, Guan F, Yang M, Zhang B. 2024. REGγ Mitigates Radiation-Induced Enteritis by Preserving Mucin Secretion and Sustaining Microbiome Homeostasis. *Am J Pathol* **194**:975–988. doi:10.1016/j.ajpath.2024.02.008

Zhu X-J, Liu X, Jin Q, Cai Y, Yang Y, Zhou T. 2010. The L279P mutation of nuclear distribution gene C (NudC) influences its chaperone activity and lissencephaly protein 1 (LIS1) stability. *J Biol Chem* **285**:29903–29910. doi:10.1074/jbc.M110.105494